DISSERTATION

ISOTOPE AND NOBLE GAS STUDY OF THREE AQUIFERS IN CENTRAL AND SOUTHEAST LIBYA

Submitted by

Mohamed S. E. Al Faitouri

Department of Geosciences

In partial fulfillment of the requirements

For the Degree of Doctor of Philosophy

Colorado State University

Fort Collins, Colorado

Summer 2013

Doctoral Committee:

Advisor: William Sanford

Michael Ronayne
Steven Fassnacht
Reagan Waskom

ABSTRACT

ISOTOPE AND NOBLE GAS STUDY OF THREE AQUIFERS IN CENTRAL AND SOUTHEAST LIBYA

Libya suffers from a shortage in water resources due to its arid climate. The annual precipitation in Libya is less than 200 mm in the narrow coastal plain, while the southern part of the country receives less than 1mm. On the other hand, Libya has large resources of good quality groundwater distributed in six basin systems beneath the Sahara. In 1983, the Libyan government established the Great Man-Made River Authority (GMRA) in order to transport 6.5 million cubic meters a day of this groundwater to the coastal cities, where over 90% of the population lives. This large water extraction of one million cubic meters per day (or greater) from each wellfield has the potential to greatly stress the water resources in these areas.

This study focuses on three GMRA wellfields in two sedimentary basins (Sirt and Al Kufra) in central and southeast Libya. The Sarir wellfield is located within the Sirt basin and consists of 126 production wells; the Tazerbo wellfield in the Al Kufra basin has 108 wells; and the proposed Al Kufra wellfield is also in the Al Kufra Basin and will have 300 production wells. With the large amount of water to be extracted from these aquifers, it is necessary perform hydrogeological studies to better characterize the physical and chemical properties of the aquifers in order to provide the information needed for planning over the proposed 50-year life span of the projects.

For this study, water samples were collected for analyses of the stable isotopes of water (^{2}H (D) and ^{18}O), ^{14}C and noble gases. These data are used to determine the age of the water in the aquifers and when recharge occurred and to estimate the climate at the time of recharge

(paleotemperatures). In addition, the helium content of the water will allow for the determination of the fluxes of helium in the crust at the locations of the aquifers. These fluxes include the helium produced in situ in the aquifer and fluxes from outside the aquifer (crust and mantle helium).

Three extraction wells were sampled from Sarir for ^{14}C analysis and the ages of these samples range from 9800 to 15200 ybp. At Tazerbo, five extraction wells were sampled and the age of the water averages 24000 ybp over a depth range of 150 m. In the Al Kufra area there were two wells sampled located approximately 100 km apart and at two different depths. The apparent age at the shallow well is 12000 ybp and at the deep well it is 21000 ybp. These ages indicate recharge during wet periods during the late Pleistocene and early Holocene. Recharge possibly occurred along ancient lakes and paleoriver channels.

The stable isotope compositions of water in all three aquifers are greatly depleted relative to that of modern precipitation. The results from the northern most aquifer (Sarir) is the most enriched and plot below the Global Meteoric Water Line (GMWL) and show evidence of potential effects of evaporation. The waters from the Al Kufra Basin aquifers are more depleted and plot on the GMWL. These results suggest that the groundwater recharge during the late Pleistocene and early Holocene was recharged at a time in which the regional monsoonal patterns were different than today. Other workers have concluded that the paleomonsoons most likely came from the southeast out of the Atlantic causing the waters to be depleted relative to modern precipitation.

Noble gas recharge temperatures (NGRTs) allow for the determination of average annual temperature during the time of recharge and to compare these values with the current annual temperatures. Noble gas recharge temperatures were determined for one sample from Sarir,

three samples from Tazerbo and one from Al Kufra (Table 4). For Sarir, the NGRT was 18°C which is about 5 degrees cooler than the average annual temperature today. For Tazerbo, one sample yielded a temperature of 20°C and the other two yielded temperatures of 25°C, compared to the present average annual temperature of 23°C. For the sample from Al Kufra, the recharge temperature is 19°C compared to the present average of 24°C. These results are consistent with findings from around the world that indicate average temperatures being several degrees cooler in the late Pleistocene than today.

The analyses of the noble gas data show that there are significant amounts of ^{4}He in the waters in excess of what is to be expected by water equilibration with the atmosphere. This indicates that for each aquifer, there is a strong component of terrigenic helium (helium produced within the earth due to radiogenic decay of U and Th decay products). Groundwater age in the aquifer can be estimated by determining the in situ production rate of ^{4}He using the U and Th content (assuming no external sources of helium). This method yields average water ages of 1.3 x 10^{5} years for Al Kufra, 5.1 x 10^{5} years for Sarir and 4.5 x 10^{6} years for Tazerbo. The ^{4}He ages for Sarir and Al Kufra are about one order of magnitude greater than the ^{14}C ages and the Tazerbo ^{4}He age is about two orders of magnitude greater. Based on looking at helium isotope ratios, it can be seen that there are external fluxes to the aquifers which would add more helium to the system than could be produced in situ.

The fluxes of helium for each aquifer system are determined by dividing the ^{4}He concentrations by the ^{14}C age. The resulting fluxes are consistent with fluxes determined elsewhere in sandstone aquifers.

Helium isotope ratios ($^{3}He/^{4}He$) provided information on the sources of helium in the aquifers. The main sources that can be identified are the ratios of helium produced in situ, the

ratio of helium from crustal rocks outside the aquifer and helium that comes from the mantle. It was determined that for the total amount of helium at Sarir, crustal helium accounts for 85%, mantle helium accounts for 14.6% and in situ produced helium accounts for 0.4%. For Al Kufra it is 95% crustal, 3.3% mantle and 1.7% in situ. For Tazerbo, values are 90% crustal, 9.7% mantle and 0.3% in situ.

ACKNOWLEDGEMENTS

I am genuinely thankful to my supervisor Dr. William Sanford, whose encouragement, guidance and support from the first to the ending level enabled me to develop an understanding of hydrogeochemistry of central and southeast Libya. Thanks are also extended to committee members Dr. Michael Ronayne, Dr. Steven Fassnacht and Dr. Reagan Waskom for their support.

Funding was generously provided by Great Man-Made River Project, without which this work would not have been possible. Mr. Fawzi Saaid, in particular, played a crucial role in his efforts in the realization of this work. Furthermore, Mr Abdusalm Al Taeeb and Mr. Hamdi El Haddad, and to all of those who supported me in any respect during the completion of the project. This work was made possible with the support of the office of higher education in Libya.

I wish to give a special greeting to my late mother and father, brothers, my wife and my kids who encouraged and supported me throughout my program.

DEDICATION

To soul of my mother and father

TABLE OF CONTENTS

LIST OF TABLES

LIST OF FIGURES

CHAPTER ONE

INTRODUCTION

1.1 Background

It is a fact that Libya receives very low precipitation due to being located in an arid climate; however, it is rich in groundwater resources. The coastal plain, only 5% of the entire area of Libya, where the majority of people live, receives around 200 mm of annual precipitation as compared to the <1 mm annual precipitation to the south. Evaporation rates are also high, ranging from 1700 mm/year in the north to 6000 mm/year in the south (Kuwairi 2006). Currently, the rainfall along the coastal zone is not sufficient for agriculture, or human demands compared with 40-50 years ago, due to low precipitation and an increase in population. Currently, groundwater is the primary source of fresh water, accounting for 96% of total Libyan consumption. However, as a result of excessive pumping, and low precipitation, seawater intrusion has taken place in the coastal aquifers: Jafara in the west, and Al Jabal al Akhder in the east (Figure 1.1), where most Libyan people are concentrated, with a marked increase in salinity, reaching over 7000 mg/l in the Tripoli region (Kuwairi 2006). In order to deal with the shortage of water in most coastal cities, water desalination, water treatment, pipeline transport from southern Europe to Tripoli, and transportation by ship have taken place.

During the 1950s, and 1960s oil production began in southern Libya. Work by Occidental (1966, 1970) led to the exploration of fossil groundwater reservoir in the Al Kufra and Sarir areas (Figure 1.1). With continuing oil exploration, more details had been reported about the fossil groundwater. During the 1960s, and 1970s, this exploration lead the Libyan government to construct farms in the Al Kufra area called the Kufra Productive Project (KPP). In 1971and 1973

the KPP had 99 wells and 27 piezometers, with discharge of 76 l/s (liter per second) per each well. Moreover, in 1974 the government constructed another project called Al Kufra Settlement project (KSP) with 55 wells each with discharge of 76 l/s. At the same time (1975), the Sarir agriculture project (North and South) was constructed in the Sarir area with 100 wells. Since that time, agriculture started to be developed by government as well as the studies of aquifers. Neither of the giant agricultural project in these areas (Sarir and Al Kufra), were suitable for population settlement due to the harsh climate.

Six groundwater basins have been identified as the main sources of groundwater resources in Libya: Cyrenaica in the northeast, Al Kufra and Sirt basins in the eastern and southeast, Jeffrah Plane, Ghadamas in the west and Murzuq in southeast (Figure 1.1).

Subsequent investigations have proved the reserves available and defined the limits of a number of potentially vast aquifers at Sirt, Kufra, Murzuq and Ghadames. Aquifers with water levels at depths of less than 100 m below ground surface were recharged by tropical rain, particularly 38 kyr – 10 kyr ago (Edmunds and Wrights 1979). Each of these basins contains reserves amounting to 3000×109 m3 of economically extractable fossil water (CEDARE 2001). In a recent study conducted under the supervision of the UN Centre for Environment & Development in the Arab Region (Libya, Egypt, Sudan and Chad) & Europe, CEDARE (2001) stated that the Nubian Basin (of which Al Kufra is part) was estimated to contain 373.3×1012m3. Therefore, in 1983 the Libyan government established the Great Man-Made River Authority (GMRA) for transporting 6.5 million cubic meters of water per day from those aquifers located beneath the deserts to the coastal cities with a minimum design life 50 years.

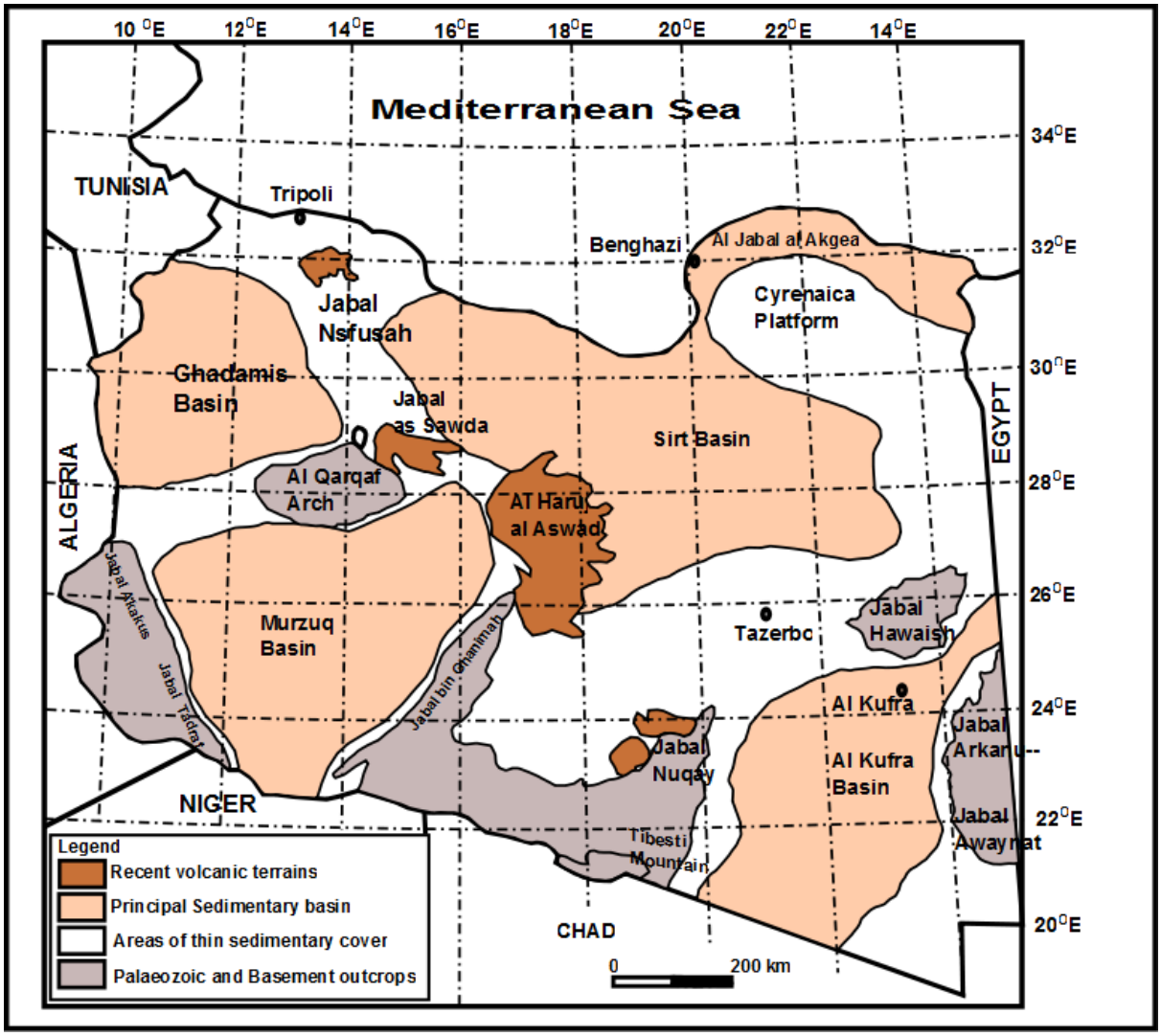

Figure 1.1. Location map of Libya, showing the sedimentary basins locations, and the surface geology, (modified after Rusk 2001, and Ramos et al. 2006)

Table 1.1 summarizes the number of wells at each wellfield within four basins, total reserves, total production and reservoir capacity of each wellfield. Figure 1.2 shows the location of these wellfileds.

To state the cost of these giant water projects, comprehensive studies have shown that the cost of pumping groundwater from the Libyan southern basins and conveying it to the northern region cost one Libyan Dinar (LD) per $9m^3$. However, compared with other options for example, desalination (1LD for 0.79 m^3), transport by pipeline from South Europe to Tripoli (1LD for 0.74 m^3), or transportation by ship (1LD for $1.03m^3$) it is the most cost effective solution for meeting the water demand. (Kuwairi 2006).

For this study, three aquifers in the Sirt and Al Kufra Basin will be the focus. In each aquifer, there are current or proposed wellfields designed to each extract 1×10^6 m^3/day or more water for transport by pipeline to Benghazi. With the plan to extract large quantities of groundwater from the Sirt and Al Kufra Basins it is necessary to characterize the hydrogeologic systems of the well fields, and to understand the behavior of aquifer flow systems before and during groundwater extraction.

1.2 Study Area

The study area consist of three wellfields (Sarir, Tazerbo, and Al Kufra) located in two major sedimentary basins located in central and southeast Libya (Figure 1.2). The three aquifers have been developed for water extraction for the GMRA. In general, Sirt and Al Kufra basins cover an area of about 650,000 km^2 within Libya, and consist of continental or marginal marine sediments of sandstone and shale with some limestone that overlie a Precambrian basement.

Table 1.1. Basins, wellfield, total reserves, total production and reservoirs capacity of GMRA projects.

Basin	Wellfield	Total Reserves (billion m^3)	No. of wells	Total Production MCM/D	Reservoirs	Capacity (MCM)
Gedammes	Gedammes	48000	144	0.25	Ajdabiya	4.0
	East & NE Jebel Hasouna		586	2.5	Al Gardabiya	6.8
Sirt	Sarir	20000	126+48 new	2	Omar Mukhtar	4.7
	Tazerbo		108		The Grand Al Gardabiya	15.4
Al Kufra	Al Kufra (planned)	25000	300	1.68	Grand Omar Mukhtar	24.0
Al Jabal Al khader	Jaghboub (Stopped)	312	40	0.137	The Total Storage Capacity	54.9

MCM = million cubic meter ; MCM/D = million cubic meter per day; NE = northeast

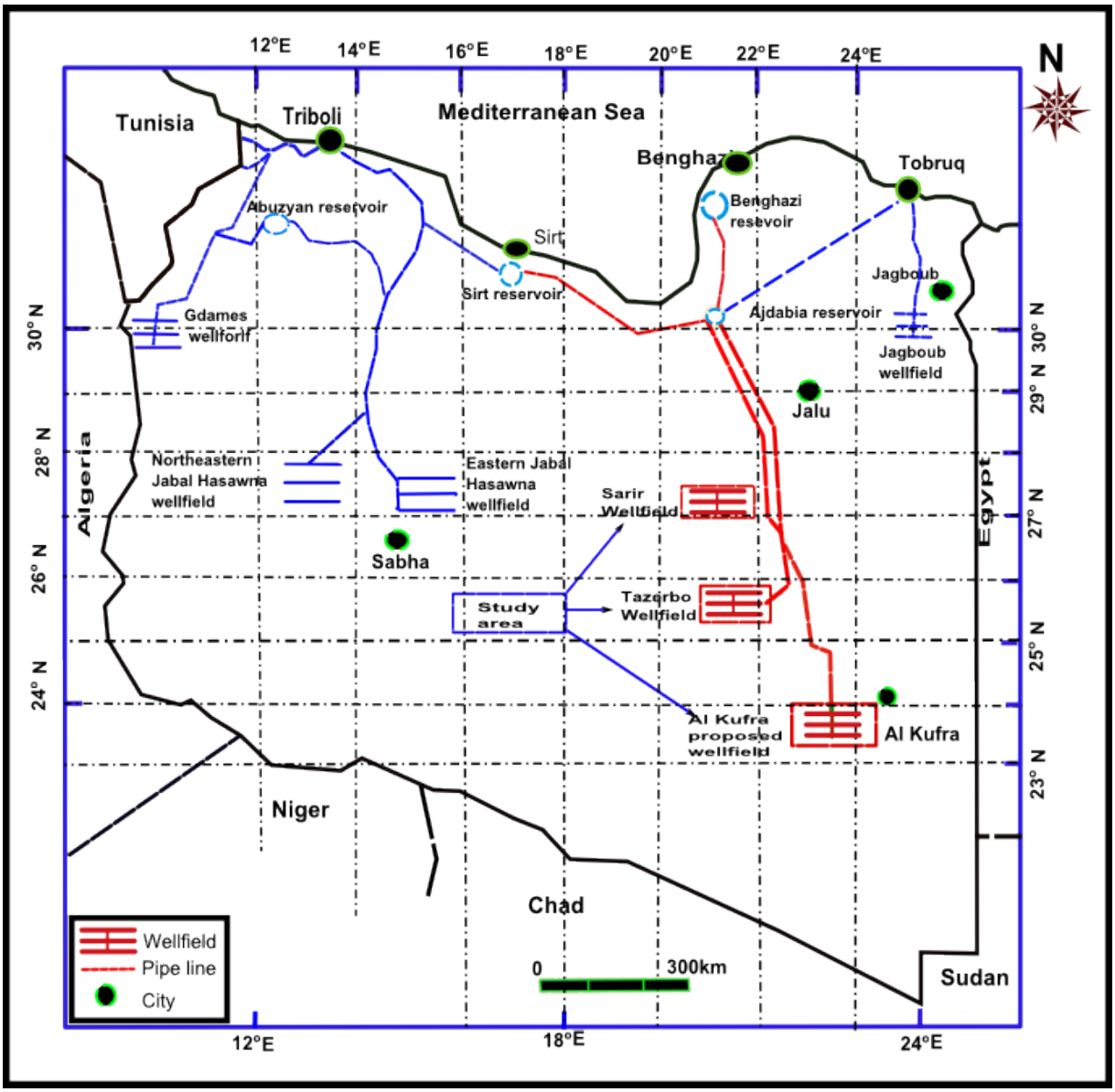

Figure 1.2. The study areas and the GMRA wellfields within Libya. Wellfields not to scale.

The Sarir wellfield is located at the southern part of the Sirt Basin, and contains of 126 production wells and 28 piezometerd. The wellfield consists of two aquifers: an unconfined shallow aquifer of Post Middle Miocene age, with depth to water table ranging from 80 m at the west part of the wellfield to about 60 m at the east part of wellfield; and a confined-semi-artesian deep aquifer of Middle Miocene age, multilayered sand, silt shale siltstone and clay, dipping generally toward the northeast. The water is being pumped only from the deep aquifer. The wellfield has been designed to produce 1,000,000 m^3/day, however at the present time it is producing only 200,000 m^3/day because some of the wells have been damaged. GMRA has decided to construct another 48 production wells that will increase the yield of the wellfield. Some of our samples were collected from these new wells during our field work in October, 2010.

The second wellfield is Tazerbo, and is located at the northern edge of the Al Kufra Basin. Three aquifers have been identified in the south part of the Tazerbo area (shallow, intermediate and deep) with relatively uniform and extensive layering separated by thick aquitards. The deep main aquifer is the target of The Great Man-made River Authority and is truncated in the north by Eocene clays. The thickness of the aquifer is 100-120 m, with a horizon of well-sorted, medium-grained, poorly cemented sands, which are encountered at 280 m in the north-west and at 500 m at the south-east of the southern aquifer (Tazerbo and Al Kufra), and dipping at an angle of about 2-3^o to the south-east. The depth to water is variable from site to another, from 260 m in NE and NW to 400 m in SE and SW, and the flow generally from S to N (e.g., Eddib 1973; Eskangi et al. 1975). Twenty one sites with piezometers have been built surrounding 108 high capacity production water wells to monitor the water level. The capacity of the wellfield has

been designed to yield one million cubic meter per day. However, at the present day, the yield of the wellfield is 490,000 m^3/day.

The Al Kufra wellfield is located in the southern part of the Al Kufra Basin, which is in the Nubian Aquifer. The area of the Nubian Sandstone Aquifer System is composed of different water-bearing strata that are differentiated into two systems, namely the Nubian Aquifer System (NAS) and the Post Nubian Aquifer System (PNAS). The NAS is comprised of the Paleozoic and the Mesozoic deposits and overlies the Pre-Cambrian basement complex. The PNAS occurs to the north part of the basin overlying the NAS in north-eastern Libya, and it is comprised of Tertiary continental deposits.

The production aquifer at the Kufra site has drained drawdown response during pumping.

The proposed wellfield will consist of 300 production wells and has 10 exploratory wells and 26 piezometer wells. The extraction rate is planned to be 1.6×10^6 m^3 per day. Al Kurfa wellfield is the most important field for GMRA because of the high production of fresh water that will be produced from the Nubian Sandstone aquifer in order to support the quantity of water being pumped from Tazerbo and Sarir wellfields.

1.3 The Objectives

Libya has many areas of hydrogeology where one needs to study and apply different methods to characterize the hydrogeologic systems in the locality of the new well fields, and to understand the behavior of aquifer flow systems before and during groundwater extraction. There have been several studies associated with the discovery of groundwater in the Sirt and Al Kufra Basins. However, there is still a lack of general knowledge on the origins, recharging zone, and the behavior of these aquifers. In order to predict the quantity of extractable water in the

aquifers, it is important to accurately determine the distribution of the aquifers within the strata in relation to stratigraphic and structural features.

The age of groundwater is a significant key for water resources, paleoclimate, waste management, and subsurface reactive transport (Sturchio et al. 2004). Therefore, one of the main objectives of this dissertation is to calculate the age of these fossil groundwaters by using different methods of isotopes. The stable isotopes and ^{14}C have been used before in these basins, however the ^{4}He chronometer to characterize the hydrogeology of the three aquifers system, such as the Post Miocene at Sarir, Tazerbo and Al Kufra, has not been established yet.

The main objectives of this study are:

- Estimate groundwater residence time in the all aquifers, and identify implications for regional recharge.
- Stable isotopes of water (^{18}O, ^{2}H), ^{3}H, ^{13}C, ^{14}C, and dissolved noble gases will be used together to calculate the groundwater recharge temperature, paleoclimate and to possibly provide important evidence of the changes in the aquifers due to water exstraction areas.
- Estimate values of crustal helium ($^{4}He_c$), mantle helium ($^{4}He_m$) in samples collected from all the aquifers to validate that the $^{4}He_c$ concentrations are representative estimates of the ^{4}He from in-situ radiogenic production.
- Estimate the helium flux for all aquifers.

1.4 Climate

Because of its location in an arid zone and the limited natural resources (water), Libya will be affected with climate change rapidly. According to Capot-Rey (1960), the Sarir Tibisti climate changed during the Quaternary based on the lake terrace found in Ouniange Kebir. Wendorf et al. (1976) stated that increasing precipitation around 7500 B.C. and 2500 B.C. followed by almost 3000 years of dry has left Libya with no surface water. Only the Mediterranean Sea plays an important role in modifying the climatic parameters temperature and moisture and only in the coastal zone, and its influence decreases gently southward to the Sahara. Therefore, the spatial pattern of annual temperatures over the country is mainly depending on latitude and elevation. Currently, the coastal cities have moderately temperatures while the south cites have high temperature.

The average annual temperature in Jalu (Figure 1.2) north of the Sarir wellfield is 23.2°C. Tazerbo has an annual average temperature of 23°C. Al Kufra has an annual average of 24°C. Average annual precipitation in Jalu is 9.3 mm, Tazerbo is 2.9 mm (Pallas 1981) and for Al Kufra is 1.3 mm (Pallas 1981). Farther to the south of Al Kufra, the annual precipitation is < 1 mm (Pachur 1996). Parts of the Tibesti Mountains to the southwest of Al Kufra receive over 30 mm of annual precipitation (Pachur 1996).

1.5 Previous Studies

Many scientists have studied the main aquifers in Libya and all have employed various methods to estimate the hydrogeologic character of these aquifers. Al Kufra and the Sirt Basins have generated much research and several estimates of groundwater reserves have been made.

Table 1.2. The annual temperature for the study area and some cities in Libya (Data source: Libyan Meteorological Department, Tripoli. Jaghboub and Jalu, (1950-2000).

Station	Latitude (N)	Elevation (m)	Summer (Jun.-Aug.) (°C)	Winter (Dec.-Feb.) (°C)	Annual (°C)	Precipitation (mm)
Al Kufra	24.13	436	30.8	14.2	23.3	2.1
Jalo	29.02	60	29.8	14.1	22.4	9.3
Agedabia	30.43	7	26.5	13.5	20.5	145.4
Benghazi	32.05	129	26.1	13.4	20.1	268.5
Tripoli	32.54	25	26.4	14.0	20.2	335.9

Some of the best known works include those of Wright and Edmunds (1971); Benifield and Wright (1980); Pallas (1981); Wright et al. (1982); Ahmad (1983); Swailem et al. (1983); Bellini and Masssa (1980); German Water Group (1977). The first groundwater study in the region was done by Ball (1927) who created a potentiometric surface map for what is now eastern Libya and western Egypt. Ball measured water levels in 30 wells over this large area and determined that the gradient of the potentiometric surface was generally to the northeast with local deviations around various oases. It was suggested that potential recharge to the Kufra Basin is from the Erdi highlands and Tibesti Mountains (Figure 1.1).

Later studies by Sandford (1935), Ezzat (1959), Gabert (1961) and Ahmad (1983) also came to the same conclusion. Pallas (1981) reviewed the previous studies of hydrogeology and water resources assessment in Libya.

Some of the flow to the north in the NAS of the Al Kufra Basin may continue into the Sirt Basin but this is not clearly established. Wright et al. (1982) showed that the potentiometric

surface in the northern part of the NAS in the Al Kufra Basin is somewhat continuous with the potentiometric surface in the Miocene aquifers in the Sirt Basin near Tazerbo, which may suggest a hydraulic connection across the basin boundaries. The NAS in the Sirt Basin is buried much deeper than in the Al Kufra Basin where it crops out at the surface. In the Sirt Basin, the NAS is confined under artesian conditions.

Groundwater models were created by Heinl and Brinkman (1989) and Gossel et al. (2004) for southeastern Libya, southwestern Egypt, and northern Chad and Sudan for the NAS of the Al Kufra Basin and the southern part of the Sirt Basin. These models, along with the work of Wright et al. (1982), suggest that there is north-northeast flow in the two aquifer systems, with flow in the NAS generally to the northeast.

The potentiometric surface maps indicate potential recharge zones for the NAS off the Tibesti Mountains and the highlands to the south in Chad and Sudan. In the Sirt Basin, the potentiometric surface in the post Oligocene aquifers shows that there may be some modern recharge around Al Haruj al Aswad to the west of Sarir. Edmunds and Wright (1979), Heinl and Brinkmann (1989), and Gossel et al. (2004) have all suggested that if there is modern recharge it is minor. There could be potential recharge to the Sirt Basin by underflow from the Al Kufra Basin through the deeper Cambrian sandstone. Numerical models mentioned above have suggested that the present recharge will be locally focused and that the current potentiometric surface formed during the past wet periods (e.g. Wright et al. 1982).

Burdon (1977) estimated storage for five basins beneath and adjacent to the Sahara to be about 60,000 km^3. Kehnde and Loehnert (1989) stated that the development of this fossil water which was recharged during the Quaternary fluvial period must be done with care; recent

recharge is relatively low or negligible. Detailed studies related to water chemistry, geology and hydrogeology description from surface and subsurface data has been carried out in these basins by Wright et al. (1982).

Comprehensive studies of water resources of the Al Kufra Basin have been done by German Water Group (1977). They believed that the aquifer at Al Kufra basin is strongly anisotropic due to lenticular beds of varying thickness and shape. Edmunds and Wright (1979) used stable and radio- isotopes to study the groundwater recharge history and paleoclimate of the Sirt and northern Al Kufra basins. They sampled wells for stable isotopes of water and ^{14}C. Their sampling included wells to the north of Sarir and near Al Kufra. Details of this study will be discussed below.

Recharge is speculated to be underflow from the south within the Nubian Sandstone and the Paleozoic aquifer systems into the Middle Miocene aquifer of Sarir. Several aspects are contrary to there being modern recharge. First, the region is currently hyper arid and the only area with any appreciable rainfall is the Tibesti Mountains. It is unlikely that the amount of precipitation is sufficient to overcome the high potential evapotranspiration rate (Pachur 1980) to provide recharge necessary to provide the inflow. Second, the geologic cross-sections beneath Kufra and Sirt basins suggest no obvious connections between the study aquifers in the south to that in the north. The Nubian Sandstone and the Tadrat Formation are not continuous into the Sirt Basin in the region around Tazerbo.

The Tadrat is separated from the overlying aquifers by confining layers, preventing or limiting potential flow from south to north. As a result it has been proposed that the observed hydraulic gradients in the region are fossil gradients established during the late Pleistocene and

early Holocene and that these gradients are slowly decaying away (e.g., Wright et al. 1982; Heinl and Brinkmann 1989; Gossel et al. 2004).

Pallas (1981) reviewed the previous studies of hydrogeology and water resources assessment in Libya. Ahmad (1983) studied the hydrological behavior of the Sarir well field by using analytical and numerical models, and concluded that there is a leaky artesian aquifer. Also, his steady-state model showed that there is an underflow entering the Al Kufra and Sarir aquifers from Tibesti, Chad and Sudan. Also, many recent research efforts took place after the GMRA started drilling water wells in Sarir, Tazerbo and Al Kufra.

Lloyd (1990) described the regional hydrogeology of the Nubian Sandstone aquifer system in eastern Libya, Sudan and Egypt and also the associated Tertiary aquifer of the Sirt Basin. Pim and Binsariti (1994) gave a general review of the geology of different areas of Libya and more details about the hydrogeological conditions in the main water wellfields in Sarir, Tazerbo, and Al Kufra. They estimated the volume of water in the aquifers by using different models and simulated drawdown from different well fields for the 50 years of life. Wheida and Verhoeven (2006) studied the water resources in Libya by describing the geographic location, population and climate to estimate the demands on groundwater by GMRA in the next 25 years. Wallin et al. (2005) recommended that isotopes can be used to garner information that is helpful in creating a long-term sustainable management plan for the Nubian aquifer.

Barr and Walker (1973) described how a canyon with a 396 m depth and a 5km wide cut into Miocene limestone north of the Sirt Basin contributed to the drainage basin known as the Sahabi River. This river was connected with lakes in the south, and it flowed to the north. During the early Pliocene subsidence took place at the Eastern area of Tibesti resulting in a lower level of the Al Kufra basin compared to the Sirt Basin (Griffin 2002, 2006).

From the early Lower Miocene to the Quaternary, tectonic activity took place in the Tibesti Volcanic Province (Furon, 1963; Gourgaud and Vincent, 2004; Geoniem et al., 2012). These resulted in a shift of the Sahabi River to the east toward the Al Kufra Basin. This has been supported by many other studies (e.g., Pachur 2000; McCauley et al. 1986). Ahmad and Goad (1978) reported that the KPP located on the paleoriver channels was recharged from the Tibesti Mountains. Pachur (1993) traced this channel from the Tibesti Mountains toward Al Kufra Basin for hundreds of kilometers. Regarding paleorecharge, Ghoneim et al. (2012) stated that there is a paleoriver discharge across the south and south east part of Libya, at Al Kufra Basin through the Sirt Basin to the Mediterranean Sea. The Al Kufra paleororiver had an extensive drainage area of about 235,500 km^2 and a length of 950 km. During the Neogene, this paleoriver formed the Sahabi River in the Sirt Basin. According to De Menocal et al. (2000) a wet period took place around 5.5 kyr ago. Runoff from the south of Sahara to the north and east of the Mediterranean Sea took place during the Miocene and Pliocene (Griffin 2002, 2006; Ghoneim et al. 2011; Paillou et al. 2012).

CHAPTER TWO

GEOLOGIC SETTING

2.1 Structural Geology

Libya is located on the northern part of the African shield, over a platform of cratonic basins. The Caledonian and Hercynian orogenies with other upheaval during the Cretaceous, Tertiary and Holocene time caused the major structural and tectonic features (uplifts, subsidence, folding, faulting, tilting and intrusions). Volcanic activity took place during the Alpine orogeny within deep seated fractures (Goudarzi 1978).

2.1.1 Al Kufra Basin

The Al Kufra Basin is a large, Palaeozoic intracratonic sag basin in SE Libya. The basin is surrounded by Jabal Az Zalmah to the north, Jabal Arknu and Jabal Al Awaynat to the east, Jabal Nugay to west, and the Borkou Massif and Ennedi Mountains to the south in Chad (Figure 1.1). The exposed sequence of Paleozoic rocks is well-preserved from Cambrian to Cretaceous time. The Northeast –Southwest trend in Al Kufra Basin is due to the Hercynian orogeny. The basin also is characterized by strike- slip faults trending northeast-southwest related to basement megashear (Bellini et al. 1991) and this shows indications of the late Pan-Africa orogeny NW-SE trend (Figure 2.1). During the Caradocian the area was affected by uplift and erosion that made some formations absent and some very thick. During the late Ordovician the basin received a thick sequence of glacio-marine sediments (Halett 2002).

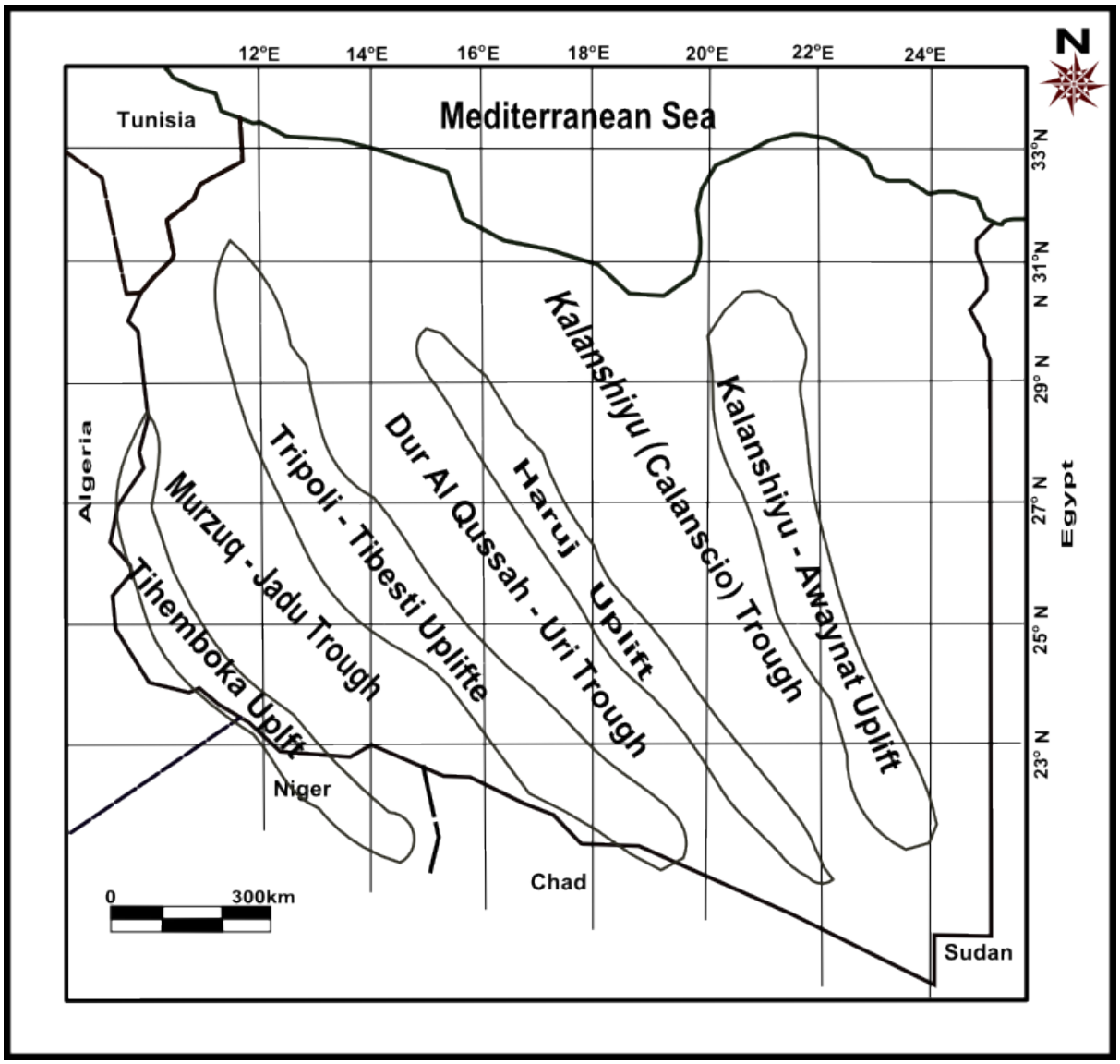

Figure 2.1. Pan-African structures that formed during late Precambrian to Late Carboniferous tectonism. Sources: Klitzsch (1971), Anketell (1996), and Hallett (2002).

According to Bellini and Massa (1980) and Klitzsch (1971) the Al Kufra Basin was affected by two tectonic cycles, the first in the Silurian resulted in a transgression with a northwest trend, According to Halett (2002) during the Carboniferous event the collision between the Gondwana and Luarasia formed the Tripoli – Tibisti Uplift, Haruj Uplift and Kalanshiyu Trough Halett (2002) (Figure 2.2). According to Lüning et al. (1999) the basin received sands of the Nubian sandstone during the Cretaceous due to major rifting related subsidence.

2.1.2 Sirt Basin

The Sirt Basin is located in central Libya and is bordered on the north by Mediterranean Sea, on the south and south east by Jabal Nugay and Jabal Dalma, and on the east by a basement high (Figure 1.1). The structural features of the Sirt Basin began in the late Precambrian by alternating periods of uplift and subsidence commencing with the Pan African orogeny (Kroner 1993). The main structure of the Sirt Basin is the result of rifting (horsts and grabens), which formed the configuration of the basin. This began to develop in the late Jurassic following a sequence of tectonic events that led to the breakup of the supercontinent Pangea (Gumati and Kanes 1985; Gumati and Nairn 1991; Van der Meer and Cloetingh 1993a, b; Baird et al. 1996; Schroter 1996) (Figure 2.1).

Uplift rises to 3000 m south of the Sirt Basin; much of the land area in the basin is characterized by desert steppes and includes eolian deposits of the Kalanshiyu and Rabyanah Sand Seas of the Sahara Desert. Rift of the Sarir Sandstone (equivalent to Nubian Sandstone) in the eastern part of the Sirt Basin region formed during the Middle and Late Jurassic and Early Cretaceous.

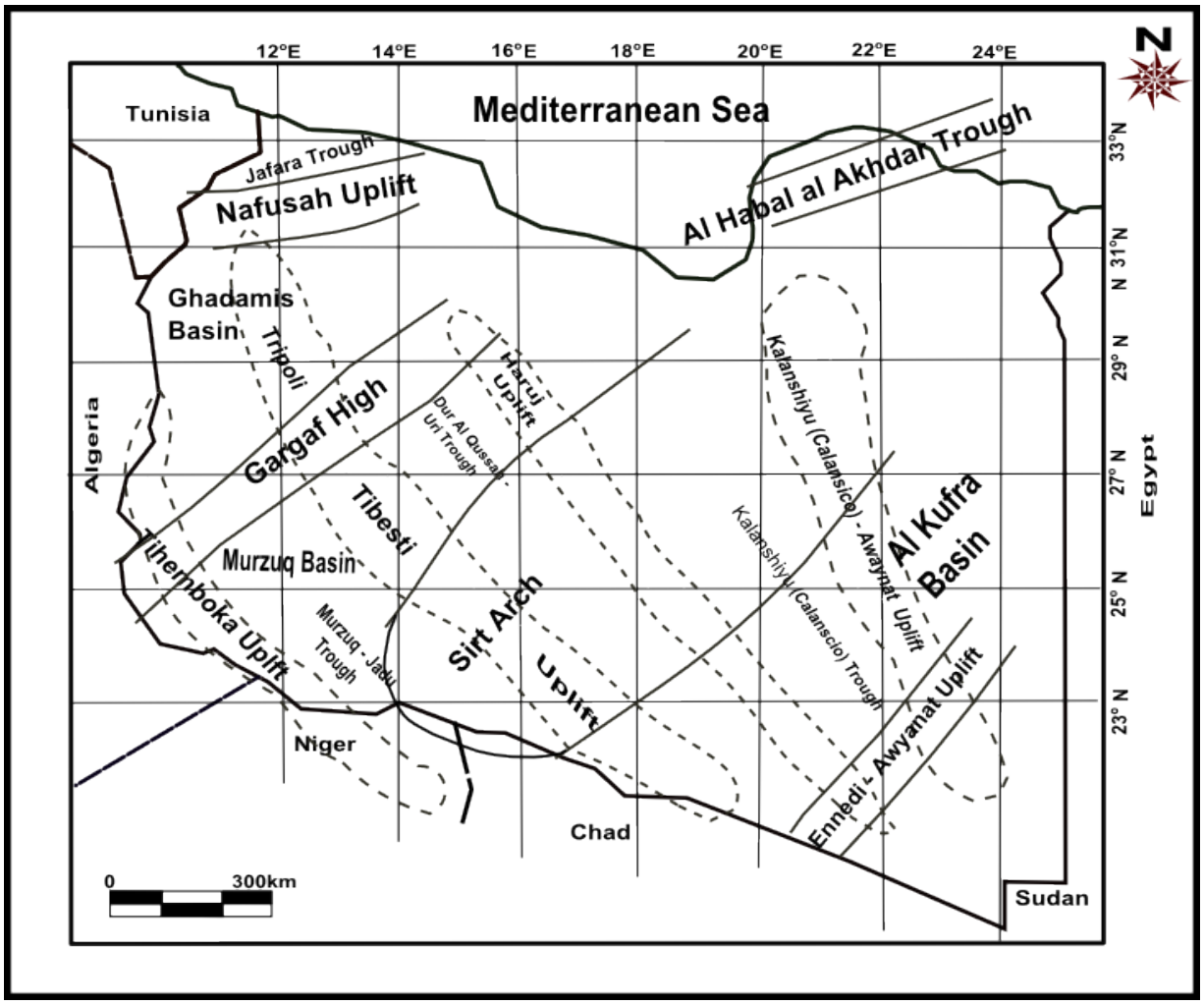

Figure 2.2. Hercynian structural trends caused by the Late Carboniferous collision between Gondwana and Laurasia. Sources: Klitzsch (1971), Anketell (1996), and Hallett (2002).

Rifting originated in the Early Cretaceous, continued through Late Cretaceous, and was completed by early Tertiary, resulting in a triple junction within the basin (Harding 1984; Gras and Thusu 1998; Ambrose 2000).

Figures 2.1 and 2.2 show the main five grabens in the Sirt Basin (Hun, Zallah, Maradah, Ajdabiya, and Hameimat) that separated the four major platforms (Waddan, Zahrah-Bayda, Zaltan, and Amal-Jalu). The general orientation of these structural features is north-northwest–south-southeast trending which persisted throughout the episodes of faulting during the Late Cretaceous and Palaeocene. During this period, a large thickness of shale and subordinate carbonates and evaporates accumulated in the troughs, while a considerably reduced thickness of dominantly shallow-marine carbonates were deposited on the platforms (Barr and Weegar 1972; Gumati and Kanes 1985; Baird et al. 1996). According to Burke and Dewey (1974) in the Early Cretaceous, the Sirt Basin was effected by extension forces along a weak zone formed by other rifts leading to the collapse of the preexisting Sirt arch. The early rifting phase corresponded with late rhyolitic and basaltic volcanism, of which granites have been dated to 152–122 Ma (Wilson and Guiraud 1998; Cahen et al. 1984).

Major basin subsidence (crustal extension, and reactivation of faults) from the northward to westward occurred in the Late Cretaceous thinning the cratonic lithosphere and fragmenting north Africa (Biju-Duval et al. 1977; Duncan 1981; Morgan 1981, 1983; Gumati and Kanes 1985; Gumati and Nairn 1991). During the Palaeocene–early Eocene, subsidence and extensional fault reactivation formed due to the relative motions of the American, African, and Eurasian plates, and the development of the Tethys on the foreland of the African plate (Anketell 1996). On the western Sirt Basin along the Hun graben, a major volcanic eruption started early Eocene to Pliocene (Wilson and Guiraud 1998). From the late Eocene until the Miocene, the Sirt Basin

begin filling with thick successions of post rift sediments. Recently, large parts of the Tertiary sequence have been eroded at the western part of the basin. Ade-Hall and Reynolds (1975) dated volcanic eruptions in Jabal As Sawda on the eastern part of the Sirt Basin to 10.5–12.3 Ma.

Another major volcanic eruption in Jabal al Haruj al Aswad in the southeast of the Sirt Basin dated to the late Pliocene (Ade-Hall et al. 1974).

2.2 Stratigraphy and Depositional History

2.2.1 Al Kufra Basin

The sedimentary succession of the Al Kufra basin was deposited on the sinking foreland between the ancient African cratonic shield and the Tethys belt (Klizch 1971). Metamorphic Precambrian basement is overlain by a very thick sequence of Cambro-Ordovician deposition. Outcrops of lower Paleozoic strata are restricted in Al Kufra Basin. Erosion surfaces separate the Cambrian (Hassaouns Formation) and the Upper Ordovician sediments (Memouniat Formation) from the time of the North Africa ice sheet (Bellini and Massa 1980). Paleozoic stratigraphy of Al Kufra Basin has been described by different scientists, e.g., Bellini and Massa (1980) ; Bellini et al. (1991); Burollet (1963); Turner (1980, 1991). The basin consists of shallow marine to fluvial deposits ranging in age from Precambrian to Cretaceous. Silurian marine transgression covers the southeast of the basin and constitutes a complete sedimentary cycle associated with a shallow marine environment (Akakus Formation) at the end of the cycle. During the Middle-Upper Devonian, a sequence of continental sediment formed (Tadrat Formation). The Carboniferous in the basin represented by the Dalam Formation with continental environment deposition after the Hercynian orogeny resulted in subsidence.

The sedimentary succession in the Al Kufra Basin can be subdivided into eight major stratigraphic units from Precambrian to Cretaceous (Lüning et al. 1999). Upper Neoproterozoic to lowermost Cambrian are undifferentiated; Cambro-Ordovician (Gargaf Group, consisting of Hassaouna, Melez Chogran and Memouniat formations); the lower Silurian Tanezzuft Formation, lower and upper Silurian (Akakus Formation), lower Devonian (Tadrat Formation), middle and upper Devonian (Binem Formation), Carboniferous (Dalma Formation) and the post-Hercynian Nubian Formation (Bellini and Massa 1980; Bellini et al. 199; Bezan 1991).

According to Bellini et al. (1991) and Turner (1980, 1991), the Al Kufra Basin was dominated by braided fluvial to shallow marine sandy facies with few marine shaly interlayers during the Cambrian and late Ordovician times when major glaciations affected large parts of North Africa. The Cambro-Ordovician succession was studied in Jebel Dalma, and north Jebel Asba. The unit is composed mainly of sandstones, fine to medium grain with some coarse, intercalations of conglomeratic beds. The sedimentary structures observed in the strata include wave and current ripples, gravel lenses, conglomeratic lag deposits, load casts and shale intraclasts (Lüning et al. 1999). Table (2.1) shows the general succession in the Kufra basin and (Figure 2.3) is a cross-section from the east to the west showing the major stratigraphic units.

2.2.2 Sirt Basin

The Mesozoic and Cenozoic sedimentary sequence in the Sirt Basin rests on a Precambrian basement and Cambrian–Ordovician clastic sediments. The Upper Cretaceous continental-marine rift consists of clastics followed by fine marine clastics and carbonates and concluding in the Paleocene and Eocene with carbonates and evaporates (Bellini et al. 1991).

Table 2.1. Shows summary of the stratigraphic section of Al Kufra Basin, showing the formation and tectonic events (Hallett 2002).

ERA	PERIOD	FORMATION	TECTONIC EVENT
CAINO-ZOIC			Mid Cainozoic uplift and erosion
MESO-ZOIC	CRETACEOUS	Nubian	Emergent, erosion and patchy continental deposition
	JURASSIC	'Continental Post Tessilien'	
	TRISSSIC		
PALAEOZOIC	PERMIAN		
	CARBON-IFERIOUS		Hercynian orogeny, uplift and erosion
		Zalmah	Conformable Dev. –Carb. contact
	DEVONIAN	Binem	Tectonically quiescent
		Tadrat	Intraplate sag basin
	SILURIAN	Akakus	Early Devonian hiatus
		Tanzuft	Liandoverain transgression
	ORDOVICIAN	Mamuniyat	Caradocian tectonism , emergent, erosion
		Milaz Shuqran	
		Hawaz	
		Ash Shabiyat	
	CAMBRIAN	Hasawnah	Passive margin sag basin
	INFRA CAMBRIAN		Extension, pull-apart basins
PRE-CAMB			Pan African orogeny

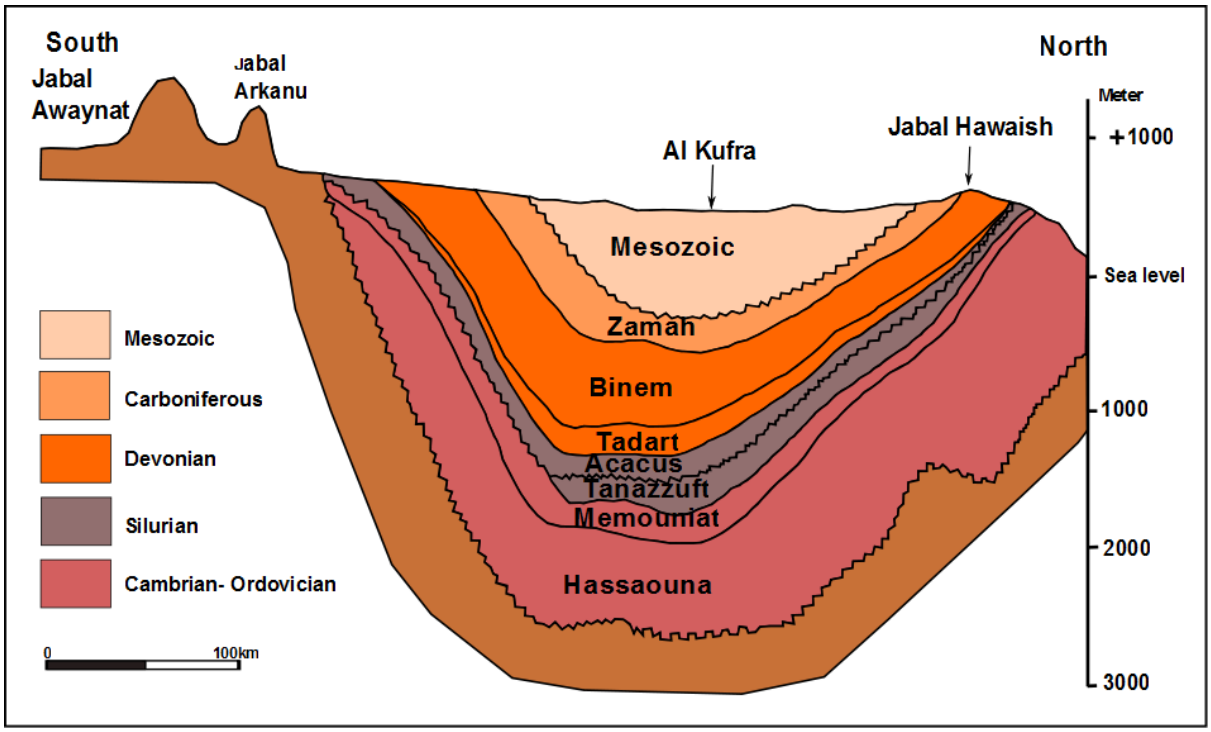

Figure 2.3. North-South cross section of Al Kufra Basin (Modified after Roohi 1996).

The basin was filled with upper Eocene to Miocene mixed carbonates and siliciclastic deposits followed by continental clastics. Sedimentary successions are characterized by cycles of transgressions and minor regressions, resulting in deposits of marine, transitional, and continental deposition.

During the first depositional period, mainly continental clastic sediments of pre-Late Cretaceous age formed. This cycle is commonly referred to as the Nubian, Sarir. In the northwest-southeast trending troughs, the sequence is shallow-marine grading into fluvial deposits in the southeast. According to Van Houten (1980); El-Hawat et al. (1996) during the Neocomian and Albian, basin deposition throughout north-eastern Africa was non-marine.

In the eastern Sirt Basin some authors have preferred to use terms such as Sarir Sandstone and Kalanshiyu (Calanscio) Sandstone to indicate late Jurassic to early Cretaceous continental clastics specific to this area. Nubian Formation is used in the sense of the non-marine sequences lying between the Taouratine Formation and the marine deposits of Cenomanian age. The Nubian Formation is widely distributed in the Sirt Basin. The formation consists of sandstones, very fine- to coarse-grained and poorly sorted, with a clay matrix (and quartzites), shale, sand, and conglomerate in some places. Sedimentary structures found in the sandstones include cross-bedding and ripple-marks. In general, the Nubian formation unconformably overlies basement Paleozoic, or Triassic-Jurassic graben fill sediments, and are overlain by the transgressive marine Cretaceous. According to Ambrose (2000), the Lower Sarir Sandstone, which rests on basement, represents early rift deposition and is typified by alluvial fans, conglomerates and braided plain deposits. According to Wennekers et al. (1996), the western part of Sirt Basin shows the presence of unsilicified Nubian rocks in both the Zallah and Abu Tumayam troughs, associated with possible lacustrine shales. The thickness of the Nubian rocks

in the Zallah Trough is 600 m, and in the Abu Tumayam Trough 450 m. During the Late Cretaceous, rifting began. Fine siliciclastic sediments were deposited in the troughs and shallow-marine carbonates prevailed on the highs (Bahi, Lidam, Etel, Rachmat, Sirt, and Kalash formations).

During the Upper Cretaceous, marine transgression took place resulting in the Bahi Formation which was deposited in shallow marine environment. The Lidam formation establishes the first marine unit in many parts of the basin and has a thickness of up to 600m in the troughs. The Etel formation is extensive across the central and southern Sirt Basin, where thickness in the troughs ranges from 660 m in the Hagfa trough to more than 700m in the Hameimat trough. The Sirt Shale is widely distributed throughout the grabens of the basin. Its thickness ranges from 500m to more than 700 m in the Zallah and Ajdabiya troughs, respectively (Bellini et al 1991). Khalash Limestone formed during the Maastrichtian, in shallow depositional environments. It occurs over most of the Sirt Basin and has a thickness of up to 600 m in the northern part of the Agedabia trough. In the Paleocene, rift evolution took place, and the basin deepened again with markedly thick (deep) marine deposition represented in the Hagfa Shale Member of the Khalifa formation and the Rabia Shale Member. Carbonate accumulated in the platform areas represented in the upper Satal, Defa, Beda, Dahra, and lower Sabil formations and the Thalith Member. According to Belazi (1989) the overlying Kheir formation (marine environment) widely developed throughout much of the Sirt Basin during the late Paleocene to early Eocene. During the early Eocene, large quantities of evaporites were deposited (Gir Formation; Hon evaporites) grading into the Mesdar Limestone. Throughout the middle and late Eocene, carbonate deposition again occurred (Gialo, Gedari, and Augila formations). According to Barr and Weegar (1972) the Oligocene succession of the Sirt Basin includes the Arida and

Diba formations. The Arida formation shows rapid changes in the lithology and environment of deposition, ranging from totally continental sandstone in the southeast to marine shale or carbonates in the north of the Basin. The Diba formation is characterized by shale intervals in the south-central basin. According to Belazi (1989), open-marine conditions took place during the middle Oligocene. Also, according to Bezan (1996) the Oligocene regression gave an increase to three major types of depositional environment represented by continental sandstone in the southeast, marine shales or carbonates in the north and northeast and marine-continental interface in west. During the Miocene, the west and southeast of the basin filled with fine to coarse-grained sands and sandstones while the northwest of the basin filled with mixed sedimentary successions. According to Benfield and Wright (1980) the carbonate and clay successions of the northeast clearly indicate marine shelf conditions. Table 2.2 shows the general succession in the Sirt basin and Figure 2.4 is a cross-section from the east to the west showing the major stratigraphic units.

Table 2.2. Summary of the stratigraphic section of the Sirt Basin, showing the distribution of major reservoirs and source rocks (Hallet 2002).

ERA	Period	Formation	Tectonic Events
CENOZOIC	Post Miocene		Maine regression continued subsidence Messinian sea level fall
	Miocene	Sahabi	
		Al Khums	Alpine orogeny, folding, tilting and warping
		Marada	
	Oligocene	Ma'zul Ninah	Coalescence of sag basins to form one large basin centered on the Ajdabiya Trough
	Eocene	Wadi Thamat	Subsidence in Hun Graben Wrenching in western Sirt Basin
		Al jir	
		Bishimah	Mid Eocene techtonism
	Paleocene	Shurfah	
		Zimam	Establishment of sag basins over site of earlier rifts
MESOZOIC	Upper Cretaceous	Algharbiyah	
		Mizdah	Slow subsidence within rifts Rifts gradually infilled
		Qasr Taghrinnah	Santonian compression Rapid subsidence within rifts
		Nalut	Cenominian transgression
		Sidi as Sid	Collapse of Sirt Arch, Formation of horsts and grabens. Subsidence in Hameimat Tough.
	Lower Cretaceous	Kiklah to Alguidr	
	Jurassic		Jurassic rifting and violence activity
	Triassic		Triassic wrenching and rifting
PALEO-ZOIC	Permian to Cambrian		Permian volcanic activity Hercynian orogeny. Formation of Sirt Arch Mid Devonian tectonism
pC			Panafrican orogeny

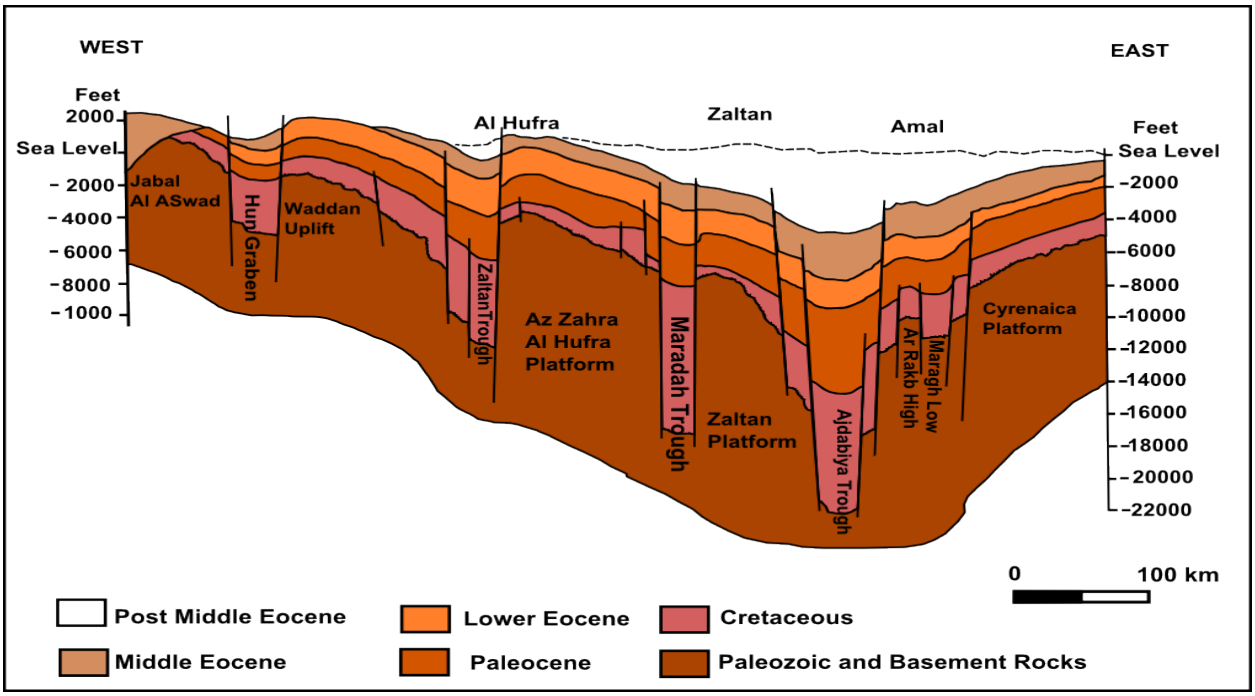

Figure 2.4. East-west cross-section of the Sirt Basin across the three major platforms: Az Zahrah–Al Hufrah, Zelten, and Amal (modified after Roohi 1996).

CHAPTER THREE

HYDROGEOLOGIC SETTING

The area of study has two regional aquifer systems, the Tertiary system of the Sirt basin (Post-Eocene aquifer) where the Sarir wellfield is located, and the Nubian system of Al Kufra basin where the Tazerbo and Al Kufra wellfields are located.

3.1 Sarir Wellfied

The Sarir wellfield is located in the southern part of the Sirt Basin and has been in operation since 1991. In the Sirt Basin, the aquifer consists of a thick deposit of Eocene clays and limestones with continental deposits of sand interbed with some clay and limestone at the north of the basin as a result of the Late of Cretaceous subsidence of the Sirt Basin (Pim and Binsariti 1994). The thickness of Post Eocene reaches up to 1600 m. The wellfield has two aquifers systems: a shallow unconfined aquifer of Post Middle Miocene age, with depth to water table from 80 m in the west part of the wellfield to about 60m in the east part of wellfield. And a deep confined-semi-artesian aquifer of Middle Miocene age, composed of multilayered sand, silt, shale, siltstone, and clay (Table 3.1). However, from the analysis of core and cutting samples, the aquifer consists mainly of silica (Table 3.2). The water flows in the Sirt basin system generally flows from S to N and finally touches the Mediterranean and the Jebel Akhdar area and discharges into coastal and inland sabkhats extending from the Gulf of Sirt to the Qattra Depression in the east (Wright et al. 1982), and probably forms the Sahabi channel. Pumping from the deep aquifer is fully balanced by vertical leakage from the shallow aquifer resulting in an effectively unconfined condition after a short period (Pim and Bensrity 1994).

Table 3.1. Lithological description of the main aquifer in Sarir wellfield (well 222; source: GMRA data).

Depth (m)		Description
From	To	
217	222	SAND, very pale orange, medium grained, subangular to subrounded, well sorted
222	225	SAND, very pale orange, medium to coarse, subangular to subrounded, well sorted. Traces of Clay greenish gray
225	228	SAND, very pale orange, coarse to very coarse, some quartz grains at granule size subangular to subrounded, well sorted, Traces of Clay greenish gray, Traces of siltstone grayish orange
228	231	SAND, very pale orange, coarse to very coarse, some quartz grains at granule size subrounded to rounded, moderately sorted, Some Clay light brown greenish gray, Traces of calcareous sandstone yellowish gray
231	234	SAND, very pale orange, fine grained subangular to subrounded, well sorted, Traces of Clay light brown
234	240	CLAYEY SAND grayish orange (fine grained sand)
240	261	SAND, very pale orange, fine to medium subangular to subrounded, moderately sorted.
261	264	CLAY and SAND, Clay yellowish gray to light brown plastic. Sand grayish orange coarse to very coarse subangular to subrounded, poorly sorted.
264	267	CLAYEY SAND grayish orange.
267	273	CLAY grayish orange.
273	276	CLAYEY SAND grayish orange fine to medium grained
276	279	SAND, very pale orange, medium to coarse, subangular to subrounded, well sorted.
279	282	CLAY and SAND, Clay light brown plastic. Sand grayish orange coarse to very coarse subangular to subrounded, well sorted
282	285	SAND, very pale orange, medium to coarse, subangular to subrounded, well sorted.
285	339	SAND, very pale orange, medium to coarse, subrounded to rounded, well sorted. Traces of Clay light brown
339	345	SAND&GRAVEL SAND very pale orange, coarse to very coarse, subrounded to rounded, poor sorted. GRAVEL to granule size. CLAY dark yellowish orange and grayish orange, plastic, some.
345	396	SAND, very pale orange, fine to medium, subrounded to rounded, well sorted. CLAY dark yellowish orange and grayish orange, plastic, traces.
396	400	CLAY dark yellowish orange, plastic.

Table 3.2. Well depth, and aquifers geochemistry analysis results for Tazerbo (well 401), Sarir (well 309A), and Al Kufra (surface sample).

Aquifer	Depth (m)	Analytic Symbol	SiO2	Al2O3	Fe2O3(T)	MnO	MgO	CaO	Na2O	K2O	TiO2	P2O5	LOI	Total
		Unit Symbol	%	%	%	%	%	%	%	%	%	%	%	%
Tazerbo	120-165	S-1	65.94	6.64	15.27	0.591	0.69	0.41	0.14	1.26	0.426	0.19	8.05	99.59
	165-219	S-2	83.38	6.97	3.62	0.137	0.18	0.22	0.12	0.19	0.333	0.05	4.1	99.28
	219-264	S-3	71.97	6.1	12.72	1.229	0.37	0.17	0.12	0.59	0.582	0.11	6.87	100.8
	264-309	S-4	61.33	4.23	25.09	1.266	0.18	0.21	0.12	0.22	0.506	0.13	7.12	100.4
	309-354	S-5	62.44	3.63	25.89	0.343	0.09	0.31	0.12	0.1	0.348	0.2	5.52	98.99
	354-399	S-6	58	7.65	26.55	0.093	0.08	0.42	0.14	0.12	0.726	0.22	6.23	100.2
	399-441	S-7 (aquifer)	94.98	1.39	2.05	0.02	0.05	0.88	0.08	0.04	0.17	0.03	1.27	101
	441-480	S-8 (aquifer)	96.97	1.53	1.28	0.002	0.03	0.16	0.09	0.02	0.15	0.01	0.59	100.8
Sarir	216-252	S-9	96.04	0.9	0.79	0.018	0.26	0.57	0.07	0.16	0.092	0.02	0.81	99.73
	252-294	S-10	94.23	1.48	1.22	0.049	0.66	0.97	0.09	0.24	0.134	0.05	1.85	101
	294-330	S-11	98.52	0.55	0.72	0.007	0.11	0.18	0.05	0.12	0.055	0.03	0.2	100.5
	333-360	S-12	97.12	0.65	0.73	0.007	0.05	0.05	0.1	0.17	0.055	< 0.01	0.21	99.14
	363-390	S-13	97.56	0.67	0.72	0.013	0.18	0.25	0.11	0.2	0.049	0.02	0.32	100.1
Al Kufra	one sample from surface	S-14	96.27	1.87	0.34	0.005	0.02	0.23	0.02	0.02	0.436	0.02	0.87	100.1

The Sarir wellfield consists of 126 production wells plus 48 new wells with a capacity of 100 l/s in order to reach the designed capacity of wellfield of 1 million cubic meters per day. The wells are arranged into three parallel lines, with 1.3km distance between each well and with 10km distance between each line and 28 piezometer wells between and surrounding these production wells (Figure 3.1).

The depth to the main aquifer is around 220 m and the aquifer thickness is around 250m through continental and some marine sediments. However, the depths of the wells were set at 450 m. At the present, the yield of the wellfield is 200,000 cubic meter per day. Transmissivity had been estimated based on recent long-term pumping tests and it is between 4.63×10^{-03} to 0.0694 m^2/s, and storativity has been calculated and it is between 2.1×10^{-04} to 3.77×10^{-04}. The aquifer has a good water quality with TDS varying between 587 to 980 mg/l.

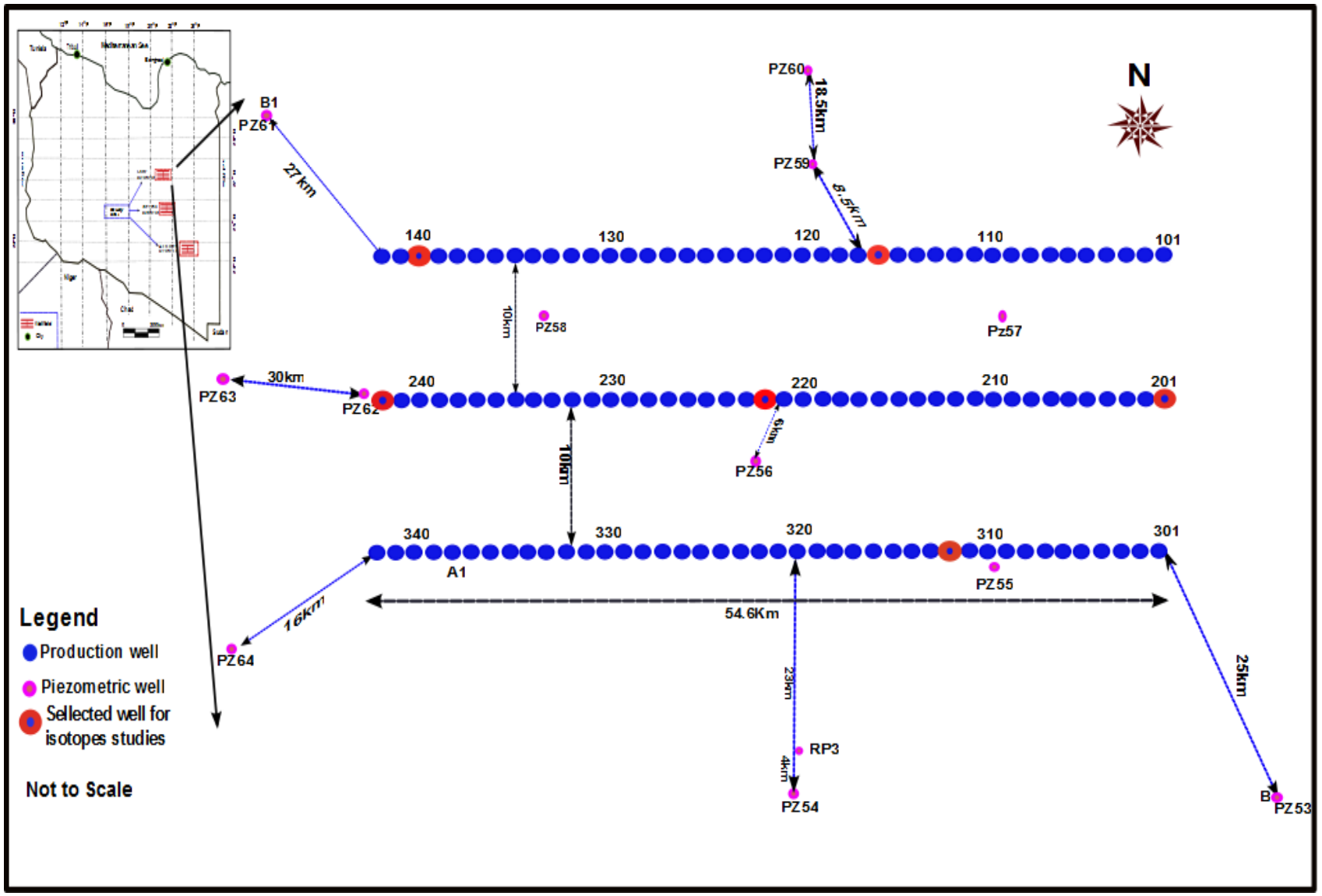

Figure 3.1 shows the Sarir wellfield design and the selected wells for this study.

3.2 Al Kufra Wellfield

The Al Kufra Basin has two aquifer systems, the Nubian Aquifer system (NAS) and the post Nubian aquifer system (PNAS). The Nubian Aquifer System is an aquifer shared by the countries of Northeast Africa and underlies an area of more than 2.2 million km^2. The NAS consists of the Paleozoic and the Mesozoic deposits and overlies the Pre-Cambrian basement complex. The PNAS occurs at the north part of the basin overlying the NAS and consists of the Tertiary continental deposits. Al Kufra Basin has two giant wellfields for the GMRA, Tazerbo and Al Kufra wellfields. According to Ahmed and Edibb (1975) the north and southwest of Al Kufra aquifer have low permeability boundaries and important fault and joint tectonics possibly affecting the hydrogeology of the area. However, according to Occidental (1970) the Al Kufra basin consists of one aquifer with discontinuous impermeable zones.

The Al Kufra aquifer is anisotropic due to interbedding of fine sediments that occur within the discontinuous lenticular beds in the Nubian Formation that make the vertical transmissivity lower than the horizontal (Tipton and Kalambach 1972). The lithological logs at Al Kufra sites show that the aquifer is highly stratified with numerous siltstone and claystone beds separating the more permeable sandstone units (Figure 3.2). Based on hydrogeological data and groundwater modeling received from the GMRA, the Upper Triassic-Early Cretaceous aquifer in the Al Kufra Basin can be subdivided into two aquifers. The upper part of the aquifer cited as shallow aquifer is composed of unconsolidated sandstone, highly interlayerd by claystone and siltstone. The lower part of the aquifer has much fewer lenticular sediments and was cited as the deep aquifer.

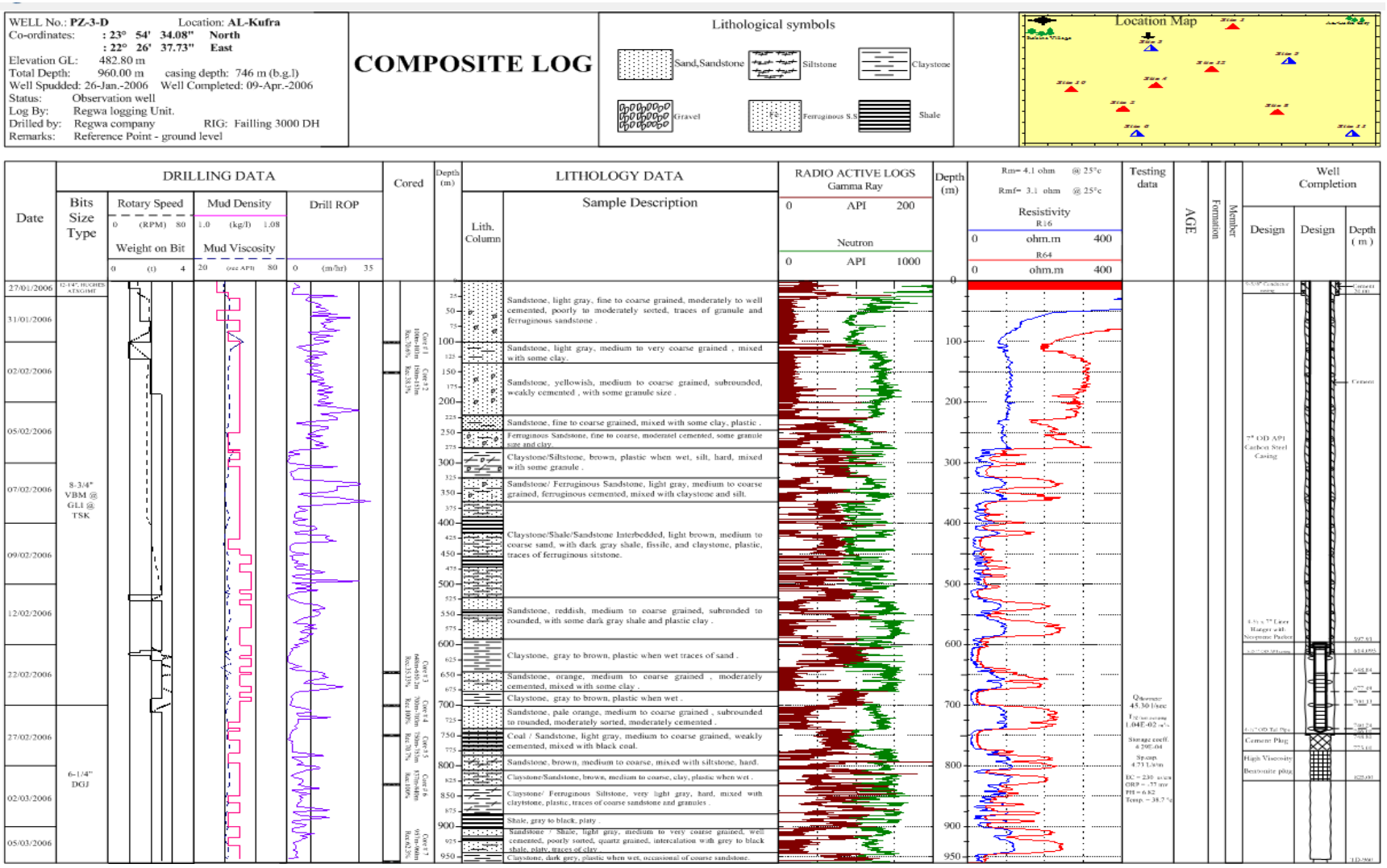

Figure 3.2. Shows the lithological log of Al Kufra aquifer that is highly stratified with numerous siltstone and claystone (source: GMRA data).

Table (3.3) shows the description of the whole sequence of the deep aquifer. However, from the analysis of core and cutting samples, the aquifer consists mainly of silica (Table 3.2).

Eddib (1973) postulated the existence of an aquifer consisting of clay with its top occurring at depths of between 70 – 130 m, in the Al Kufra area acting as an aquiclude to separate the shallow aquifer from the deep aquifer. Ahmed and Eddip (1975) came to the same conclusion. Comparing our new well log and drilling data and the new geophysics well log interpretation along with hydraulic consideration of the old information of KPP and KSP lead us to the conclusion that the existence of the aquiclude cannot be confirmed.

The Al Kufra wellfield with 300 production wells is under construction. However, 10 exploratory wells and 26 piezometric wells have been completed (Figure 3.3). As we said, the Al Kufra area has another water project, Kufra Productive Project (KPP), which was started in 1972, and it is located at the northern part of the Al Kufra basin. The formation of the basin in this area (KPP) consists of continental fluvial deposits of lenticular layers. Variation in lithology horizontally and vertically makes the permeability different from one place to another. The upper part of the aquifer is sand (700 m) above series of clay layers that separate the shallow and deep aquifers.

Transmissivity has been estimated based on the recent long-term pumping tests that took place in 2004 to 2008 and it is between 0.07090 – 0.0284 (m^2/s) while the storativity of GMRA wellfield has been calculated and it is between 4.85×10-05 – 2.21×10-05. The aquifer has a good water quality with TDS varying between 98 to 538 mg/l.

Table 3.3. The description of the whole sequence of the Al Kufra aquifer (source: GMRA data).

Depth (m)	Description
154-168	SANDSTONE; yellowish white coarse grained sand subrounded to subangular well sorted.
168-180	SANDSTONE / SILTSTONE; pale brown medium to coarse grained with bluish gray siltstone fragments.
180- 182	SANDSTONE / SHALE; yellowish brown medium to coarse grained subrounded to subangular moderately sorted. Brownish gray mudstone fragments.
182-212	SANDSTONE; whitish yellow medium to coarse grained subrounded to subangular well sorted
212-225	SILTSTONE / SANDSTONE; brownish gray micaceous fragments moderately hard. Sandstone yellowish brown fine to medium grained, poorly sorted.
225-250	SANDSTONE; yellowish brown medium to coarse grained subrounded to subangular moderately sorted. With minor traces of siltstone bluish gray fragments.
250 -303	SANDSTONE; light brownish yellow coarse grained subrounded to subangular well sorted with traces of black iron oxids.
303 -314	SANDSTONE / SILTSTONE; pale brownish gray medium to coarse grained subrounded to subangular poorly sorted weakly cemented quartz grains mixed with siltstone fragments light gray to pale yellowish gray, moderately hard, micaceous.
314-340	SANDSTONE / SILTSTONE; light olive yellowish coarse grained subrounded to subangular moderately sorted with brownish gray siltstone, micaceous moderately hard.
340-349	SILTSTONE / SANDSTONE; pinkish brown to gray, fragments micaceous moderately hard mixed with brownish gray mudstone fragments.
349-350	SANDSTONE / SILTSTONE; light yellow medium to coarse grained subangular to subrounded poorly sorted. Siltstone pale brown fragments moderately hard.
350-377	SANDSTONE; whitish yellow coarse grained subrounded to subangular, well sorted, weakly cemented quartz grains.
398-410	CLAYSTONE / SILTSTONE; pinkish brown,. Light bluish gray siltstone fragments, moderately hard, slitly micaceous.
410-430	GRAVELS / SILTSTONE; whitish yellow to pink, with pinkish to white fragments siltstone. With black fragments of iron oxides.
430-448	SANDSTONE / SILTSTONE; yellowish brown coarse grain, subangular to subrounded moderately sorted. Pink micaceous fragments moderately hard.
448-450	FERRUGINOUS SANDSTONE; reddish brown, subangular to subrounded, ferruginous cemented moderately sorted.
450-465	CLAYSTONE; grayish brown, moderately hard.
465-467	CLAYSTONE / BLACK ORGANIC MATERIALS; dark gray to black, plastic. With organic material.
467-469	COAL CLAYSTONE; black, massive fragments mixed with dark gray to black organic play.
469-470	CLAYSTONE; gray to dark gray, with traces of siltston.
470-519	FERRUGINOUS CLAYSTONE; dark grayish brown, plastic, iron oxides.
519-529	CLAY SANDYSILT STONE ; reddish brown ferruginous mixed with reddish clay silt, iron oxides.
529-550	CLAYSTONE; dark brown, plastic, with iron oxides.

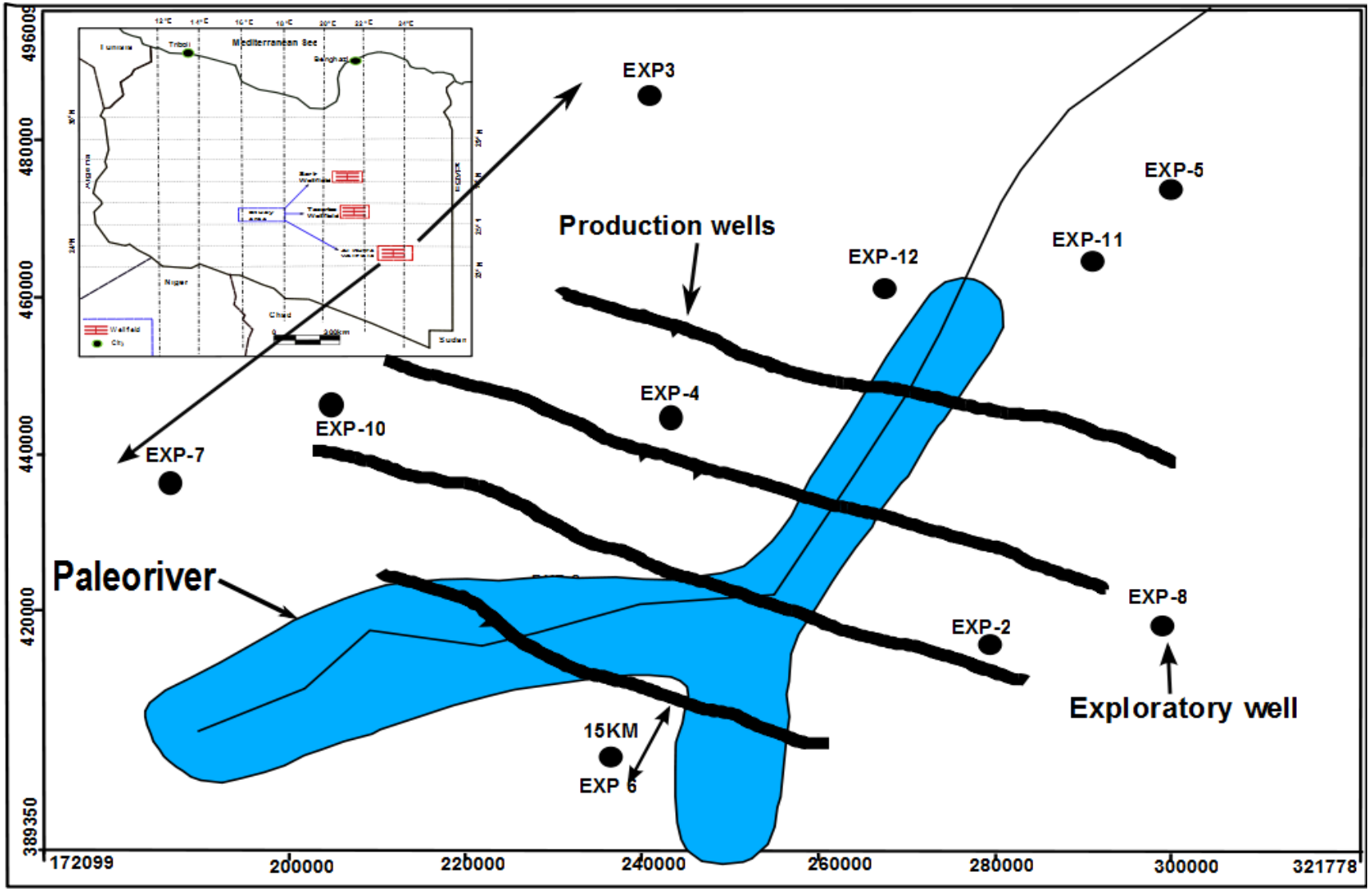

Figure 3.3. Shows the Al Kufra proposed wellfield design and the selected wells.

3.3 Tazerbo Wellfield

The Tazerbo wellfield is located in the northern edge of the Al Kufra Basin, above the SW- NE alignment of the south flank of Hercynian uplift that was transected by the Caledonian movements (Wright et al. 1982). The whole sedimentary sequence within the wellfield, reaching up to 800 m thickness, is of Lower Devonian age, mainly consisting of marginal marine deposits (Pim and Bensrity 1994).

Three aquifers have been identified in the south (shallow, intermediate and deep) with relatively uniform and extensive layering and separated by thick aquitards. The deep/main aquifer is the target of The GMRA. It is truncated in the north by Eocene clays, and is a 100-120 m thick horizon of well-sorted, medium-grained, poorly cemented sands (Table 3.4), which are formed at 280 m depth in the north-west and at 500 m depth in the south-east of the southern aquifer (Tazerbo and Al Kufra). Analysis of core and cutting samples, the aquifer consists mainly of silica (Table 3.2). The aquifer dips at an angle of 2-3^{o} to the south-east. Aquitards lying above and beneath the main aquifer consist of shale, fine grained argillaceous, ferruginous sandstones with mudstone interbeds (Pim and Binsariti 1994) (Table 3.2). The depth to water is variable from one site to another, from 260 m in the NE and NW to 400 m in the SE and SW.

The wellfiled consist of 108 high capacity production water well at 100 l/s of each well and surrounding by twenty one piezometers for monitoring the static water level and for estimation of the transmissivity and storage coefficient in the deep, intermediate and shallow aquifers (Figure 3.4).

The capacity of the wellfield was designed to yield 1 million cubic meter per day; however, at the present the yield of the wellfield is 490000 cubic meter per day.

Table 3.4. The description of the whole sequence of the Tazerbo aquifer (source: GMRA data).

Depth (m)	Description	
404.28-438	SANDSTONE, dark yellowish orange, fine to medium grained, rounded to subrounded, well sorted, weakly cemented, quartz grained, clayey.	MAIN AQUIFER
438-441	SANDSTONE with SILTSTONE interbeds, pale yellowish brown sandstone, fine grained, rounded to subrounded, well sorted,weakly cemented, with dusky brown siltstone interbeds, very soft.	
441-456	SANDSTONE, grayish orange pink, fine to medium grained, rounded to subrounded, well sorted, weakly cemented quartz grained. Traces of light gray shale chips, thinly laminated.	
456-459	SANDSTONE, grayish red, coarse to medium grained, subrounded to subangular, well sorted, weakly cemented quartz grained, clayey.	
459-462	SANDSTONE, grayish brown, coarse to medium grained, subangular to subrounded, well sorted, weakly cemented. Traces of light gray to dusky red shale chips.	
462-471	SANDSTONE with SILTSTONE interbeds, dark grayish red to dark reddish brown sandstone, fine to medium grained, subrounded to rounded, well sorted, weakly cemented, with dusky brown siltstone interbeds, very soft.	
471-474	SANDSTONE, dark grayish red, fine to medium grained, subrounded to rounded, well sorted, weakly cemented. Traces of dusky brown silt stone.	
474-477	SANDSTONE with SILTSTONE ineterbeds, blackish red sandstone, fine to medium grained, subrounded to rounded, well sorted, weakly cemented, with dusky brown to black siltstone interbeds, very soft.	
477-486	SANDSTONE with SHALE interbeds, pale red sandstone, fine to medium grained, subrounded to rounded, well sorted,weakly cemented, with light red to dusky red shale chips interbeds, thinly laminated.	MAIN AQUIFER
486-495	SANDSTONE, grayish orange pink, fine to medium grained, subrounded to rounded, well sorted, weakly cemented quartz grained, slightly clayey.	
495-501	SANDSTONE, grayish red, fine to medium grained, subrounded to rounded, well sorted, weakly cemented, clayey.	
501-507	SANDSTONE, pale gray to grayish pink, fine to medium grained, subrounded to rounded, well sorted, weakly cemented quartz grained, slightly clayey.	
507-519	SANDSTONE with SHALE interbeds, grayish orange pink sandstone, fine to medium grained, subrounded to subangular, well sorted, weakly cemented, with light gray shale chips, thinly laminated.	
519-537	SANDSTONE, grayish orange pink, fine to medium grained, subrounded to rounded, well sorted, weakly cemented, slightly clayey.	
537-543	SANDSTONE, dark reddish brown, fine to medium grained, subrounded to subangular, well sorted, moderately cemented. Traces of silica cemented black iron oxides.	
543-552	SANDSTONE, grayish orange pink, fine to medium grained, subrounded to subangular, well sorted, weakly cemented quartz grained, clayey.	
552-561	SANDSTONE, dark reddish brown, fine to medium grained, subrounded to subangular, well sorted, weakly cemented quartz grained, clayey.	
561-564	SANDSTONE, grayish orange pink, fine to medium grained, subrounded to rounded, well sorted, weakly cemented. Traces of light gray shale chips.	
564-570	SANDSTONE with SILTSTONE and SHALE interbeds, grayish orange pink sandstone, fine to medium grained, subrounded to rounded, moderately sorted, weakly cemented with dusky brown to black siltstone and reddish purple shale chips interbed, moderately hard.	
570-573	SANDSTONE, pale greenish yellow, fine to medium grained, subrounded to rounded, well sorted, weakly cemented quartz grained. Traces of light gray shale chips.	
573-578.25	SANDSTONE, grayish orange pink, fine to medium grained, subrounded to rounded, well sorted, weakly cemented. Traces of light gray shale chips, thinly laminated.	

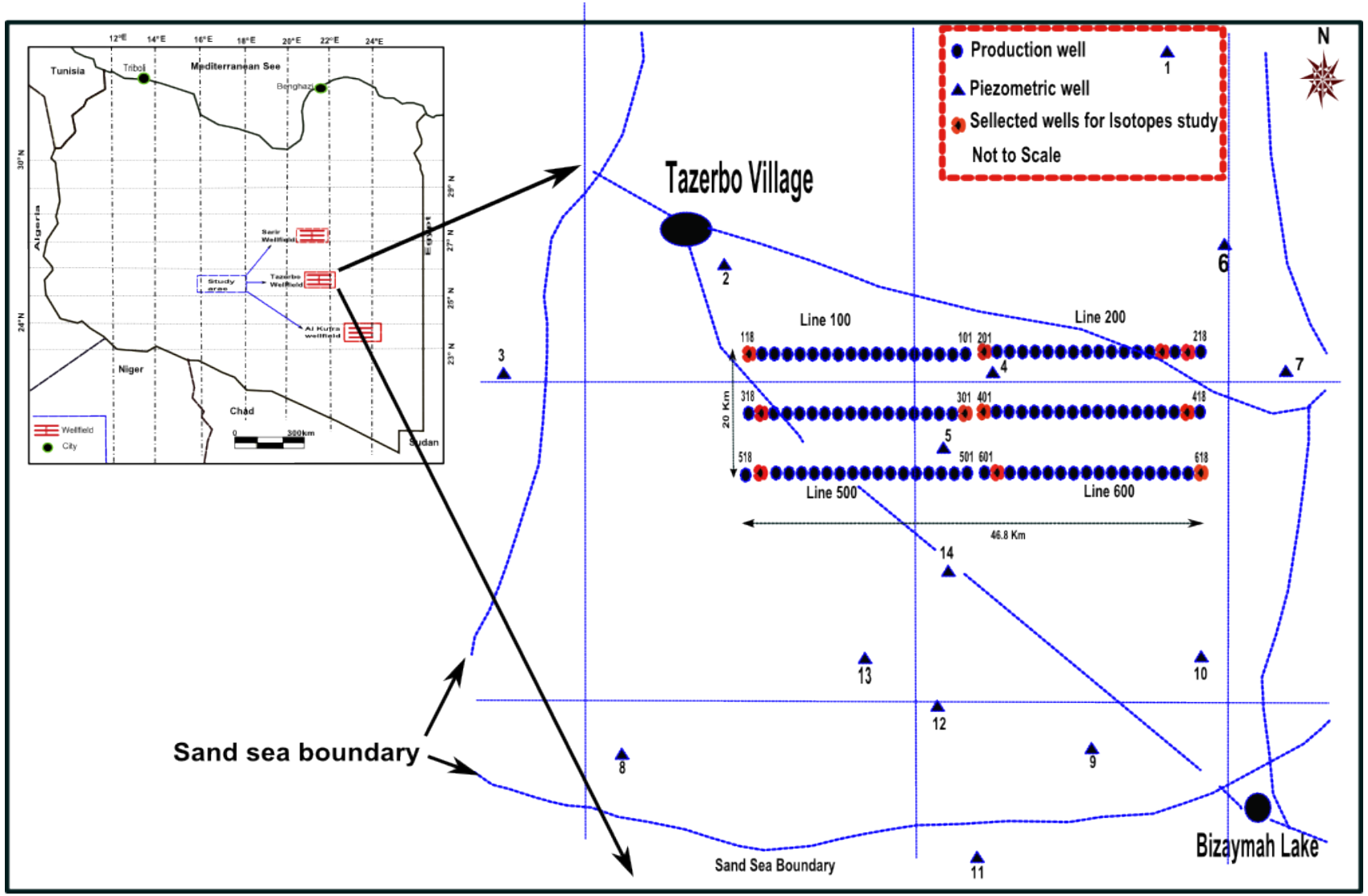

Figure 3.4. Shows the Tazerbo wellfield design and the selected wells for this study.

Based on our geophysical data and previous studies, the upper 500 m represent the aquifer with $10^{12}m^3$ of reserves water which is large enough for a long project life under good groundwater management. Transmissivity had been estimated based on the recent long-term pumping tests is between 3.71×10^{-02} to 7.92×10^{-03} m^2/s, and the storativity is between 2.1×-04^{-3} to 0.77×10^{-04}. The aquifer has a good water quality with TDS varying between 212 to 266 mg/l.

The groundwater flow in the Al Kufra and Tazerbo wellfields (Al Kufra Basin) trend from south to north-northeast as many other previous studies have concluded (e.g. Eddib 1973; Eskangi et al. 1975).

3.4 Recharge Area

The Sirt and Al Kufra Basins have been studied since the early 20^{th} century in order to determine the original source and recharge area of these groundwaters, which were the main target for many scientists; however, some of them believed that the Al Kufra basin is recharging, while others believed no recharge happened since the water formed in these basins. For example, Ball (1927); Sandford (1935); Ezzat (1959); Gabert (1961) believed that the Al Kufra basin is recharging by rainfall at high elevation regions from the Erdi area and Tibesti mountains (Ahmad, 1983). On the other hand, Murray (1952); Hellstrome (1940); Edmunds and Wright (1979); Swailem et al., (1983); believed that there is no current recharge or that any recharge is negligible in these aquifers.

Regardless, GMRA has been pumping water from the Sarir wellfield since 1991, the Tazerbo wellfield since 2004 and the Al Kufra will be in the near future with a total capacity 1.6

MCM/D. However, the Al Kufra aquifer has been pumping from agriculture projects since 1972 as well as for the Al Kufra settlement.

Now the ground water table is decreasing and the Al Kufra oasis is drying. Pumping of 1.6 MCM/D from the AL Kufra aquifer will definitely decrease the water table. Today, the Al Kufra and Sirt Basins receive no recharge or negligible recharge, which means the basin is slowly depleting because of the long period of high pumping that took place 40 years ago from the KPP, KSP and Sarir agriculture projects and we saw this fact in the Al Kufra oasis and Bezzima oasis (near Tazerbo wellfield) in 2010 during our field work. However, according to some previous studies, these aquifers could receive some recharge from the Tibesti and the highlands west of the Al Kufra Basin.

CHAPTER FOUR

SAMPLE COLLECTION AND METHODS

Groundwater age can be predicted in many ways, for example, by measurements of time-dependent abundances of natural isotopic tracers (Sturchio et al. 2004). In order to predict the quantity of extractable water in the aquifers, it is important to accurately determine the distribution of the aquifers in relation to stratigraphic and structural features.

Numerous radiotracers have been used to estimate the residence time of elements in groundwater. Noble gases and ^{14}C are the most applicable for dating groundwater. Carbon isotopes for example require application of a model to convert ^{14}C concentrations into ages but significant error is possible. In addition, ^{14}C can only be applied for groundwater younger than 40 kyr old. Chlorine 36 has been applied over a time scale of millions of years (Bentley et al. 1984; Torgersen et al. 1991). Another method to date groundwater is by using radiogenic ^{4}He (Marin et al. 1979; Torgersen 1980; Andrews 1983; Marty et al. 1988; Ballentine and Hall 1999; Aeschbach-Hertig et al. 1999, 2000). In this study, Noble gases (N_2, Ar, Ne, Kr, Xe, He), ^{14}C, ^{18}O, ^{2}H will be applied to all groundwater samples.

4.1 Data Collection

Over 100 water and rock samples were collected from three deep confined and semi-confined aquifers. The samples were collected from the wellfields in a rattem to be representative of the system. The water samples were collected from production wells after sufficient water was pumped out to the collected pipe. The first samples were collected from the Sarir wellfield of the Sirt basin during our our field work in October 2010.

The wellfield has started pumping water in 1991. The water wells are screened almost 170 m in the deep aquifer, and 18 inch (457.2 mm) stainless steel casings were installed from the surface to the top of the main aquifer. Submersible pumps were installed at the same depth of the water table. The samples were selected based on the wellfield design and the distribution of wells (Figure 2.4) to represent the whole aquifer area. The same methodology was applied to the Tazerbo and Al Kufra wellfield. Although Tazerbo well field has the same well design and well distribution within the wellfield (Figure 2.8), they are different in depth and formations. Also some samples from Tazerbo well field were collected from artesian wells (TZ 517, TZ 217, TZ 218, and TZ 518). Al Kufra wellfield samples were collected from shallow and deep wells; the deep wells have been pumping since 1971, while the shallow wellfield was drilled in 2004.

The data are:

- Field chemical measurements of pH, water temperature (^{o}C), and specific conductance (SC).
- Alkalinity measurements had been determined at the GMRA Laboratory in Sarir, Tazerbo, and Al the Kufra wellfield (Figure 3.1b).
- Water samples for isotopic analyses (^{18}O, ^{2}H, ^{3}H, ^{14}C) and dissolved noble gases will be used to estimate the residence time (age) of groundwater, to determine groundwater fluxes and paleotemperature, and to estimate recharge rates.
- Core and rock cuttings: Determination of rock mineralogy and whole rock chemistry are necessary to understand water-rock interactions and to determine the uranium/thorium content that is needed to determine the production rate of ^{4}He (See chapter 6).

Another dataset was used for the description of the wellfield and for some calculation of some hydrogeological parameters:

- Well data: construction/completion information, geophysical logs and hydraulic heads. This information was used for identifying the stratigraphy and structural trends, delineation of aquitards and aquifers and to develop potentiometric surfaces.
- Well production information and results of pumping tests to estimate hydraulic conductivity and transmissivity.

4.2 Stable Isotopes

Stable isotope samples ($\delta^{18}O$, $\delta^{2}H$) were collected from each wellfield in 50 ml bottles with tight closures. The samples were sent to the University of Wyoming Lab. Deuterium (^{2}H) and oxygen-18 (^{18}O) contents are expressed as δ values in parts per thousand (‰) relative to the International Standard, VSMOW (Viena Standard Mean Ocean Water), and the analytical uncertainties of the individual measurements are better than 0.1‰ for $\delta^{18}O$ and 1‰ for δD.

4.3 Radioactive Carbon Isotopes

Samples for carbon isotopes (^{13}C and ^{14}C) were collected in 1 liter plastic bottles instead of glass because the glass bottles are susceptible to breakage during the transportation from Libya to the USA (Figure 3.1). Carbon Isotope samples were sent to Beta Analytic Inc., Miami, Florida and the analysis was performed on the DIC within the submitted waters, and determined by mass spectrometry. The age of ^{14}C was corrected by using the model of Fontes and Garnier (1979).

(a)

(b)

(c)

Figure 4.1. Sample Collection Photographs, Tazerbo production artesian well a) tritum sample, b) ^{14}C sample from Al Kufra water well, c).

Both $^{13}C/^{12}C$ and $^{14}C/^{12}C$ ratios were measured at Beta Analytic Inc., Miami, Florida by conventional and accelerator mass spectrometry, respectively. ^{13}C results are reported as δ values relative to the VPDB (Vienna Pee Bee Belmenite) standard and have an overall precision of ± 0.3 ‰. ^{14}C results are normalized to the NBS OX-1 standard, corrected for background and isotopic fractionation using the measured $\delta^{13}C$ values, and reported as percent modern carbon (pmc). The analytical precision of the AMS ^{14}C results is ± 0.7% and the background corresponds to a conventional ^{14}C age of 45 kyr or = 0.4 pmc (Roberts et al. 1997). In view of the uncertainties related to sample preparation we adopt an overall uncertainty of ± 1 % of the given value or at least ±0.4 pmc.

4.4 Noble Gases

Noble gas samples were collected in copper tubes, about 60 cm in length with 1 cm diameter that were connected to transparent plastic tubes with valve to control the volume of water (Figure 4.2). The pressure of the water flushing into the tubes was controlled to avoid bubbles and once the plastic tubes became free of bubbles, stainless steel pinch off clamps were applied to each end of the tubes. Clamps were placed on the tubing about 1 to 2 inch from the ends. Jigs were used to set clamp positioning and the tubing was centered in the clamp. The clamps were tightened with alternating hex nuts. The two halves of the clamp were brought together exactly. A gap of almost 1mm was observed when tightening the clamps to prevent the user from over tightening (Figure 4.2). Care was also taken to avoid damaging or deforming the tube ends.

a

b

C

Figure 4.2. Noble gas samples were collected in copper tubes connected to transparent plastic tubes, a), water flushing into the tube was controlled to avoid bubbles, b), clamps were placed on the end of the tube, c).

Absolute concentrations were determined with a precision of 1 % and 2 % for the heavier noble gases (Ne, Ar, Kr, and Xe) and He, respectively. In order to estimate recharge temperatures, noble gas concentrations needed to be corrected for excess air.

In these calculations, the salinity effect on noble gas concentrations was not explicitly calculated because the salinity of the water was low (< 500 ppm), and the salinity effect is negligible. Noble gases samples were taken to the University of Utah's, Department of Geology and Geophysics, Noble Gas Laboratory Utah. Noble gas recharge temperature, and excess air, and ^{4}He terrigenic were calculated by using the Andrew Manning (2009) model.

4.5 Tritium Samples

Although glass bottles are preferred for tritium collection (^{3}H), they could break during collection or transportation. However, 1 liter factory fresh plastic bottles were used for sample collection. All bottles were filled to the top and trapped; air was minimized prior to the lids being applied. The analytical precision as well as the detection limit of the tritium measurements was approximately ± 0.1 TU (tritium units, 1 TU is equivalent to a $^{3}H/^{1}H$ ratio of 10^{-18}, which represents one atom of tritium in 101 atoms of hydrogen).

Tritium contents were measured at the Utah Laboratories by converting water into methane gas and subsequently counting, after an enrichment step, with a counter having a low-level background and a sensitivity of 1 TU. Tritium, which is reported in tritium units (TU), was measured by ^{3}He accumulation method where the samples were vacuum degassed and shelved for 60 days to allow for the growth of ^{3}He from tritium decay.

4.6 Whole Rock and Trace Element Analysis

Samples of aquifer material were collected from all three sites and sent to Activation Laboratories LTD in Ontario Canada, for whole rock and trace element analyses. The purpose of the analyses were to determine if there are significant carbonates in the rock which will affect the age calculation using ^{14}C and to determine the uranium, lithium, and thorium content that is needed to determine the subsurface production of ^{4}He and ^{3}He, which is needed to estimate the age of the water and to determine the potential contribution of mantle ^{4}He to the terrigenic ^{4}He component (See chapter 6). The sample numbers, aquifers and sample depths are shown in table (3.2).

CHAPTER FIVE

STABLE AND CARBON ISOTOPES

5.1 Stable Isotopes

A mass spectrometer was used to measure the ratio of the rare isotope to the common isotope ($^{2}H/^{1}H$ and $^{18}O/^{16}O$) instead measure the concentration of ^{2}H and ^{18}O individually. The variations in many isotopic abundances are relatively small, therefore, stable isotope ratios are reported relative to a standard as δ values in units of parts per thousand (per mil, and written as ‰). Values for water are reported relative to VSMOW (Vienna Standard Mean Ocean Water). A stable isotope has a general expression:

$$\delta_s = \left(\frac{R_s}{R_{std}} - 1\right) \times 1000 \qquad (5.1)$$

where R_s and R_{std} are $^{2}H/^{1}H$ or $^{18}O/^{16}O$ of the sample and standard, respectively. When δ has a negative value means the sample is depleted in the heavy isotope relative to the standard and it is isotopically light relative to the standard isotope.

The relationship between $\delta^{2}H$ and $\delta^{18}O$ in precipitation worldwide is called the global meteoric water line (GMWL) and is represented by Craig (1961). The hydrogen and oxygen isotopic compositions of precipitation samples have direct relationship.

$$\delta^{2}H = 8\delta^{18}O + 10 \qquad (5.2)$$

Evaporation from surface water is a nonequilibrium process that augments the residual water such that the $\delta^{2}H/\delta^{18}O$ slope is below the GMWL (Coplen 2000). This slope is a function of temperature, salt concentration, and humidity (Gat 1981).

5.1.1 Stable Isotopic Data Results and Discussion

The stable isotope compositions of the three aquifers studied differ from one another (Table 5.1). The δD and $\delta^{18}O$ data show two different groups as shown in Figure 5.1. The Sarir wellfield samples have a stable isotope composition of δD ranging from -76.7 to -69.4 ‰ and $\delta^{18}O$ ranging from -9.9 to -8.7 ‰, while the stable isotope composition of the Al Kufra wellfield are depleted relative to Sarir, δD from -85.7 to -82.3 ‰ and $\delta^{18}O$ from -11.6 to -11.2 ‰, and the corresponding values for the Tazerbo wellfield that are the most depleted are δD from -86.5 to -81.9 ‰ and $\delta^{18}O$ from -12 to -11.5 ‰, as shown in table (5.2) .The five samples from Sarir are the most enriched and plot below the Global Meteoric Water Line (GMWL) (Figure 5.1). The nine samples from Tazerbo are depleted relative to those at Sarir and plot on the GMWL. The three samples from the Kufra aquifers (shallow and deep) plot just below the GMWL, near the composition of those from Tazerbo (Figure 5.1) suggesting that the waters have experienced some evaporation.

Figure (5.1) also shows the intercept and the trends of the meteoric lines that indicate these waters were light isotopically and the climate was cooler than the present. Of course, some samples will not follow these two groups because they could be mixtures of young and old groundwater.

Acording to Edmunds and Wright (1979) the pluvial period during the late Pleistocene and Holocene is the source of groundwater in the Sirt and the Al Kufra Basins, and these rains had been driven from the south. On the other hand, Swaliem at el (1983) said that the source of these groundwaters is the pluvial period but were came from the east (Atlantic Ocean). The result of this study agree that this water is fossil water, and the age could be late Pleistocene and Holocene.

Table 5.1. Stable Isotope Compositions in per mil

Location	Well (ID)	$\delta^{2}H$	$\delta^{18}O$
Al Kufra	41	-84.7	-11.5
Al Kufra	85	-84.8	-11.4
Al Kufra	RGWA	-83.2	-11.3
Sarir	116	-74.3	-9.4
Sarir	140	-72.2	-9.0
Sarir	222	-69.4	-8.7
Sarir	242	-75.9	-9.7
Sarir	312	-76.7	-9.9
Tazerbo	118	-86.3	-12.1
Tazerbo	201	-84.9	-11.8
Tazerbo	217	-83.0	-11.8
Tazerbo	317	-86.5	-12.0
Tazerbo	401	-86.2	-12.0
Tazerbo	417	-82.1	-11.6
Tazerbo	517	-86.0	-11.9
Tazerbo	602	-84.7	-11.9
Tazerbo	618	-81.9	-11.5

It is clearly seen that the compositions of the three aquifers are quite depleted relative to that of modern precipitation (e.g. Tunis $\delta^{18}O$ = -3.5 ‰, and δD = -20.6 ‰; Faya-Largeav $\delta^{18}O$ = -1.9 ‰, and δD = -22.8 ‰; IAEA GNP). In general, all values are similar to those reported from the same areas by Edmunds and Wright (1979). Groundwaters from the Nubian sandstone at Al Kufra have a uniform isotopic composition $\delta^{18}O$ = -11.5 ‰, δD = -82 ‰, and lie close to the meteoric line. The compositions seen in all groundwaters are significantly lower than those expected to be found in modern precipitation. Edmunds (2009) suggests that this is evidence of Late Pleistocene recharge from Atlantic rainfall that was modified as it passed over the Sahara region (see section on 14-Carbon as to estimated age of groundwater).

During Pleistocene times the Sirt and Al Kufra Basins were several degrees cooler than during Holocene times, therefore $\delta^{2}H$ and $\delta^{18}O$ of groundwaters recharged during Pleistocene times should be more negative than those of groundwaters recharged during Holocene times.

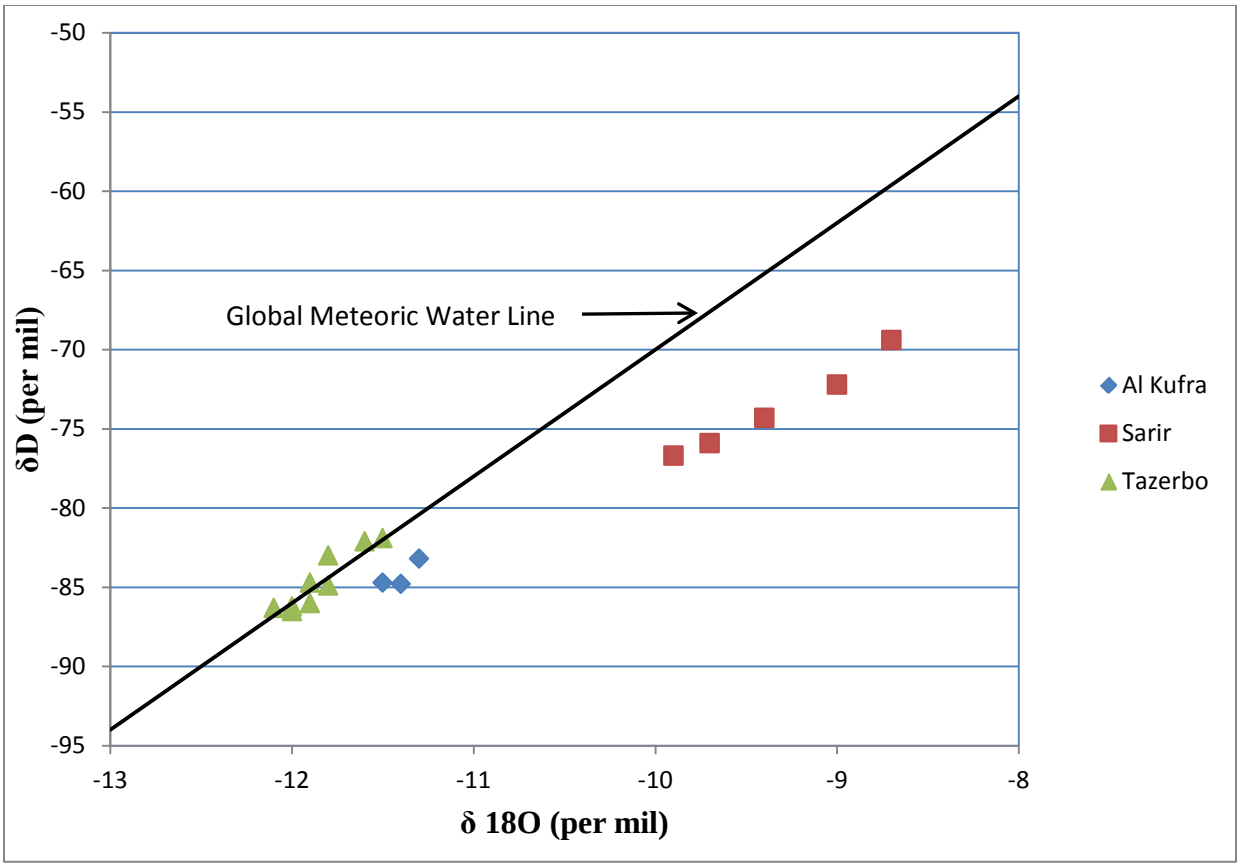

Figure 5.1. Stable isotope compositions from this study compared to the Global Meteoric Water Line.

5.2 Carbon Isotopes

The ^{14}C radio isotope has been used extensively for environmental studies.^{14}C age calculations for groundwater are based on the assumption that the initial activity of the CO_2 is 100 % modern carbon (100 pmc) (Fontes and Garnier 1979).

The main sources of the dissolved carbon in groundwater are: (1) active carbon from the soil zone, from carbon dioxide of soil gases and solid carbonate from the soil, and (2) less active carbon of inorganic origin, formed during the production of the bicarbonate. Moreover, dissolved CO_2 or carbonate is depending on the pH (Fontes and Garnier 1979).

$$CO_2 + H_2O + MeCO_3 \leftrightarrows Me(HCO_3)_2 \qquad (5.3)$$

where Me is generally Ca^{2+} or Mg^{2+} or $2Na^{+}$.

The time (t) elapsed in aquifers by ^{14}C is given by the general law of radioactive decay (Fontes and Garnier 1979):

$$t = \frac{\tau}{\ln 2} \times \ln \frac{A_0}{A_t} \qquad (5.4)$$

where τ is the half-life of ^{14}C in time units equal to 5730 ± 30 years (Godwin 1962); A_0 is the specific activity at time equal to zero and generally it is referred to as the ^{14}C content of the atmospheric CO_2 (percent modern carbone,pmc); A_t is the specific activity of sample (pmc).

Different models can be used to calculate (A_0), for example, Vogel 1967, 1970 and Vogel and Ehhalt 1963; Tamers 1967, 1975 and Tamers and Scharpensee (l970); Ingerson and Pearson (1964), Pearson and Hanshaw 1970, Pearson et al. 1972 and Pearson and Swarzenki 1974; Mook 1972, 1976.

In this study we used the Fontes and Garnier (1979) model to estimation of the initial activity of the total dissolved ^{14}C and then corrected the groundwater age. Fontes and Garnier (1979) model is based on chemical concepts for approximating amounts of inactive and active carbon, and on an isotopic reaction to estimate further exchange within the aquifer.

The field measurement of pH is very important here since it allows one to calculate the ^{14}C-bearing aqueous carbon. The active carbon content in groundwater samples was calculated indirectly from knowledge of the inorganic and total dissolved carbon contents. The inorganic carbon was assumed to be released into the solution when alkaline-earth carbonates are dissolved, and its concentration will be equal to the molality of $Ca^{2+} + Mg^{2+}$.

The total alkalinity of a groundwater sample is given by its total strong acid equivalent (Fontes and Garnier 1979) :

$$mH^+ \cong 2mCO_3^{2-} + mHCO_3^- \qquad (5.5)$$

where m denotes molal concentration.

Therefore, the inorganic carbon molality, as given by the ionic balance of major ions, is equal to half of the carbonate alkalinity. On the other hand, the less active or dead carbon content can be calculated from the ionic balance expression as:

$$mC_M = mCa^{2+} + mMg^{2+} - mSO_4^{2-} + \frac{1}{2}(mNa^+ + mK^+ - mCl^- - mNO_3^-) \quad (5.6)$$

where

$$mC_M = \frac{2mCO_3^{2-} + mHCO_3^-}{2} \qquad (5.7)$$

and mC_M is the molal concentration of carbon of inorganic origin.

And the initial activity of the total dissolved carbon can be calculated (Fontes and Garnier 1979) as:

$$A_0 = \left(1 - \frac{C_M}{C_T}\right) A_g + \frac{C_M}{C_T} A_M + \left(A_g - 0.2\epsilon - A_M\right) . \frac{\delta_T - (C_M/C_T)\delta_M - [1-(C_M/C_T)]\delta_g}{\delta_g - \epsilon - \delta_M} \quad (5.8)$$

where:

- C_T, the molal concentration of the total dissolved inorganic carbon, is the sum of the dissolved carbonate, bicarbonate, and CO_2 (= H_2CO_3).

- C_M, the molal concentration of the dissolved carbon coming from solid carbonates, is calculated from the chemical model (5.7) or from half of the carbonate alkalinity measured in the field.

- δ_T is measured.

- δ_M can be measured (or assumed to be near zero in the case of marine carbonates).

- δ_g can be adjusted according to the literature.

- A_g is generally taken as 100 % of modern carbon (if the waters do not contain tritium and can be considered free of 'bomb' ^{14}C
- A_M is generally taken as 0 % of modern carbon (less or dead carbon) but should be measured, as pointed out by Geyh (1970, 1972);
- ϵ isotopic enrichment factor (per mil) at equilibrium between gaseous CO_2 and solid carbonate and it is calculated at the temperature of the aquifer from the values given by Deines et al. (1974). Generally it is assumed that $\epsilon\ ^{14}C\ \% = 0.2\ \epsilon\ ^{13}C\ ‰$
- T, M, and g are total, solid, and gaseous carbon, respectively.

5.2.1 Isotopic Reactions

Isotope fractionating is formed by a series of chemical reactions as shown in equations below and every single compound will exchange with the other coexisting carbon species:

$$CO_2\,(gas) \leftrightarrows CO_2\,(aqueous)$$
$$CO_2\,(aqueous) \leftrightarrows HCO_3^-$$
$$H\,CO3^- \leftrightarrows CO3^-$$
$$CO_3^{2-} \leftrightarrows \text{solid carbonate}$$

Equilibrium for each compound may not be completed because of the differences in reaction rates and large variations in the relative amounts of coexisting carbon species. Considering the multistage reactions of the different carbon-bearing compounds as a simple two-term exchange- mixing process were took place in these equations. The end-members of this mixing process are the soil CO_2, and the solid carbonate of the soil and of the aquifer (Fontes and Garnier 1979).

5.2.2 Carbon Isotope Results

In this study, we calculate the age of groundwater from three wellfields representing two sedimentary basins by using ^{14}C activities and $\delta^{13}C$ of dissolved inorganic carbon (DIC), and by noble gases in Ch. (6).

The ^{14}C activities and $\delta^{13}C$ values were determined on ten groundwater samples from the three sites: the locations of these samples are indicated in Figures 3.1, 3.3, and 3.4. Results are presented in Table 5.2. ^{13}C analyses are reported as δ values relative to the PDB standard and ^{14}C abundances are reported as percent modern carbon (pmc) (table 5.2). The estimated age of the groundwater was determined using the method of Fontes and Garnier (1979).

Table 5.2. ^{14}C activities and values of field-measured parameters.

Sample No.	Temp. °C	pH	Conductance (µS/cm)	Alkalinity (mg/l)	$\delta^{13}C$ (‰)	^{14}C (pmc*)	^{14}C Age (yr)
KF85	29.2	6.4	220	36	-14.3	5.27	20500
KFRGA	25	6.8	560	49	-26.3	32.49	12000
SR116	32.3	7.5	1340	221	-8.8	6.30	15200
SR242	31.7	7.4	2100	187	-25.7	41.42	9800
SR312	32.1	7.3	1750	190	-19.7	26.89	10800
TZ 118	29.6	6.7	290	100	-9.9	1.88	26000
TZ217	27.9	6.8	340	152	-9.4	1.51	27500
TZ401	31.8	6.8	310	119	-9.5	2.29	24100
TZ517	31.3	6.5	280	102	-9.3	2.39	23500
TZ618	29.9	7.2	350	148	-9.2	2.44	23400
*Percent Modern Carbon							

5.2.3 Radiocarbon Data Interpretation and Discussion

^{14}C concentration and $^{14}C/^{12}C$ ratios were converted into groundwater ages and corrected base on Fontes and Garnier (1979) (Table 5.2).

The result of ^{14}C analysis of groundwater samples from the three aquifers have $\delta\ ^{13}C$ values ranging from -23.94 ‰ from a shallow well at the Al Kufra wellfield to -10.379 ‰ from a deep well; the ^{14}C values range from 32.5 pmc at the shallow well to 5.3 pmc at the deep well. The Tazerbo wellfield has $\delta\ ^{13}C$ values range from -8.2 ‰ to -5.99 ‰, and ^{14}C ranging from 1.9 to 2.4 pmc.

The three extraction wells that were sampled from Sarir wellfield show a relatively large spread of values of carbon isotopes (Table 5.2). For all three wells water is being drawn from the same depths. Pim and Bensrity (1994) stated that the aquifer at Sarir is leaky and receives water from the overlying aquifer. This leakage would allow younger water from the overlying aquifer to mix with the older deeper water.

Though there is a large range of carbon isotope values, the field parameters and alkalinity values are similar in all three wells. The relationship we see here is that samples with lower percent modern carbon (pmc) are more enriched in ^{13}C.

The results of ^{14}C analysis shows that the north part of the wellfield has older groundwater than the south part with a 5 ka difference. This could be the result of groundwater flow which is from the south to the north. The values of $\delta^{13}C$ and ^{14}C at Sarir exhibit ranges from -25.7 ‰ to -8.8 ‰ and 5.27 pmc to 41.4 pmc, respectively. These numbers are close to the previous study (e.g. Edmunds and Wright, 1979).

Based on the Fontes and Garnier (1979) analyses, the ages of these samples range from 9.8 kyr to 15.2 kyr and there does not appear to be any spatial trend in the data.

At Tazerbo wellfield, five extraction wells were sampled for carbon isotope analyses (Table 5.2). The values of $\delta^{13}C$ and ^{14}C activity are similar for all wells as are all the field parameters and alkalinities. The $\delta^{13}C$ values range from -8.20 to -5.99 ‰. The age of the water averages 25 kyr over a depth range of 150 m. The uniformity of all water quality parameters and ages over this depth range suggests that there is no leakage into the Tadrat Formation due to pumping. There is a trend in the data where the age of the groundwater is younger in the south and older in the north. The age is corresponding to the late Pleistocene.

There are no data upgradient of the potentiometric surface to determine groundwater flow rates. Pachur (1996), Pachur and Hoelzmann (2000), and Al Ramly (1980) have identified paleolakes and drainages from the Tibesti Mountains and the surrounding Sarir Tibesti. Pachur (1980) and Ghoneim at el. (2012) have identified paleodrainages that are directed from the Tibesti Mountains directly toward the Tazerbo area. These features could possibly provide the necessary pathways for recharge to the Tadrat formation.

In the Al Kufra area there were two wells sampled for carbon isotopes (Table 5.2). These wells are located approximately 100 km apart and are at two different depths. KF85 is one of the extraction wells as part of the KPP, has a depth of 300 m and has been in operation for nearly 40 years. KFRGA is a shallow well with a depth of 30 m and was originally installed as a piezometer. It currently is used as a water supply well for a small field camp. KF85 has a lower ^{14}C activity and is enriched in $\delta^{13}C$ compared to KFRGA. All field parameters and alkalinity values are similar at each location. The apparent age at KFRGA is 12 kyr and at KF85 it is 21 kyr. The shallow sample age is of early Holocene while that of the deep well is late Pleistocene.

The late Pleistocene age of the well for the KPP is consistent with the Edmunds and Wright (1979). However their data show the percent modern carbon values to be lower than those of our sample. Therefore, it is likely that the continued pumping from the KPP is beginning to extract water of a younger age as the influence of pumping has expanded, yet the stable isotope values are still the same. Pachur (1996), Robinson et al. (2006), Griffen (2006) and Ghoneim et al (2012) have identified paleodrainages that extend from the Tibesti Mountains, Chad and northern Sudan to the north. Some of these drainages have been traced for over 950 km. These large drainages were probably formed during the late Miocene wet periods and were subsequently intermittently active in the Pleistocene and early Holocene. Spaced-based radar data have been used to identify a major drainage (Kufra River) that at one time flowed directly towards the present day Al Kufra oasis. This drainage continued to the north and at one time connected with the Sahabi River and drained to the Mediterranean Sea. El Ramly (1980) discusses the evidence of lakes and swamps surrounding Tibesti Mountains during the Holocene and a Pleistocene lake around Al Kufra. These drainages could possible supply the source of water for extended widespread recharge periods during the Pleistocene and short periods of more localized recharge during the Holocene.

In general, the oldest ages are from the Tazerbo well field, which is using water from the Devonian-age aquifer that is confined. In Al Kufra it is interpreted at this time that the wide range of ages is due to the fact that the KFRGA well is shallower than KF85 and hence samples groundwater of a younger age. It is recommended that samples be collected from deeper wells around the Al Kufra as the well field planned for the area will extract water from deeper depths than that sampled at the RGWA well.

The variable nature of groundwater ages at the Sarir wellfield may be due to the fact of the extensive pumping from the main aquifer that is resulting in the addition of groundwater from overlying aquifers with younger water. In Figure (5.2) plots the $\delta^{18}O$ values against the percent of modern carbon for the wells in which there are both sets of data. The graph also contains data from Edmunds (2009) for comparison. Our results are similar to those of Edmunds (2009), and it can be seen that the lighter values of $\delta^{18}O$ are associated with older water (as shown by percent modern carbon (pmc) – lower pmc indicates older water). This comparison suggests that the waters in Tazerbo were recharged during the Late Pleistocene (see section on stable isotopes).

In brief, it is highly likely that the ages represent various amounts of mixing of younger shallower water with deeper older water. This suggests that water from the late Pleistocene is mixing with shallow water recharged during the Holocene. Several researchers have found evidence of paleodrainages that cross through the area around Sarir. North of Sarir, Edmunds and Wright (1979) identified a channel of fresh water which they attribute to recharge along a former wadi line. The age of this water is put at 5000 – 8000 ybp, which generally corresponds to wet periods during the early Holocene. Pachur (1980) has traced a paleodrainage for over several hundred kilometers from Al Haruj al Aswad located to the west towards the Sarir wellfield. This drainage may have allowed recharge during the more extended wet periods of the late Pleistocene with episodic recharge during the short lived wet periods of the Holocene. Presently, there may be some local recharge off of Al Haruj al Aswad as evidenced by the shape of the potentiometric surface (Wright et al 1982.)

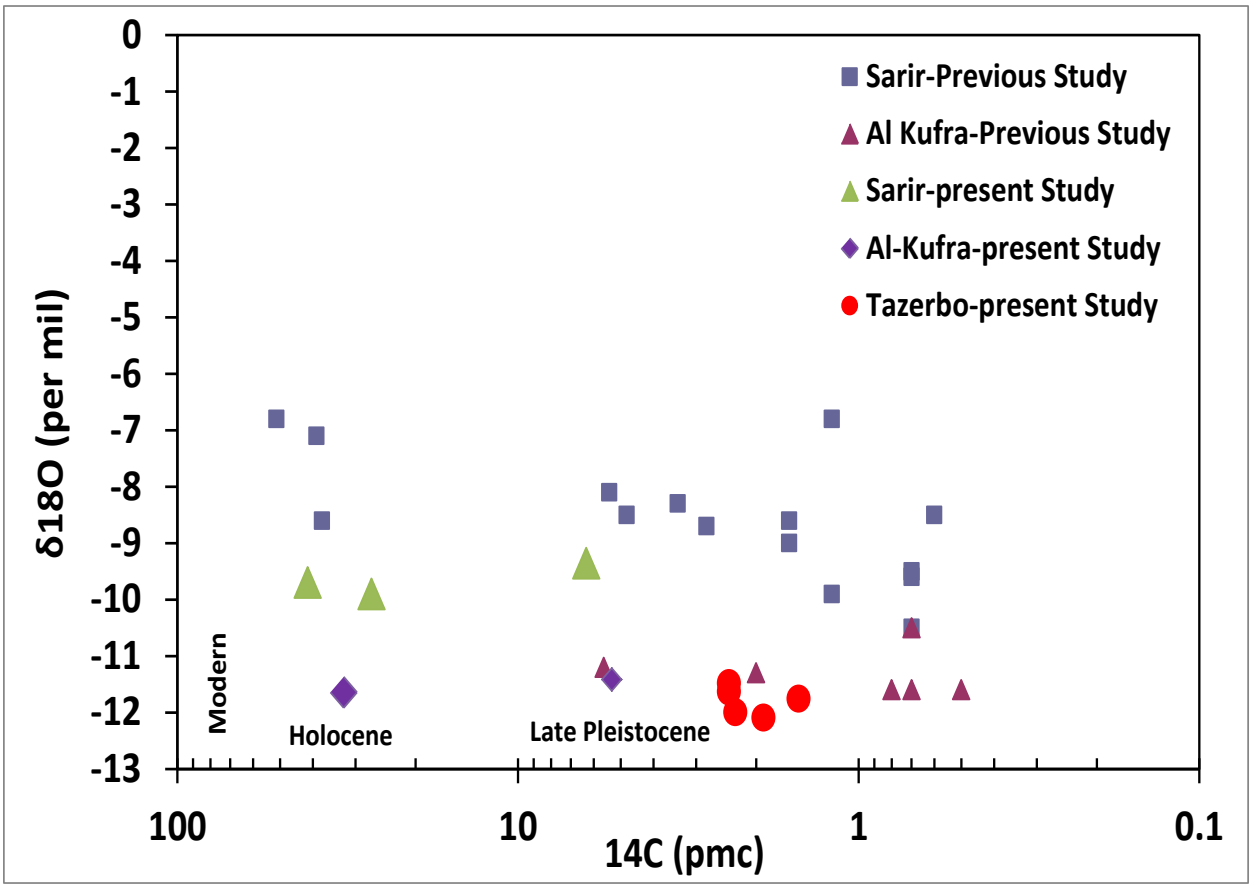

Figure 5.2. Comparison of $\delta^{18}O$ vs. ^{14}C for this study and that of Edmunds (2009).

CHAPTER SIX

NOBLE GASES

6.1 Background

Noble Gases are outstanding tracers of physical transport in groundwater. Moreover, they are excellent tools to investigate the paleotemperature of groundwater and many other physical parameters of environmental systems (Andrews and Lee 1979; Stute and Schlosser 1993; Stute and Deak 1989; Pinti et al. 1997). The radiogenic accumulation rate of crustal ^{4}He is a function of the concentrations of the radioisotopes in the formation solids. Most of the crustal ^{4}He is produced from the uranium and thorium decay series (Solomon 2000).The concept of ^{4}He as tools for dating groundwater is based on the constant accumulation of helium (^{4}Hec) in the reservoir such that the ^{4}Hec concentration is proportional to the residence time of the fluid.

There are several sources of helium in an aquifer (Figure 6.1). One source is dissolved helium from the atmosphere ($He_{atomsphere}$) which enters the aquifer in the recharge area. There is a production of helium within the aquifer material from radiogenic production from U and Th decay and nucleogenic reactions with Li ($He_{in\text{-}situ}$). Helium is also being produced by the same reactions outside the aquifer within the crust and mantle (He_{crust} and He_{mantle}) which can then diffuse into the aquifer, adding additional He to what would be produced in-situ. The total concentration of helium within the water in the aquifer will increase along the flow path from point 1 to point 3 in Figure 6.1.

Because ^{14}C has different sources and the way dissolved carbon sinks in groundwater, the dependability of ^{14}C ages is limited. Therefore, radiogenic He calculated from noble gas provides a good time scale for groundwater.

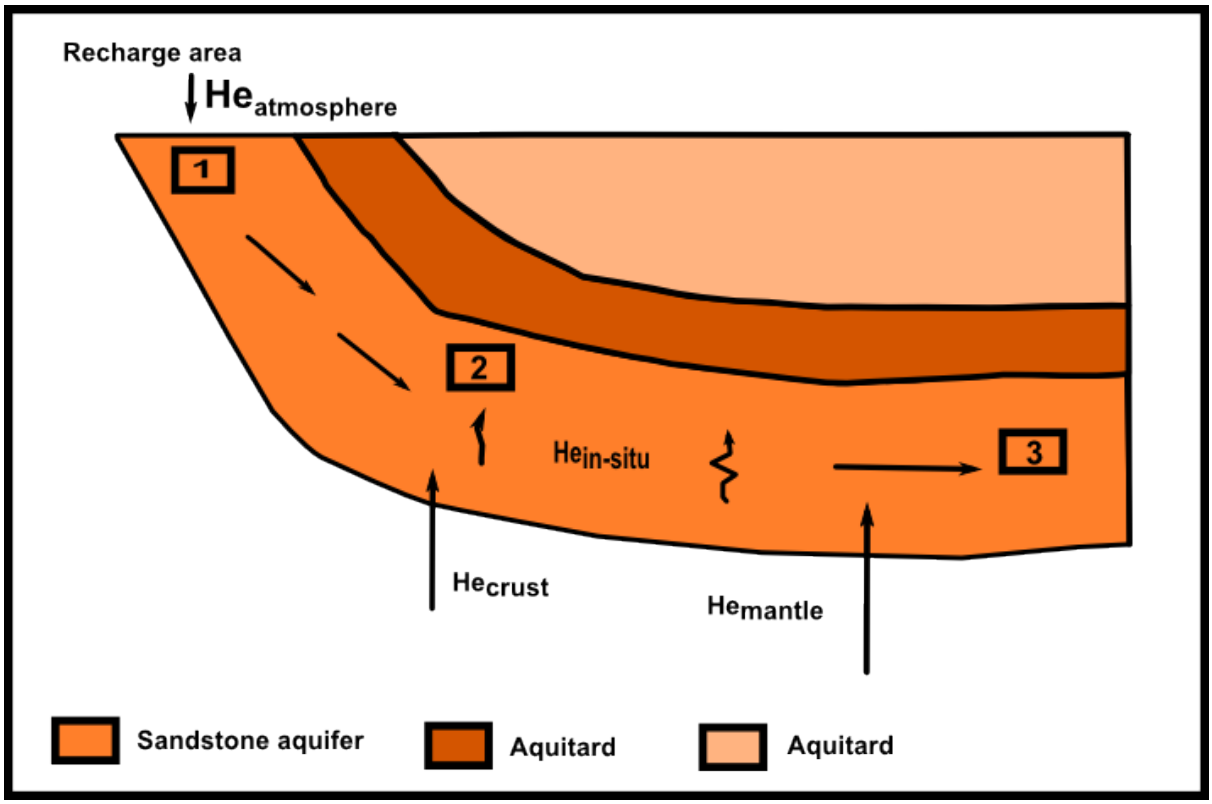

Figure 6.1. Conceptual model illustrating the sources of helium found in an aquifer.

Calculation of residence time requires estimates of the radiogenic accumulation rate and the ^{4}Hec component of the total ^{4}He in the sample ($^4He_{tot}$). Concentration of helium in the samples (^4He_c) can be resolved by a mass balance approach with known estimates of ^{4}He and/or R (^{3}He/^{4}He) for the various source components described below (Ballentine et al. 1991; Stute et al. 1992; Castro et al. 1998a).

Groundwater residence time can be estimated by (Andrews and Lee 1979):

$$t = \frac{^4Hec}{p} \qquad (6.1)$$

where:

- t = residence time [T]
- ^{4}Hec = concentration of radiogenic ^{4}He [mol L^{-3}]
- p = radiogenic accumulation rate [mol L^{-3} T^{-1}] (see equation 6.8)

The relatively small accumulation rate of ^{4}Hec in reservoir allows for the potential to estimate the residence time of relatively old fluids.

The radiogenic helium that is produced by the radioactive decay series of uranium (U) and thorium (Th) is used as a time indicator tool for dating waters. The present study presents the dissolved noble gas concentration from three aquifers in two sedimentary basins located in central and south east Libya. The accumulation of radiogenic helium has two formulas ^{3}He and ^{4}He, and they originally formed in three main reservoirs; the atmosphere, the mantle, and the crust. Groundwater can contain measurable amounts of He from all three reservoirs. Atmospheric helium (He_a) can be formed in groundwater by solubility equilibrium or/and by the dissolution of entrapped air. A fluctuating water table causes air to be trapped in dead-end pore spaces. The air bubbles eventually dissolve and become part of the He signature (Heaton and

Vogel 1981). The concentrations of He_a have a characteristic $^3He/^4He$ ratio (Ra) of 1.36×10-6 (Clarke et al. 1976).

Radioisotopes decaying in the earth's crust produce the crustal helium (He_c) and it can be found in groundwater. The average crustal $^3He/^4He$ ratio (Rc) was determined by Mamyrin and Tolstikhin (1984) to be 2.0×10^{-8}. Tritium is naturally produced in the earth's crust by a nucleogenic reaction with lithium, ^6Li (n, α) ^3H (Solomon and Cook 2000). However, post 1950 tritium could be produced from atmospheric testing of nuclear weapons (Solomon and Cook 2000). When the crustal helium (^4He_c and ^3He_c) is produced in the formation solids, they accumulate by direct release and solid-state diffusion.

Due to the occurrence of U and Th in nearly all crustal rocks, the concentration of ^4He in the pore fluid should increase linearly with time because of the long half-lives of U and Th (Torgersen and Clarke 1985). Radiogenic ^4He_c is produced from the uranium (^{238}U, ^{235}U), and thorium (^{232}Th) decay series (Solomon 2000), while the radiogenic ^3He_c is produced by the beta-decay of tritium (^3H) in the crust. Also, ^3He could be produced from the decay of anthropogenically-derived tritium ($^3He_{ant}$).

The third component of helium is derived in the mantle where it forms from the same reactions as in the crust (Solomon and Cook 2000). Mantle helium (He_m) has a high ratio of $^3He/^4He$ typically 1.2×10^{-5} (Ozima and Podosek 1983).

Formation porosity plays a role in the rate of ^4He accumulation that is produced by the crustal degassing flux which is controlled by local advection/diffusion (Torgersen and Ivey 1985). Therefore, ^4Hec and ^3Hec that produced in the formation solids, they accumulate in the formation pore space via direct production and solid-state diffusion.

The release of helium from this rock will also create a high ^4He flux into the aquifer but is unlikely to be as constant or as widespread as the observations.

Numerous studies have found that ^4He residence times are significantly larger than those from well-established hydrological and geochemical methods (^{14}C for example). These differences have mainly been attributed to external flux of ^4Hec from underlying rocks. For example, Torgersen and Clarke (1985), Torgersen and Ivey (1985), Solomon (1996), Castro et al. (2000) observed this phenomenon in different basins with different models. Also, dating groundwater by using radiogenic ^4He has been done by many scientists (e.g Marin et al. 1979; Torgersen 1980; Andrews 1983; Marty et al. 1988).

6.2 Noble Gas Results

Samples were collected from wells at each location and analyzed for their noble gas and tritium content at the University of Utah Noble Gas Laboratory in Salt Lake City, Utah USA. The results are presented in table (6.1).

Tritium content of the groundwater in Al Kufra and Sirt basin is very low with an average of 0.076 T.U.. These low content of tritium is another indication that this groundwater is a fossil water and has no recent recharge. The total concentration of ^4He in groundwater can be separated into four components (Solomon 2000), ^4He concentrations resulting from equilibrium solubility with air ($^4He_{sol}$), radiogenic helium ($^4He_{rad}$), mantle helium (^4He_m) and excess air helium ($^4He_{ea}$).

$$^4He_{tot} = {}^4He_{sol} + {}^4He_{rad} + {}^4He_m + {}^4He_{ea} \qquad (6.2)$$

Excess ^3He can be calculated as follows

$$^{3}He_{exc} = (^{4}He_{tot} - R_s) - (^{4}He_{sol} - R_{sol}) - (^{4}He_{ea} - R_a) \quad (6.3)$$

R_s is the measured $^{3}He/^{4}He$ ratio in the groundwater samples; R_{eq} is the $^{3}He/^{4}He$ ratio of water in solubility equilibrium with the atmosphere, i.e., $R_{eq}= 0.983 \times Ra = 1.360 \times 10^{-6}$ (Benson and Krause 1980).

Independent noble gas components are formed during groundwater infiltration, e.g. excess air makes the application more or less complicated that will affect the He age. (Heaton and Vogel 1981).

6.3 Noble Gases Result Interpretation and Discussion

The helium concentration, ^{4}He terregenic ($^{4}He_{terr}$), ^{3}He, and $^{3}He/^{4}He$ (R_{terr}) are listed in table (6.2 and 6.3). Where R_{terr} originating from terrigenic source (radiogenic ^{4}He, nucleogenic ^{3}He and mantle He, which means composed of crustal plus mantle He).

As described above, calculating the groundwater residence time with the ^{4}He chronometer and reconstructing the paleotemperature require quantification of the ^{4}He component produced from in situ alpha decay (^{4}Hec), and the radiogenic accumulation rate (Λ). The origin of these parameters is discussed in the following sections.

6.3.1 Radiogenic Accumulation Rate

The ratios of $^{3}He/^{4}He$ will be normalized relative to Ra, where Rs/Ra is ratio sample, Ra/Ra = 1, Rm/Ra = 8, and Rcrust/Ra = 0.02. The radiogenic accumulation rate of ^{4}Hec, and R/Ra_{terr} have been calculated as described above and the result listed in table (6.2).

Table 6.1. Dissolved gas and tritium concentrations results from groundwater samples from Al Kufra, Sarir and Tazerbo wellfields.

Sample I.D.	N2 total (ccSTP/g)*	Ar total (ccSTP/g)	Ne total (ccSTP/g)	Kr total (ccSTP/g)	Xe total (ccSTP/g)	He-4 (ccSTP/g)	He-3 (ccSTP/g)	Tritium (TU)**
KF-85	2.33E-02	4.95E-04	4.72E-07	8.86E-08	1.14E-08	3.78E-07	1.399E-13	0.00
KFRGA	2.04E-02	4.43E-04	4.26E-07	6.39E-08	7.78E-09	2.93E-07	1.345E-13	0.11
SR-116	1.75E-02	4.07E-04	3.15E-07	6.58E-08	1.01E-08	5.87E-07	9.878E-13	0.10
SR-222	2.63E-02	5.06E-04	4.47E-07	9.63E-08	1.17E-08	2.28E-07	3.480E-13	-
SR-140	2.17E-02	4.67E-04	4.71E-07	7.45E-08	9.28E-09	3.96E-07	6.422E-13	-
TZ-118	3.87E-02	5.95E-04	6.95E-07	6.61E-08	8.13E-09	4.42E-06	8.504E-12	0.11
TZ-217	2.88E-02	5.13E-04	5.80E-07	8.95E-08	1.03E-08	6.69E-06	5.534E-12	0.05
TZ-317	3.90E-02	6.00E-04	7.03E-07	1.10E-07	1.19E-08	4.47E-06	8.906E-12	-
TZ-401	3.75E-02	6.25E-04	7.53E-07	1.03E-07	1.14E-08	5.28E-06	7.620E-12	0.09
TZ-618	3.13E-02	5.23E-04	5.61E-07	6.70E-08	7.69E-09	6.83E-06	4.526E-12	0.04
SR-242	-	-	-	-	-	-	-	0.08
SR-312	-	-	-	-	-	-	-	0.04
TZ-517	-	-	-	-	-	-	-	0.14

*cm^3 of gas at standard temperature and pressure per gram of water;
**Tritium Units; 1 TU is equal to 3.22 picocuries per liter.

Table 6.2. ^{4}He, ^{4}He terregenic, and tritium mearments for the Sarir, Tazerbo and Al Kufra wellfields.

Sample	Depth	He	4Heterr	Delta Heterr	R/Ra	Rterr	3Hetrit	14C	Tritium	Hydro age	(3He/4He)
	(m) (ASL)	(ccSTP/g)	(ccSTP/g)	solubility (%)			(ccSTP/g)	(yr)	(TU)	yr	
KF-85	347.56	3.78E-07	2.56E-07	5.99	0.2670	3.68E-07	9.28E-14	2.05E+04	0	1.53E+05	3.63E-07
KFRGA	30	2.93E-07	1.78E-07	4.37	0.3317	4.58E-07	8.03E-14	1.20E+04	0.11	1.07E+05	4.51E-07
SR-116	456	5.87E-07	5.08E-07	11.72	1.2159	1.68E-06	8.40E-13	1.52E+04	0.1	8.81E+05	1.65E-06
SR222	452	2.28E-07	1.14E-07	2.597	1.1050	1.52E-06	1.71E-13	7.00E+03	0	1.97E+05	1.50E-06
SR-140	450	3.96E-07	2.71E-07	6.4048	1.1709	1.62E-06	4.32E-13	9.86E+03	0	4.71E+05	1.59E-06
TZ-118	461	4.42E-06	4.23E-06	95.828	1.3913	1.92E-06	8.00E-12	2.61E+04	0.11	3.52E+06	1.89E-06
TZ-217	458	6.69E-06	6.54E-06	153.073	0.5972	8.24E-07	5.31E-12	2.75E+04	0.05	5.45E+06	8.12E-07
TZ-317	533	4.47E-06	4.28E-06	98.88	1.4397	1.99E-06	8.38E-12	2.41E+04	0	3.57E+06	1.96E-06
TZ-401	578	5.28E-06	5.08E-06	118.91	1.0423	1.44E-06	7.20E-12	2.35E+04	0.09	4.23E+06	1.42E-06
TZ618	600	6.83E-06	6.68E-06	156.094	0.4785	6.60E-07	4.35E-12	2.34E+04	0.04	5.57E+06	6.51E-07

The majority of ^{4}He is most originally from external flux and a small amount is from in-situ production. From the R/Ra_{terr} (R_{ter}: crustal plus mantle He) it is clear that all aquifers received a significant amount of mantle derived $^{4}He_{terr}$. The average values of this ratio are (0.267 - 0.332) for the Al Kufra wellfield, and (1.105 - 1.216) for the Sarir wellfield, and (0.479 - 1.440) for the Tazerbo wellfield. These values are all above the typical crustal production values (R/Ra) = 0.02 (Andrews 1985).

The R/Ra in the Tazerbo wellfield increases from the east toward the west consistently with the distance between the wells in the wellfield, from 0.5 to 1.042 in the central of wellfield to 1.40 at the west of wellfield (See figure 3.4). Moreover, this ratio decreases with depth to the main aquifer. For example the south wells have a depth of 650 m to the top of the main aquifer while the north wells have 280 m to the top. A similar trend occurs from the east to the west of the well field.

In the Al Kufra wellfield, the shallow aquifer has a higher ratio of R/Ra than the deep aquifer. On the other hand, the R/Ra ratios for the Sarir wellfield are more or less the same throughout the wellfield. As we can see, the R/Ra ratio provide information on whether the terregenic helium is predominated by the helium of radiogenic origin, or it is a mixture between crustal and mantle sources.

6.3.2 Source of ^{4}He (internal or external origin) and Helium Flux in Aquifers

He concentrations increase with groundwater age due to the accumulation of radiogenic He that produced by the decay of U and Th series nuclides in crustal minerals (e.g., Andrews and Lee 1979; Torgersen and Clarke 1985; Stute et al. 1992b).

Table 6.3. Parameters were used to calculate the steady-state ^{4}He and ^{3}He production rate of the Sarir, Tazerbo and Al Kufra wellfields.

Site	depth (m)	Li ppm	Th Ppm	U ppm	P(3He) ccSTPg-1 rock yr-1	P(4He) ccSTPg-1 rock yr-1	Density (ρ)	($^{3}He/^{4}He$) rock	(R/Ra) rock	P(3He)H2O ccSTPcm$^{-3}_{H2O}$ yr-1	P(4He)H2O ccSTPcm$^{-3}_{H2O}$ yr-1
KF	-	4.1	4.4	1.4	6.23E-22	2.70E-13	2.65	2.31E-09	0.0017	3.07E-21	1.67E-12
SR	216-252	7.1	1.7	0.5	3.99E-22	1.00E-13	2.65	3.98E-09	0.0029	1.96E-21	6.19E-13
SR	252-294	7.2	1.8	0.8	5.52E-22	1.34E-13	2.65	4.12E-09	0.0030	2.72E-21	8.27E-13
SR	294-330	6.4	1.3	0.4	2.82E-22	7.84E-14	2.65	3.60E-09	0.0026	1.39E-21	4.84E-13
SR	333-360	6	1.3	0.4	2.64E-22	7.84E-14	2.65	3.37E-09	0.0024	1.30E-21	4.84E-13
SR	363-390	6.1	1.2	0.4	2.60E-22	7.55E-14	2.65	3.44E-09	0.0025	1.28E-21	4.67E-13
Sr-averag	0.35	6.56	1.46	0.5	3.46E-22	9.32E-14	2.65	3.71E-09	0.0027	1.70E-21	5.76E-13
Tz	120-165	11.5	7.1	2.5	3.00E-21	4.60E-13	2.65	6.51E-09	0.0047	1.48E-20	2.85E-12
Tz	165-219	11.9	5.4	1.3	1.90E-21	2.88E-13	2.65	6.60E-09	0.0048	9.38E-21	1.78E-12
Tz	219-264	10.9	7.4	2	2.54E-21	4.18E-13	2.65	6.09E-09	0.0044	1.25E-20	2.58E-12
Tz	264-309	12.2	6.5	2.5	3.07E-21	4.43E-13	2.65	6.94E-09	0.0050	1.52E-20	2.74E-12
Tz	309-354	11.6	6	2.5	2.84E-21	4.29E-13	2.65	6.62E-09	0.0048	1.40E-20	2.65E-12
Tz	354-399	20.8	11.7	4.4	9.30E-21	7.87E-13	2.65	1.18E-08	0.0086	4.58E-20	4.87E-12
Tz	399-441	6.4	3.5	0.8	6.46E-22	1.83E-13	2.65	3.54E-09	0.0026	3.19E-21	1.13E-12
TZ	441-480	7.2	4.3	0.8	8.10E-22	2.05E-13	2.65	3.94E-09	0.0029	3.99E-21	1.27E-12
Tz-average	0.35	6.8	3.9	0.8	7.28E-22	1.94E-13	2.65	3.75E-09	0.0027	3.59E-21	1.20E-12

Porosity (ɵ) is 0.35 for all aquifer. SR: Sarir wellfield well # 309A; Tz: Tazerbo wellfield well # 401.

There are three potential sources of radiogenic He in groundwater: 1-in situ production within the aquifer matrix; 2-release of stored He from sediments; and 3-flux from adjacent layers or underlying crust.

The rate of He accumulation due to the first source can be estimated if U and Th concentrations of the aquifer material are known. However, the strength of the two other sources can vary by orders of magnitude depending on the geological setting. Therefore, He accumulation in groundwater typically provides only a qualitative timescale.

The He excess air found in the three aquifers is remarkably acceptable in view of the presumed groundwater age. Significant release of stored He from the sediment is expected because of the volcanic area near the wellfields. The ^{4}He accumulation rate, due to in situ production can be calculated following (Stute et al. 1992b) and the results are listed in table (6.3).

From the results of all the aquifers, it is clear that this water has received some external ^{4}He out of the aquifer. Our Ra is high for all samples mean that these waters have extra helium not in-situ. Therefore, we had to concern about the other source of helium (mantle and crust).

The mantle component is a significant amount in our samples in all the aquifers. However, the crustal ^{4}He observed in our He samples could be the result of in-situ production or from the external source. Therefore, core and cutting samplings from all the aquifers were analyzed for Li, U, and Th to calculate the in-situ production rates of ^{4}He and ^{3}He according to Ballentine et al. (1991) (See table 6.2 and 6.3). In-situ production rates are given by

$$P(^{3}He) = [6.35(U)+ 1.434(Th)]x(Li)\ x10^{-23}\ cm^{3}\ STP\ g^{-1}_{rock}\ yr^{-1} \quad (6.6)$$

$$P(^{4}He)=1.207x10^{-13}(U)+ 2.867x10^{-14}(Th)\ cm^{3}\ STP\ g^{-1}_{rock}\ yr^{-1} \quad (6.7)$$

where (Li), (U) and (Th) represent the Li, U, and Th concentrations (in ppm), in the aquifer rock, respectively. The porosity ($\emptyset$) of the aquifer matrix have to be measured. Estimate the accumulation rate of the He isotopes in the water by

$$[p^{i}_{He}] = P(\ ^{i}He)\rho\Lambda_{He}\left(\frac{1-\emptyset}{\emptyset}\right) \qquad cm^3\ STP\ cm^{-3}{}_{H2O}\ yr^{-1} \quad (6.8)$$

where **i** represents ^{3}He or ^{4}He, ρ is the mass density of the rock in gcm^{-3} and is taken as 2.6 gcm^{-3} for the predominant quartz sand, $\emptyset$ is the porosity of the reservoir rock and Λ_{He} is the fraction of produced ^{4}He which is released from minerals into the water; For sediments, it can be assumed that Λ_{He} =1 (e.g., Torgersen 1980; Torgersen and Clarke 1985).

Table (6.3) lists for all aquifers the Li, U and Th concentrations, the average porosity and the density of the reservoir rocks, as well as the in-situ production rates of ^{3}He and ^{4}He in the rock matrix, and the rate of ^{3}He and ^{4}He accumulation in the water.

Samples from the Sarir and Tazerbo wellfields were obtained from two cores from the northwestern part of Sarir wellfield and from the central region of the Tazerbo wellfield (Figures 3.1; 3.4). The U concentrations in the Sarir wellfield range from 0.4 to 0.8 ppm with a mean value of (0.5) ppm. The Th concentrations range from 1.2 to 1.8 ppm with a mean value of (1.46) ppm. The Li concentrations range from 6 to 7.2 ppm. The concentrations in the aquitards are higher, particularly in the overlying clay in the Tazerbo wellfield (mean values 0.8 ppm for U, 3.9 ppm for Th, and 6.8 ppm for Li). The total porosity $\emptyset$ was measured to be 0.35.

With the above mean values, equation (6.8) yields a He accumulation rate of 5.768×10^{-13} $cm^3STP\ g^{-1}\ yr^{-1}$ for the Sarir well field aquifer, 9.56×10^{-13} $cm^3STP\ g^{-1}\ yr^{-1}$ for the Tazerbo aquifer, and 1.669×10^{-12} $cm^3STP\ g^{-1}\ yr^{-1}$ for Al Kufra (outcrop sample).

The He ages may be interpreted as maximum estimates, because an additional He flux from adjacent aquitards or deeper layers of the crust is present.

The isotope ratio $^3He/^4He$ (R) may be used to discern different sources of the accumulated He. Although a detailed knowledge of the sediment composition would be required for a precise calculation of the $^3He/^4He$ production ratio, rough estimates can be made on the basis of the measured Li concentrations (Table 6.2 and 6.3).

We estimate $^3He/^4He$ (R) production ratios of less than 10^{-8} (3.71×10^{-9}) for the Sarir sand, (3.75×10^{-9}) for the Tazerbo, and (2.31×10^{-9}) for Al Kufra. Since the data from well Tz 618 yield an upper limit of 1.18×10^{-8} for the radiogenic $^3He/^4He$ ratio in the Tazerbo, a major contribution of He produced in the aquitards.

Nevertheless, some He diffusion from the aquitards into the aquifer appears likely, given that the U and Th concentrations in the aquitards are higher. Moreover, the upward gradient that can see in the artesian wells will increase the flux.

If it is assumed that the entire He results from in-situ production with consideration to all ^4He can come from the aquifer rock. The time to produce this amount of helium in Sarir has been calculated to be between $1.9x10^5$ to $8.8x10^5$ yr. Comparing with the ^{14}C age (9 to 15 kyr) this seems to be very high. Tazerbo and Al Kufra have the same results. Tazerbo has ^4He accumulation in water between $8.99x10^{-13}$ to $3.8\ x10^{-12}$ $ccSTPcm^3_{H2O}yr^{-1}$ with a groundwater age between $1.7x10^6$ to $2.69x10^6$ yr, while the Al Kufra has ^4He accumulation in water was $1.669x10^{-12}$ $ccSTPcm^3_{H2O}yr^{-1}$ with a groundwater age between $1.07x10^5$ - $1.57x10^5$ yr. These

ages are also far away from the ^{14}C age (See Figures 6.2 and 6.4). When we looked at the $^{3}He/^{4}He$ ratios in the water and in the rocks, we found them far away from each other, which mean this helium is not from in-situ production, it came from another source of helium outside of the aquifer, and the rock-water system is not closed.

The amount of helium that we have is significantly high to have been produced only from in-situ. Therefore, external sources should be considered and have to be estimated. This high concentration of ^{4}He in all the aquifers that gave high water residence times indicates that the ^{4}He has an external source that could be vertical flux from a deeper level, or could be from the volcanic activity in the region.

Since the aquifer thickness are known for all the aquifers (Tazerbo is 150m, Sarir is 170 m and Al Kufra is 200 m) and we have calculated the ^{4}He accumulation rate in water for all the aquifers, the crust ^{4}He flux (J_{Hec}) can be calculated for all samples from the excess ^{4}He according to equation (6.9) and the result is shown in table (6.4)

$$J_{Hec} = P_{He} * h * \emptyset \quad (6.9)$$

where J_{Hec} is crust ^{4}He flux, P_{He} is the in-situ production rate; $\emptyset$ is porosity, and h is aquifer thickness. Therefore, the average ^{4}He flux for the Sarir aquifer is 1.17×10^{-7} $cm^3STPg^{-1}yr^{-1}$, for the Al Kufra is 4.5×10^{-8} $cm^3STPg^{-1}yr^{-1}$, and for Tazerbo is 7.8×10^{-7} $cm^3STPg^{-1}yr^{-1}$.

On the other hand, an estimate of helium flux following base on ^{14}C age is (Trogersen & Ivery 1985):

$$J_{He} = \left(\left(\frac{C_{He}}{t}\right) - \left(\frac{A_{Is}}{\emptyset}\right)\right)\emptyset h \quad (6.10)$$

Where C_{He} is terrigenic helium, t is time from ^{14}C (in our case); A_{Is} is the In-situ production rate; ∅ is porosity, and h is the aquifer thickness. The ^{4}He flux was estimated by the authors base on equation (6.10); for the Sarir aquifer is 1.043 x 10^{-7} cm^3STP/cm^2yr^{-1} and 9.567x10^{-7} $cm^3STP/cm^2yr^{-1}$for Tazerbo and 5.818 x 10^{-7} cm^3STP/cm^2yr^{-1} for Al Kufra.

Castro et al. (2000) have calculated the ^{4}He fluxes for several sandstone aquifers and they got these results, the Auob Sandstone Aquifer has ^{4}He fluxes with value 6 x 10^{-6} cm^3 STP cm^{-2} yr^{-1} and the Carrizo aquifer has ^{4}He fluxes 3.6 x 10^{-7} cm^3 STP cm^{-2} yr^{-1} and the Ojo Alamo and Nacimiento aquifers a value of 3 x10^{-6} cm^3 STP cm^{-2} yr^{-1}. To explain the amount of the in-situ helium production we could assume these huge quantity came of ^{4}He produced in the rock is released to the water or at least part of the ^{4}He produced in the rock is released Castro et al. (2000).

With average ^{4}He production rates 5.7×10 -^{12} $cm^3STPcm^{-3}H_2Oyr^{-1}$ for the Carrizo aquifer, 3.7×10^{-12} ^{f} $cm^3STPcm^{-3}H_2Oyr^{-1}$ for the San Juan Basin aquifers, and 2.9×10^{-12} $cm^3STPcm^{-3}H_2Oyr^{-1}$ for the Stampriet aquifer which take between 2 kyr - 1 Ma, 2 kr -5 Ma, and 2-50 Ma, respectively, to produce the measured ^{4}He concentrations.

These groundwater ages seem to be far too high, being in contradiction with the ^{14}C ages. On the other hand, to say that all the produced ^{3}He and ^{4}He were released from the rock, one would expect the measured and calculated R/Ra ratios in the waters and in the rocks to be similar, which was not observed.

Table 6.4. ^{4}He, ^{3}He and helium flux results for the the Sarir, Tazerbo and Al Kufra wellfields.

Sample I.D.	4He (ccSTP/g)	3He (ccSTP/g)	R/Ra	14C(yr)	4Heterr (ccSTP/g)	JHe (ccSTP/gyr)	Helium Flux Cm3STP/Cm2/yr	AVG.JHe mol/gyr	AVG.JHe atmos4He/m^2yr	AVG.JHe atmos4He/m^2yr/Ø	AVG.JHe atmos4He/m^2yr*
KF-85	3.78E-07	1.01E-07	0.267	2.36E+04	2.56E-07	1.08E-11	3.15E-08	1.46E-12	8.81E+11	2.52E+12	2.85E+08
KFRGA	2.93E-07	9.72E-08	0.332	9.03E+03	1.78E-07	1.97E-11	8.49E-08	3.95E-12	2.38E+12	6.79E+12	7.70E+08
SR-116	5.87E-07	7.14E-07	1.216	2.22E+04	5.08E-07	2.29E-11	1.07E-07	4.97E-12	2.99E+12	8.54E+12	9.68E+08
SR222	2.28E-07	2.51E-07	1.105	7.00E+03	1.14E-07	1.62E-11	7.29E-08	3.39E-12	2.04E+12	5.83E+12	6.61E+08
SR-140	3.96E-07	4.64E-07	1.171	9.86E+03	2.71E-07	2.75E-11	1.31E-07	6.07E-12	3.65E+12	1.04E+13	1.18E+09
TZ-118	4.42E-06	6.14E-06	1.391	2.61E+04	4.23E-06	1.62E-10	7.11E-07	3.30E-11	1.99E+13	5.69E+13	6.44E+09
TZ-217	6.69E-06	4.00E-06	0.597	2.75E+04	6.54E-06	2.38E-10	1.05E-06	4.89E-11	2.95E+13	8.42E+13	9.54E+09
TZ-317	4.47E-06	6.44E-06	1.440	2.41E+04	4.28E-06	1.78E-10	7.81E-07	3.63E-11	2.19E+13	6.25E+13	7.08E+09
TZ-401	5.28E-06	5.51E-06	1.042	2.35E+04	5.08E-06	2.16E-10	9.54E-07	4.44E-11	2.67E+13	7.64E+13	8.65E+09
TZ618	6.83E-06	3.27E-06	0.479	2.34E+04	6.68E-06	2.86E-10	1.27E-06	5.9E-11	3.55E+13	1.01E+14	1.15E+10

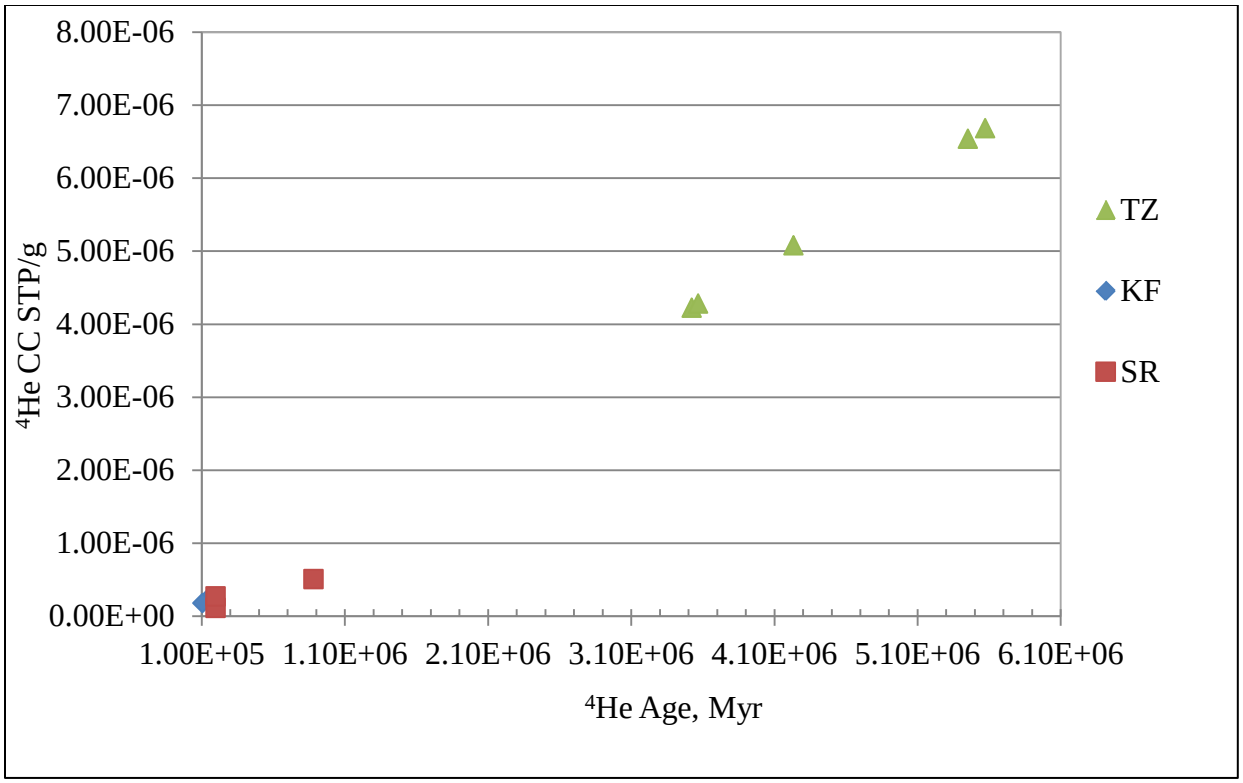

Figure 7.2. ^{4}He concentration vs. measured groundwater age as determined by He

6.3.3 Separation of ^{4}He Components

Table (6.2) shows the $^4He_{tot}$ and $^3He_{tot}$ with R values for each sample location. Magnitudes of R measured in the Sarir samples are well constrained around a value of 3.63×10^{-7}. This value is less than those documented for the atmosphere (Ra = 1.36×10^{-6}) and mantle (Rm = 1.2×10^{-5}), but greater than He produced in the crust (Rc = 2.0×10^{-8}).

Magnitudes of R measured in the Al Kufra samples are well constrained around a value of 1.59×10^{-6}. This value is close to the documented value for the atmosphere (Ra = 1.36×10^{-6}) and less than the mantle (Rm = 1.2×10^{-5}), but greater than He produced in the crust (Rc = 2.0×10^{-8}). Magnitudes of R measured in the Tazerbo samples are well constrained around a value of 1.346×10^{-7}. This value is less than the documented value for the atmosphere (Ra = 1.36×10^{-6}) and less than mantle (Rm = 1.2×10^{-5}), but greater than He produced in the crust (Rc = 2.0×10^{-8}). This indicates that He in all the aquifers is a mixture derived from the crust as well as the atmosphere and/or mantle. $^3He/^4He$ ratios above the atmospheric value indicates an accumulation of ^{3}He from tritium decay, whereas $^3He/^4He$ ratios below the atmospheric value indicates an accumulation of radiogenic He. The concentration of the other noble gases indicate that our samples are not contaminated with atmospheric noble gases, therefore, that ratio near the atmospheric values are due to terrigenic production

To calculate each type of helium (in-situ, mantle, or crust) for all well fields we used equation (6.11) as described below:

$$R_s = x(R_{in}) + y(R_c) + z(R_m) \qquad (6.11)$$

where: x+ y + z = 1, $x = \frac{P_{in}}{J_{He}}$, $R_m = 8$, $R_c = 0.02$, R_{in} = calculated for each wellfield

6.3.3.1 The Tazerbo Wellfiled

Table (6.3) shows the terrigenic helium of our samples with average R of $1.34x10^{-6}$ which is one order of magnitude lower than $1.25x10^{-5}$ for the He mantle (Ozima and Podosek 1983). Most samples have a He ratio within one order of magnitude less than the mantle He or one order of magnitude higher than the crustal Helium 10^{-9} - 10^{-7} with a typical value of 2 x 10^{-8} (Mamyrin and Tolstikhim 1984). All samples contain originally radiogenic ^{4}He and nucleoginic ^{3}He with no tritiogenic ^{3}He because of very low tritium in all samples (0.04 - 0.11 TU). Very high ratios of $^{3}He/^{4}He$ are found in sample TZ118 and TZ317 with values of $1.86x10^{-6}$ to $1.96x10^{-6}$. These ratios can be explained by the existence of mantle helium. We then determined the concentration of $^{4}He_{c}$ was then determined by subtracting the calculated concentrations of in-situ He_{terr} and ^{4}Hem from $^{4}He_{tot}$ (Equation 6.11). The helium here is consisting of 90 % crustal, 9.73 % mantle, and only 0.27 % in-situ helium.

6.3.3.2 The Sarir wellfield

Excess He in the Sarir wellfield samples is due to radiogenic ^{4}He and nucleogenic ^{3}He with average ratio $1.58x10^{-6}$ which represents the terregnic He value. Here, we can see this He was produced in the crust and mantle. This interpretation is based on the high value of He which may have been contributed by the mantle.

It is clear in He_{terr} that it is accompanied by He radiogenic and nucleogenic ^{3}He that do not follow the depth concentration relationship. ^{3}H measurements were 0.1TU to below detection limit meaning no modern recharge and suggests it is fossil water.

The R ratio of theses samples are too high to be explained by crustal production only. Therefore, it should be mixture from different regions. We estimate the percentage of mantle helium is 14.58%, crustal helium is 85%, and the in-situ is 0.42% according to equation (6.11).

Considering the depth of the Sarir samples, all wells have more or less the same depth 452m ± 4m, the $^{4}He_{terr}$ concentration in sample SR116 is higher than sample SR222 and SRP140. This difference could be due to aquifer and formation lithology or upward leakage of water in this area. Since the Sarir aquifer has varying lithology throughout the wellfield, correlation between the wells is difficult. This diversity in lithology in the Sarir wellfield and in the Sirt Basin in general (the north part of the aquifer has more limestone and clay than the south part) definitely will affect the ^{14}C age, as it clear in the samples SR116 SR222 and SR140. Even when all samples have the same depth, however, the ^{14}C age is highly different from 9 kyr to 15 kyr, see table (5.2).

6.3.3.3 The Al Kufra Wellfield

Samples were taken from the deep and shallow aquifers. While the concentrations of He are very close, the ^{14}C ages are different. The deep aquifer has a ^{14}C age 20kyr, while the shallow aquifer has a ^{14}C age 12 kyr. Deep aquifer has ^{3}H of 0 or below the detection limit, which means the tritiogenic ^{3}He can be excluded. All samples from deep and shallow aquifers have $^{3}He/^{4}He$ ratios of $3.6x10^{-7}$ - $4.5x10^{-7}$ which means these samples also have mantle Helium like the other aquifers. R/Ra for all samples are also high (0.267) for the deep and (0.33) for the shallow, which indicate this water contains mantle helium. The contributions of mantle, crustal and in-situ helium in these samples were estimated by the author to be 3.23 %, 95 % and 1.7 % respectively. This could be interpreted as the wellfield being located near a magmatic formation represent in

Jabal as Saeda, west of Sirt Bsin, Al Haruj Al Aswas (Miocene – Qyaternary) in west south west of Sirt Basin, and Tibessti Mountain (Pliocene – Recent) south of Al Kufra Basin that could release a weak mantle component that was incorporated into that water.

6.3.4 ^{3}He and ^{4}He

The ^{3}He excesses are higher than ^{4}He for both shallow and deep aquifers in al Kufra area (Figure 6.3). On the other hand, the Sarir wellfield has ^{4}He excesses higher than ^{3}He. However the Tazerbo wellfield has samples with both cases. ^{4}He concentrations in the deep well samples at the Al Kufra wellfield are higher than those from the shallow aquifer. The Tazerbo and Sarir wellfields have ^{4}He concentration increases from east to west. The same scenario exists for ^{3}He in the Tazerbo wellfield, where it increases from $4.3x10^{-12}$ to $8x10^{-12}$ ccSTP g^{-1}. The ^{3}He concentration in the Al Kufra wellfield is consistent with depth, from $8x10^{-14}$ to $9.28x10^{-14}$ ccSTP g^{-1}.

The amount of terrigenic helium (radiogenic ^{4}He, nucleogenic ^{3}He and mantle He) is compared to the percent modern carbon (Figure 6.4) shows that there is more helium in the groundwater with increasing groundwater age. This is consistent with their being a longer time period for helium to be added to the system due to natural uranium/thorium decay in the aquifer material.

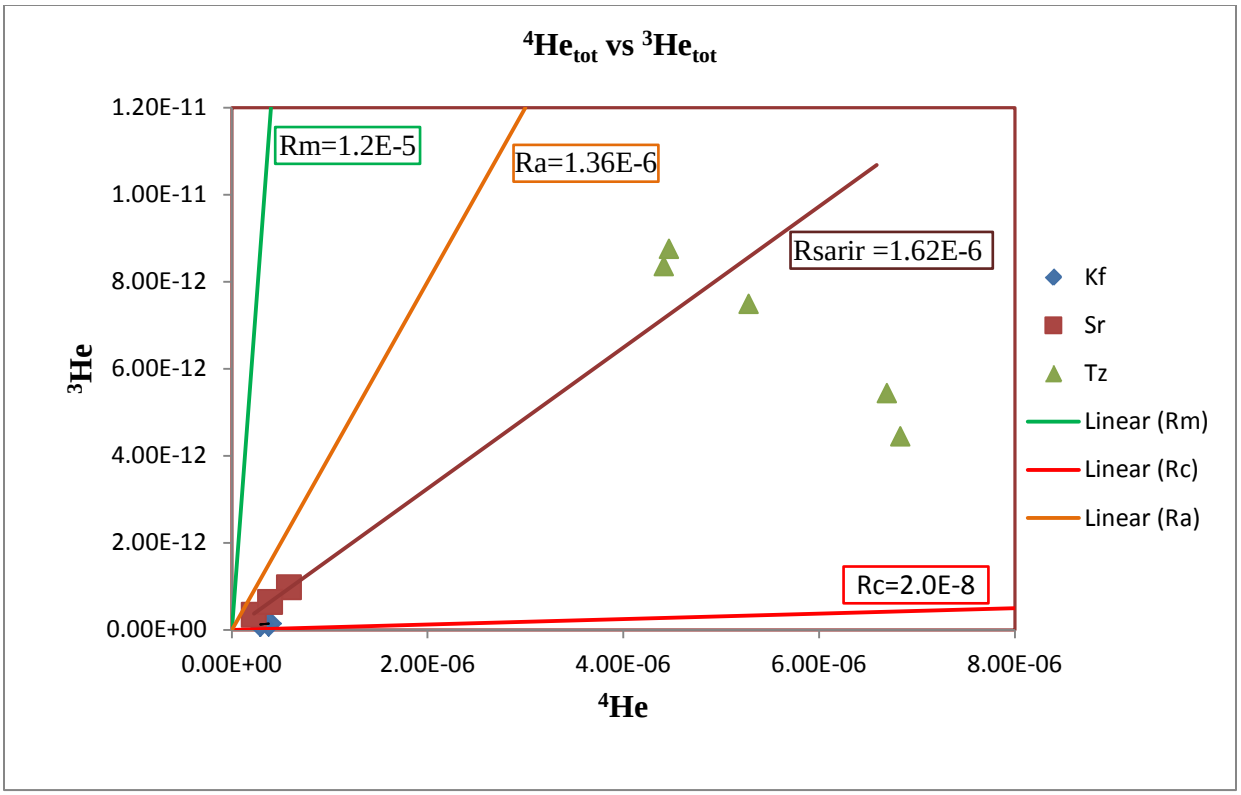

Figure 6.3. ^{4}He versus ^{3}He. Sarir samples plot on a line with a slope of R = 1.62E-06. Tazerbo and Al Kufra samples display more variation.

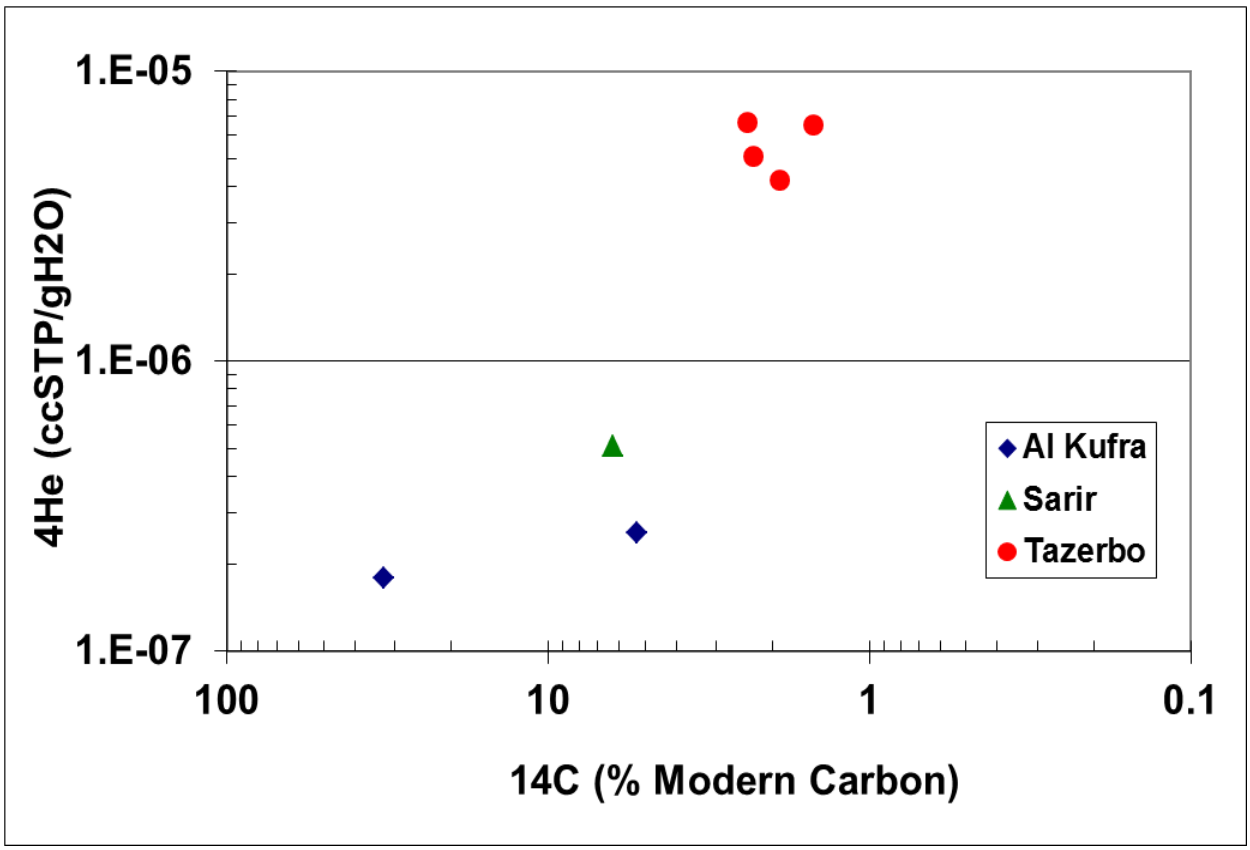

Figure 6.4. Terrigenic helium versus ^{14}C activity.

It seems there is no correlation between the ^{4}He concentration and (^{14}C) age in the Sarir well field; this may be because the Sarir well field is located near volcanic activities area called the Al Harruj al Aswad almost 250 km west of the wellfield. However, Al Kufra and Tazerbo have more or less direct correlation, increasing He is associated with increasing in (^{14}C) age.

6.3.5 Reconstruction Paleoemperature and Age of Groundwater

The results of noble gas temperature analyses for each aquifer provide a snapshot in time of the state of the aquifer. As we mention in chapter (5) there are no flow path data available due to the limit of wells for access. What has been developed is a baseline to which later results can be compared in order to identify changes in apparent ages and other parameters due to continued extraction of water from the three aquifers.

A methodological model similar to (Aeschbach-Hertig et al. 1999, 2000; Ballentine and Hall 1999) was used to measure noble gas concentrations in groundwater with uncertainties r within ±1 to 2% in order to calculate the noble gas temperature (NGT).

Noble gas concentration depends on the solution of atmospheric noble gases in water. Several parameters control the equilibrium concentration in surface waters, temperature (recharge temperature), pressure (elevation), excess air, reequilibrium and salinity (Aeschbach-Hertig et al. 2000) the results of these paramters are listed in table (6.5a). The salinity of water effects the concentration of noble gases, therefore it has to be calculated for fresh water from the electrical conductivity at 20^{o}C (Wüest et al. 1996).

$$S\ (‰) = 0.87x10^{-3}\ k_{20}\ (\mu S\ cm^{-1})\ldots \qquad (6.12)$$

Calculating noble gases concentration (He, Ne, Ar, Kr, and Xe), requires knowing two or three of these parameters (Aeschbach-Hertig et al. 1999). The resulting excess of dissolved gases is often best detected by Ne, therefore ΔNe which is (Ne_{meas}/Ne_{eq} - 1) × 100 %, is the relative Ne excess above the solubility equilibrium, and is used for the temperature calculations (Aeschbach-Hertig et al. 2001).

The model is a closed-system equilibration (CE) of groundwater with only partially dissolved entrapped air, resulting in a solubility controlled fractionation has been used in order to correct for the excess air component during the calculation of noble gas concentration. The CE-model provides good results for the noble gas data set from all the aquifers:

$$Ci_{(T,S,P,A,F)} = C^*_{i\ (T,S,P)} + \left(\frac{(1-F)\,Az_i}{\frac{1+FAz_i}{C^*_i}} \right) \text{ (i = He, Ne, Ar, Kr, Xe)} \qquad (6.13)$$

where

- $C_i^*(T,S,P)$ are the moist air solubility equilibrium concentrations as a function of temperature, salinity, and atmospheric pressure, and can be calculated by one of these methods, Clever 1979; Weiss 1970, 1971; Weiss and Kyser 1978, Smith and Kennedy 1983. z_i are the noble gas volume fractions in dry air, *Ae* is the initial amount of dry entrapped air per unit mass of water, *F* is the fractionation of excess air.

χ^2-test, the sum of the squared deviations between the modeled and measured concentrations of noble gases was used in the model to describe the data within their uncertainty for each sample individually (Ballentine and Hall 1999; Aeschbach-Hertig et al. 1999). Equation (6.13) is a nonlinear least squares method to calculate the values of the model parameters that minimize χ^2. The model has two important parameters, (*Ae*) is the STP-volume of the initially entrapped air per mass of water, and the fractionation parameter (*F*), reflecting the reduction of the entrapped gas volume in the final and initial state (*v*) and the dry gas pressure in the trapped

gas to that in the free atmosphere (q), which is expressed as: $F = v/q$. Those two parameters have a physical interpretation that should be used to check the best of the fit results (Aeschbach-Hertig et al. 2000, 2001). The χ^2 -test was first applied to individual samples to identify irregular samples that cannot be described by the model, the sample that has an χ^2 model value equal to or bigger than the probabilities of p (χ^2) 0. 1= (2.71) or p (χ^2) 0.05 = (3.84) will be rejected. Although the uncertainty parameters are very small in our samples, the model calculates them from the covariance matrix in the least squares fitting algorithm.

The results are shown in table (6.5 a and b). Four samples with high χ^2-values (TZ612, TZ118, SR116, and KFRG) fail to pass the model, however all other samples fit acceptably. This means the concentrations of the parameters derived from fitting more or less match the weighted means of the parameters derived from the individual samples. The parameters derived from the inverse modeling of the heavier noble gases were used to calculate the atmospheric He component.

The terrigenic He (He_{terr}) that we calculated from the difference between the measured total He and the calculated atmospheric He has been used for groundwater dating. However, equation (6.13) is applicable to the observed He for the three aquifers because of the presence of radiogenic He.

Entrapped air fraction (Ae) has a range from 0.0240 to 0.0436 $cm^3STP\ g^{-1}$, and q has a range from 0 to 0.910, and v has a range from 0 to 0.3914, see all results in table (6.3a). The best results of fits are samples KF85, and TZ118 as they listed in Table (6.5b) using the scale of the errors by the factor $(\chi^2/\ v)^{1/2}$. It is note that all samples produce a more or less low value of Ae which is well constrained by the data.

Table 6.5 a. Results of fitting equation 6.4 to the measured concentrations of Ne, Ar, Kr, and Xe.

Input Information			Recharge Parameters				
Sample Name	Salinity	Recharge Elevation	Recharge T	*Ae*	F	EA	Delta Ne
	(per mil)	(masl)	(C)	(ccSTP/g)		(ccSTP/g)	(% Solubility)
KF-85	0.09	400	19.4	0.0275	0.15	0.0186	166.9%
KFRGA	0.25	400	-	0.0240	0.15	0.0162	161.7%
SR222	0.60	200	18.6	0.0286	0.42	0.0098	77.3%
SRPW-140	0.60	200	-	0.0331	0.23	0.0178	145.5%
TZ-118	0.12	250	-	0.0317	0.17	0.0192	181.6%
TZ-217	0.14	250	25.1	0.0291	0.00	0.0291	317.1%
TZ-317	0.14	250	20.3	0.0295	0.07	0.0241	236.3%
TZ-401	0.13	250	25.2	0.0364	0.05	0.0309	292.6%
TZ618	0.15	250	-	0.0436	0.06	0.0348	336.7%
						0.0189	157.5%

Table 6.5 b

	Recharge Model Fit														
Sample Name	Chi^2	Chi^2 Ceiling		He		Ne		Ar		Kr		Xe		N2	
		P = 0.1	P = 0.05	Chi^2	Misfit	Chi^2	Misfit	Chi^2	Misfit	Chi^2	Misfit	Chi^2	Misfit	Chi^2	Misfit
KF-85	0.62	2.71	3.84	1495.45	184.8%	0.01	0.0%	0.05	0.55%	0.89	-2.0%	0.057	1.56%	0.40	-9.3%
KFRGA	0.52	2.71	3.84	1139.64	207.9%	0.00	0.0%	0.04	0.6%	0.39	-3.6%	0.09	1.8%	0.92	-8.8%
SR-116	14.00	2.71	3.84	926.92	155.7%	0.05	-0.4%	4.65	6.9%	6.92	-13.6%	2.38	-8.5%	0.56	-7.0%
SR222	0.00	2.71	3.84	1870.09	640.1%	0.00	0.0%	0.00	0.0%	14.63	-18.7%	0.00	0.0%	0.26	-4.8%
SR-140	0.00	2.71	3.84	622.81	99.6%	0.00	0.0%	0.00	0.0%	0.00	0.3%	0.00	-0.1%	0.16	4.2%
TZ-118	2.33	2.71	3.84	1165.32	215.2%	0.00	-0.1%	0.39	1.9%	1.86	-7.6%	0.08	1.7%	1.47	-11%
TZ-217	50.92	2.71	3.84	2284.46	2168.7%	0.01	-0.2%	16.30	13.8%	26.93	-23.7%	7.68	-14.3%	2.58	19.1%
TZ-317	0.00	2.71	3.84	2384.23	4168.2%	0.00	0.0%	0.00	0.0%	0.00	-0.2%	0.00	0.1%	0.01	-0.9%
TZ-401	0.72	2.71	3.84	2292.39	2257.3%	0.00	0.0%	0.05	-0.6%	0.58	4.8%	0.10	-1.9%	0.91	10.5%
TZ618	0.02	2.71	3.84	2310.35	2485.4%	0.00	0.0%	0.00	0.1%	0.01	-0.7%	0.00	0.3%	0.00	0.5%

Because *Ae* are small values (from 0.0240 to 0.0436) cm3STP g^{-1}, we have good fits (χ^2) increasing from 0 to 50.92 at the Tazerbo aquifer. Howevere, the Sarir aquifer has *Ae*-values from 0 to 2.33 and The Al Kufra aquifer has an *Ae*-value of 0.0275 for the deep aquifer with temperature 19.4°C and 24°C for the shallow aquifer.

The non-atmospheric He components are calculated from the measured He by subtracting the equilibrium and excess air components, as defined by equation (6.13) with the parameters obtained from the fit to the other noble gases. The CE-model (Eqn. 6.13) gives us the best fit for the heavier noble gases and the most realistic results for the radiogenic He.

Degassing during sampling appears doubtful because the noble gas concentration pattern is consistent with Eqn. (6.13). The great He accumulation rates may be due to a He flux from deeper strata. Such a flux may be particularly significant at all the wellfields because of the long residence times, allowing the He to diffuse vertically through the strata. Because of its high He concentrations, most samples give the best constraints for the isotopic signature of the radiogenic He in all aquifers.

In addition, the contribution of ^{3}He from the decay of tritium in the groundwater could be significant. However, tritium concentrations in our samples are very low (<0.1 TU) in all the wellfields indicating a negligible addition of water younger than 50 yr to these aquifers including the shallow aquifer in Al Kufra with its Holocene noble gas signature.

The noble gas data are used to estimate the temperature of the region during recharge of the groundwater and to determine the amount of ^{4}He that was produced in the subsurface (terrigenic He, He_{terr}), which is an indicator of groundwater age. The paleotemperatures are determined following the methodology of Aeschbach-Hertig et al. (1999) which also allows for the determination of the He_{terr}.

The recharge temperatures and terrigenic He components are presented in Tables (6.2) and (6.4). Figure (6.5) shows these noble gas temperatures as a function of the calculated ^{4}He and ^{14}C ages. A generally well developed correlation between the ^{4}He concentration and ^{14}C age for the three aquifers exists. Noble gas recharge temperatures (NGRTs) were determined for one sample from Sarir, three samples from Tazerbo and one from Al Kufra. For Sarir, the NGRT was 18°C, which is about 5 degrees cooler than the average annual temperature today. For Tazerbo, one sample yielded a temperature of 20°C and the other two yielded temperatures of 25°C, compared to the present average annual temperature of 23°C. For the sample from Al Kufra, the recharge temperature is 19°C compared to the present average of 24°C. A sensitivity analysis showed that if the elevation of recharge was increased by 500 – 600 m, the NGRT will decrease by ~2°C. Therefore, these reported NGRT should be considered as maximum values since the elevations of the wellfields were used.

Our NGRT values for the various aquifers yield recharge temperatures that are a few degrees cooler than the current average annual temperatures from as far south as Al Kufra to as far north as Sarir. These values, determined from wells that have evidence of late Pleistocene water, suggest that the climate at that time was cooler than today. This is consistent with the findings of others that indicate a lowering of temperatures by several degrees around the world during the last glacial maximum (e.g., Stute et al. 1995; Aeschbach-Hertig et al. 2001; Edmunds et al. 2004). The lower temperatures are consistent to temperatures being a few degrees cooler during the Late Pleistocene compared with today. Fontes and Garnier's (1979) model indicate all samples are of Pleistocene and Holocene age, and most of them are older than 10 kyr.

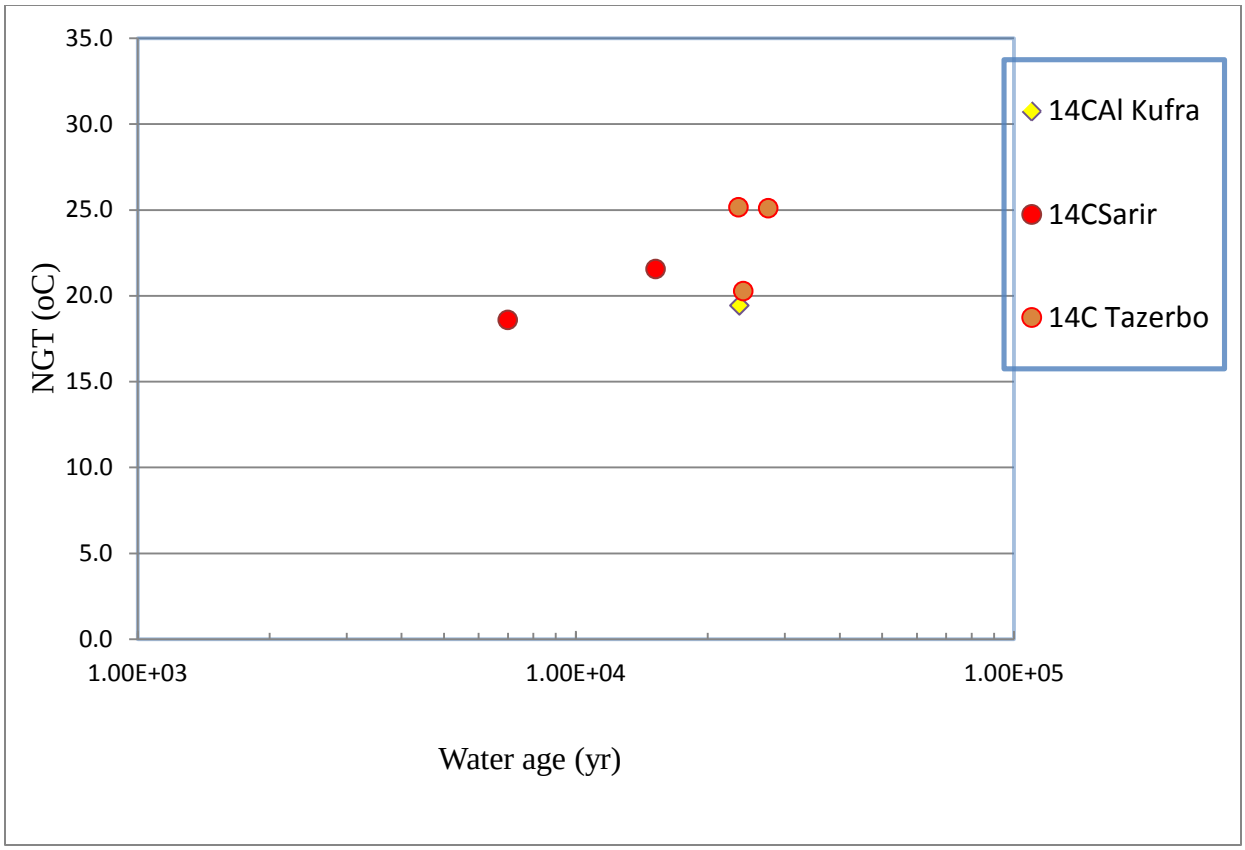

Figure 6.5. Noble gas temperatures for the Al Kufra wellfield, Sarir wellfield, and Tazerbo wellfield as a function of the calculated ^{4}He and ^{14}C ages.

These ages seem to be consistent with several indications from the climate-sensitive variables. The amount of terrigenic helium is compared to the percent modern carbon shows that there is more helium in the groundwater with increasing groundwater age. This is consistent with their being a longer time period for helium to be added to the system due to natural uranium/thorium decay in the aquifer material.

Samples with low NGTs seem to indicate a cold climate, i.e., KF85 at ^{14}C ages of 20 kyr. However, samples with ^{14}C activities (41.4 pmc) suggest age for$^{14}C \approx 10$ kyr are independent of the model used to calculate the initial ^{14}C activity. Clearly, the interpretation of the carbon isotope data is consistent with the interpretation of NGRTs, and stable isotopes as climate indicators. On the other hand, noble gas gave us very large groundwater ages compared with ^{14}C as shown in table (6.4).

CHAPTER SEVEN

CONCLUSIONS AND RECOMMENDATION

The stable isotope compositions of the three aquifers studied differ from one another. The δD and δ18O data show two different groups. The Sarir wellfield samples have an average stable isotope composition of δD = -73.7 ‰ and δ18O = -9.3 ‰, which generally these value are indicate Holocene ages, while the averge of stable isotope composition of the Al Kufra wellfield are δD = -4.1 ‰ and δ18O = -11.4 ‰, and the corresponding values for the Tazerbo wellfield are δD = -84.6 ‰ and δ 18O = -11.8 ‰, which generally indicate Pleistocene age. The isotope values for the Sarir plot below the global meteoric water line (GMWL) suggesting that the waters have experienced some evaporation, while the Tazerbo samples are depleted relative to those at Sarir plot on the GMWL. However, Al Kufra samples are plot below the GMWL but close to Tazerbo samples. The compositions seen in all groundwaters are significantly lower than those expected to be found in modern precipitation. During Pleistocene times the Sirt and Al Kufra Basins were several degrees cooler than during Holocene times, therefore δ2H and δ18O of groundwaters recharged during Pleistocene times should be more negative than those of groundwaters recharged during modern times.

^{14}C concentration and $^{14}C/^{12}C$ ratios were converted into groundwater ages and corrected base on Fontes and Garnier (1979). The carbon isotopes are varying between the three aquifers. The result of ^{14}C analysis of groundwater samples from the three aquifers have relatively small negative $\delta^{13}C$ values ranging from -23.94 ‰ from a shallow well at the Al Kufra wellfield to -10.379 ‰ from a deep well. The Tazerbo wellfield has $\delta^{13}C$ values ranging from -8.2 ‰ to -5.99 ‰. The values of $\delta^{13}C$ at Sarir exhibit ranges from -25.7 ‰ to -8.8 ‰.

Determination of ^{14}C ages as outlined above yields a range of 9.9 kyr to 15.2 kyr at the Sarir wellfield. For Tazerbo, the range is much narrower, yielding ages from 23.4 kyr to 27.5 kyr. The shallow sample from the Al Kufra wellfield has an age of 12.0 kyr while the deep sample has an age of 20.5 kyr. There is a relationship between well depth and age in the Al Kufra Basin.

The groundwaters in Sarir and Al Kufra could be divided into two main isotopic groups: strongly negative stable ^{13}C-isotope ratios combined ($\delta^{13}C$ = -25.7 to -23.94 ‰) with low ^{14}C activity; and less negative in ^{13}C (-10.379 to -8.8 ‰) with higher 14C values. The first group corresponds either to the shallow groundwaters in Al Kufra or to some deep wells in the Sarir wellfield. The second group corresponds generally to deeper groundwaters in Tazerbo and Al Kufra wellfields.

In general, the oldest ages are from the Tazerbo well field, which is using water from the Devonian-age aquifer that is confined. The Tadrat Formation is confined and underlies the Nubian Sandstone and they would have a limited area of recharge to occur, assuming recharge comes from the south following the regional hydraulic gradient. Since we have no samples along the potential flow path, we do not know how the ages progress from the recharge area to the discharge area near Tazerbo.

The consistency of the ages suggests that recharge occurred 25 kyr, corresponding to the Late Pleistocene. During this time period, the climate was cooler and more humid as our results from the noble gas. Recharge at this time may have occurred due to the precipitation in the highlands to the south (Tibesti Mountains) with flow to the north through the channel deposits discussed in previous study. It has been suggested that during this time, the channels were flowing more regularly, potentially providing recharge to the Tadrat Formation.

In the Al Kufra area, there are two different ages that are dependent upon the depth of sampling. The deep sample from the agricultural fields near the town of AL Kufra, give an age of 20.5 kyr Table (5.2). The shallow sample has an apparent age of 12.0 kyr. The Nubian Sandstone throughout this area is exposed at the surface and is well above the Tadrat. These locations are along the paleochannel discussed earlier. Therefore, recharge could have been from the south, including the Tibesti Mountains, Awynat and farther to the south in northern Chad.

It has been suggested that the end of the Pleistocene humid period was around 11.7 kyr, which corresponds to the apparent age of the shallow groundwater at Al Kufra. In Sarir, there is a relatively wide spread of apparent groundwater ages (9.9 kyr – 15.2 kyr). These groundwater samples are from Middle Miocene the fluvial sands, with interbedded clays, of the southern Sirt Basin. Though no depth relationship between apparent age and depth, there are more clay layers above the well screen with the greatest apparent age. As the Sarir wellfield has been pumping for over 20 years, it is most likely that the apparent age range is due to a mixing of deeper older water with younger shallow water. The source of recharge for this area is unclear. The large paleochannel does flow to this direction but is farther to the east (See fig. 3.3). It is possible that there was some recharge from the Al Haruj al Aswad to the west.

For the three well fields there have been no groundwater ages younger than about 10 ka. Therefore, there is no evidence of recharge during this time period and no evidence of modern recharge. As a result, it has been proposed that the observed groundwater gradients in the area are from fossil gradients established during the late Pleistocene/early Holocene and that these gradients are slowly decaying. Tritium content of the groundwater in Al Kufra and Sirt basin is very low, with an average of 0.076 T.U. The low content of tritium is another indication that this groundwater is fossil water and has no recent recharge.

This study shows how a simple analytical model for the accumulation of ^{4}He in groundwater allows the simultaneous estimate of the crustal ^{4}He flux in relatively simple flow systems and under certain assumptions. The accumulation of ^{4}He in groundwater helps to estimate of the crustal ^{4}He flux. ^{4}He ages obtained from a model simulations are not consistent with those obtained from ^{14}C. All the aquifers, have received some external ^{4}He out of the aquifer. The mantle component is a significant amount in our samples in all the aquifers. However, the crustal ^{4}He observed could be the result of in-situ production or from the external source.

The rate of accumulation of ^{4}He in the Al Kufra Basin is the result of two processes. In young water (age < 10 kyr) the rate of accumulation of ^{4}He can be accounted for by the in-situ production of ^{4}He by the alpha-decay of U and Th series elements with the release factor for helium near 100 %. However, in the main part of the basin (> 26 kyr), the rate of accumulation of ^{4}He is 55 times the rate of in-situ production and cannot be accounted for by in-situ weathering and the subsequent release of ^{4}He trapped in mineral grains over geologic time. The rate of accumulation of ^{4}He in the older waters of the Tazerbo can be accounted for by the flux of ^{4}He from the whole crust as well as the large amount that could come from the aquitard as it has large amount of U and Th.

Sarir wellfield would also appear to reflect such a whole crust ^{4}He flux and the data of numerous other authors strongly suggests large ^{4}He sources outside the confines of the individual groundwater bodies. The observation of a whole crust ^{4}He flux and crustal degassing of ^{4}He may therefore be widespread.

The studies generally yield a nearly linear rate of increase in ^{4}He with age but the agreement between the ^{14}C and the calculated ^{4}He age is often somewhat poor; ^{4}He ages tend to be greater, oftentimes by factors of up to 50-70 times.

This study reports the rate of accumulation of ^{4}He in the Sirt and Al Kufra Basins the possible mechanisms which could provide a source for this ^{4}He. The results indicate that these confined aquifers are accumulating ^{4}He at a rate that is initially controlled by crust production and later by the mantle production of ^{4}He. This mechanism could explain the discrepancies in ^{4}He ages observed by other workers.

Al Kufra aquifer samples show that the recharge temperature was 20^{o}C, cooler than today, between 20 - 22 kyr, and Tazerbo aquifer samples show that the recharge temperature was 20-25^{o}C, cooler than today, between 24 - 28 kyr, while Sarir aquifer ample show that the recharge temperature was 18°C, cooler than today between 10 - 15 kyr.

There are no flowpath data available in this study due to the limit of well access; what has been developed is a baseline to which later results can be compared in order to identify changes in apparent ages and other parameters due to continued extraction of water from the three aquifers.

We recommended for the further study that samples must be collected from deeper wells around the Al Kufra as the well field planned for the area will extract water from deeper depths than that sampled at the RGWA well. Some limited regional recharge by direct infiltration from the surface aquifers in all wellfields are to be expected. Although a detailed knowledge of the sediment composition would be required for a precise calculation of the $^{3}He/^{4}He$ production ratio, rough estimates can be made on the basis of the measured Li concentrations.

REFERENCES

Ade-Hall, J. M., and P. H. Reynolds, 1975, Geophysical studies of North Africa Cenozoic volcanic areas: II. Jabal Soda, Libya: Canadian Journal of Earth Science, v. 12, p. 1257–1263.

Ade-Hall, J. M., P. H. Reynolds, P. Dagley, A. E. Musette, T. P. Hubbard, and E. Klitzsch, 1974, Geophysical studies of North Africa Cenozoic volcanic areas: I. Hrauj Assuad Libya: Canadian Journal of Earth Science, v. 11, p. 998– 1006

Aeschbach-Hertig, W., Stute, M. Clark, J.F., Reuter, R.F., and Schlosser, P., 2001, A paleotemperatures record derived from dissolve noble gases in groundwater of the Aquia Aquifer (Maryland, USA): Geochimica et Cosmochimica Acta, 66(5):797-817

Aeschbach-Hertig W., Peeters F., Beyerle U. and Kipfer R., 1999, Interpretation of dissolved atmospheric noble gases in natural waters. Water Resour. Res. 35, 2779–2792.

Aeschbach-Hertig W., Peeters F., Beyerle U. and Kipfer R.,2000, Palaeotemperature reconstruction from noble gases in ground water taking into account equilibration with entrapped air. Nature 405, 1040–1044.

Ahmad, M. and Edibb, A., 1975, Resources in Libyan Sahara. In Proceedings Second World Congress. International Water Resources Association, New Delhi, volume 101, pages 1–10.

Ahmad, M. U., 1983, A quantitative model to predict safe yield for wellfield in the Kufra and Sarir Basins, Libya. Groundwater J., 1983, 21, 1, Jan., Feb., pp. 58-66.

Ahmad, M., Goad, M., 1978, Discovery of an ancient underground channel in the north Sarir well fields, Libya. Proc. Symp. On Investigation, Exploitation, and Economy of Underground Waters, Jagreb, Yugoslavia, pp. 77–85.

Ambrose, G. 2000, The geology and hydrocarbon habitat of the Sarir Sandstone, SE Sirt Basin, Libya. Journal of Petroleum Geology, 23(2), 165-191.

Andrews J. N. and Lee D. J.,1979, Inert gases in groundwater from the Bunter Sandstone of England as indicators of age and palaeoclimatic trends. J. Hydrol. 41, 233–252.

Andrews, J. N., 1983, Dissolved radioelements and inert gases in geothermal investigations, Geothermics,12, 67-82.

Andrews, J.N., Lee, D.J., 1979, Inert gases in groundwater from the Bunter Sandstone of England as indicators of age and paleoclimatic trends. J. Hydrol. 41, 233–252.

Anketell, J. M., 1996, Structural history of the Sirt Basin and its relationships to the Sabratah Basin and Cyrenaican platform, northern Libya, in M. J. Salem, A. S. El-Hawat, and A. M. Sbeta, eds., Geology of the Sirt Basin: Amsterdam, Elsevier, v.3, p. 57–88.

Baird, D.W., Aburawi, R.M., and Bailey, N.J.L., 1996, Geohistory and petroleum in the central Sirt Basin, in Salem, M.J., El-Hawat, A.S., and Sbeta, A.M., eds.,The geology of Sirt Basin: Amsterdam, Elsevier,v. III, p. 3–56.

Ball, J., 1927, Problems of the Libyan Desert. The Geographical Journal, 70(1):21–38.

Barr, F. and Walker, B.,1973, Late tertiary channel system in northern Libya and its implications on Mediterranean sea level changes. Initial Reports of the Deep Sea Drilling Project, 13:1244–1250.

Barr, F.T., and Weegar, A.A., 1972, Stratigraphic nomenclature of the Sirte basin, Libya: Tripoli, Libya, Petroleum Exploration Society of Libya, 179 p.

Ballentine, C. J., and C. M. Hall, 1999, Determining paleotemperature and other variables by using an error-weighted nonlinear inversion of noble gas concentrations in water, Geochim. Cosmochim. Acta, 63(16), 2315– 2336.

Belazi, H. S. (1989).The Geology of the Nafoora oilfield, Sirte Basin, Libya. Journal of Petroleum Geology, 12(3), 353-366.

Ballentine, C.J., R.K. O'Nions, E.R. Oxurgh, F. Horvath, and J. Deak. 1991, Rare Gas Constraints in Hydrocarbon Accumulation, Crustal Degassing and Groundwater Flow in the Pannonian Basin. Earth and Planetary Science Letters, v. 105, p. 229-246.

Bellini, E., Giori, I., Ashuri, O., and Benelli, F. 1991, Geology of Al Kufrah Basin, Libya. The Geology of Libya, 6:2155–2184.

Bellini, E., and Massa, D., 1980, A stratigraphic contribution to the Paleozoic of the southern basins of Libya: In M. J. Salem, M. T. Busrewil, The geology of Libya, London, Academic Press, v. 1, p. 3-56.

Benfield, A. and Wright, E, 1980, Post-Eocene sedimentation in the eastern Sirt Basin, Libya. In Symposium on the Geology of Libya, volume 2, pages 463–500.

Benson, B.B., Krause Jr, D., 1980, Isotopic fractionation of helium during solution. A probe for the liquid state. J. Soln. Chem. 9, 895-909.

Bentley h. W., Phillips F. M., Davis s. N., Airev P. L., Calf g. E., Elmore d., Gove h. E.. Habermehi. M. A. and Torgersen t., 1984, Chlorine-36 dating of very old groundwater: 1. The Great Artesian Basin. Australia, Water Resour. Res., 22,1991-2001, 1986.

Bezan, A. M. 1991, The Kufra Basin. In Proceedings of APPA Conference. Yaounde. 3_5 June 1991 (pp. 20).

Bezan, A.M. 1996. The Palaeocene sequence in Sirt Basin. First Symposium on the Sedimentary Basins of Libya, Geology of the Sirt Basin, vol. 1. (eds. M.J. Salem, A.J. Mouzughi and 0,S. Hammuda), Elsevier, Amsterdam, p. 97-118.

Biju-duval, B. and Montadert, L. (Eds.), 1977, Structural history of the Mediterranean basins. Editions Technip, Paris, 448 p.

Burden DJ. 1977, Flow of fossil groundwater. Quarterly Journal of Engineering Geology 10:97–124.

Burke, K., and Dewey, J. 1974, Two plates in Africa during the Cretaceous Nature, vol. 249, p. 313-316

Burollet, P.,1963, Field trip guidebook of the excursion to jebel nefusa. Petrol. Explor. Soc. Libya.

Cahen, L., Snelling, N.J., Delhal, J., Vail, J.R., Bonhomme, M. and Ledent, D., 1984, The Geochronology and Evolution of Africa. Clarendon, Oxford, 512 pp.

Capot-Rey, R.,1960, Comptes rendus. Forschungen in der zentralen Sahara Trav. Inst. Rech. Sahariennes, Alger, 19.

Castro, M.C., Jambon, A., de Marsily, G., Schlosser, P., 1998a, Noble gases as natural tracers of water circulation in the Paris Basin. 1. Measurements and discussion of their origin and mechanisms of vertical transport in the basin. Water Resour. Res. 34 (10), 2443-2466.

Castro, M.C., Stute, M., Schlosser, P., 2000, Comparison of 4He ages and 14C ages in simple aquifer systems: implications for groundwater flow and chronologies. Appl. Geochem. 15, 1137–1167.

CEDARE, 2001, Nubian Sandstone Aquifer System Programme,Regional Maps. Cairo Office, Heliopolis, Cairo.

Clarke W. B., Jenkins W. J. and Top Z., 1976, Determination of tritium by mass spectrometric measurement of 3He. Int. J. Appl. Rad. Iso. 27, 515–522.

Clever H. L., 1979, Krypton, xenon and radon - gas solubilities. In Solubility data series Vol. 2, pp. 357. International Union of Pure and Applied Chemistry, Pergamon Press, Oxford.

Coplen, T. B., Herczeg, A. L., & Barnes, C. 2000. Isotope engineering—using stable isotopes of the water molecule to solve practical problems. InEnvironmental tracers in subsurface hydrology (pp. 79-110). Springer US.

Craig, H. (1961). Standard for reporting concentrations of deuterium and oxygen-18 in natural waters. Science, 133(3467), 1833-1834.

Deines, P., D. Langmuir, and R. S. Harmon, 1974, Stable carbon isotope ratios and the existence of a gas phase in the evolution of carbonate groundwaters, Geochim. Cosmochim. Acta, 38, 1147-1164.

Demenocal, P., 2004, African climate change and faunal evolution during the Pliocene–Pleistocene. Earth and Planetary Science Letters, 220(1):3–24.

DeMenocal, P., Ortiz, J., Guilderson, T., Adkins, J., Sarnthein, M., Baker, L., and Yarusinsky, M., 2000, Abrupt onset and termination of the African humid period::: rapid climate responses to gradual insolation forcing. Quaternary Science Reviews, 19(1-5):347–361.

Duncan, R. A., 1981. Hotspots in the southern oceans-an absolute frame of reference for motion of the Gondwana continents.

Eddib, A., 1973, A quantitative study of ground water in the Kufra Basin. Master's thesis, Ohio University.

Edmunds, W. M. 2005, Groundwater as an archive of climatic and environmental change. In: Isotopes in Water Cycle: past, Present and Future of a Developing Sciences (ed. By P. k. Aggarwal, J. Gat & K. Froehlich), 341-352. Springer- Verlage, Berlin, Germany.

Edmunds, W. M. 2009, Palaeoclimate and groundwater evolution in Africa – implications for adaptation and management, in Hydrological Sciences-journal des Sciences Hydrologiqiues, 54(4), Special issue: Groundwater and Climate in Africa.

Edmunds W.M., Dodo A, Djoret D., Gasse F., Gaye C., Goni I.B., Travi Y., Zouri K. and Zuppi G.-M., 2004, Groundwater as an archive of climate and environmental change: Europe to Africa: In: Barttarbee, R.W. et al. (eds) Past climate variability through Europe and Africa, Springer, Dordrecht, The Netherlands, 279-306.

Edmunds, W. and Wright, E., 1979, Groundwater recharge and palaeoclimate in the Sirte and Kufra basins, Libya. Journal of Hydrology, 40(3-4):215–241.

El-Hawat, S. A., A. A. Missallati, M. A. Bezan, and M. T. Taleb, 1996, The Nubian Sandstone in the Sirt Basin and its correlatives, in M. J. Salem, M. T. Busrewil, A. A. Misallati, and M. A. Sola, eds., The geology of the Sirt Basin: Amsterdam, Elsevier, v. 2, p. 3–30.

El Ramly, I.M., 1980. Al Kufrah Pleistocene lake — its evolution and role in present-day land reclamation. In: Salem, M.J., Busrewil, M.T. (Eds.), The Geology of Libya, vol. 2. Academic Press, London, pp. 659–670.

Eskangi, A. M. and Swailem, F. M, 1975, Studies on Groundwater Parameters in Kufra Basin (Libya) using Radioisotope Techniques, Peaceful Uses of Atomic Energy for Scientific and Economic Sevelopment, Proc. Symp. Baghdad, Iraq, 517.

Ezzat, A., 1959, Ecological studies of bottom living Amphipods in the Nozha Hydrodrome. Extension Department, Editing and Publication Section.

Fontes, J. and Garnier, J., 1979, Determination of the initial 14c activity of the total dissolved carbon: A review of the existing models and a new approach. Water Resources Research, 15(2):399–413.

Fontes, J.-C., and J.-M. Garnier, 1 977, Determination of the initial 14C activityo f the total dissolvedc arbon:A ge estimationo f waters in confined aquifer, in Proceedings of Second International Symposium on Water-Rock Interaction, vol. 1, edited by H. Paquet and Y. Tardy, pp. 363-376, Universitĕ Louis Pasteur Strasbourg.

Furon, R., 1963, Geology of Africa: Edinburgh. Oliver and Boyd.

Gabert, G., Kleinsorge, H., Kreysing, K., and Venzlaff, H., 1961, Some results of ground water investigations in the republic of Sudan. In Symposium of Athens. IASH Publication, number 56, pages 201–213.

Gat JR. 1981., Lakes. In Stable Isotope Hydrology—Deuterium and Oxygen-18 in the Water Cycle, Gat JR, Gonfiantini R (eds). IAEATechnical Report Series No. 210. IAEA: Vienna; 203–221.

Geyh, M. A., 1970, Carbon 14 concentration of lime in soil sand aspects of the carbon 14 dating of groundwater, in Isotope Hydrology 1970, pp. 215-222, International Atomic Energy Agency, Vienna.

Geyh, M. A., 1972, On the determination of the initial 14C content in groundwater, in Proceeding of Eighth International Conference on Radiocarbon Dating, vol. l, Royal Society of New Zealand,Wellington.

Ghoneim, E., Benedetti, M., & El-Baz, F., 2012, An integrated remote sensing and GIS analysis of the Kufrah Paleoriver, Eastern Sahara. Geomorphology,139, 242-257.

Ghoneim, E., Benedetti, M., and El-Baz, F, 2011, An integrated remote sensing and GIS analysis of the Kufrah paleoriver, eastern sahara. Geomorphology.

Godwin, H.,1962, Half-life of radiocarbon. Nature, 195, 984.

Gossel, W., Ebraheem, A. M., Wycisk, P., 2004, A very large scale GIS-based groundwater flow model for the Nubian sandstone aquifer in Eastern Sahara (Egypt, northern Sudan and eastern Libya): Hydrogeology Journal (2004) 12:698–713.

GoudarzI, G.H. and Smith, LP. 1978, Preliminary structure-contour map of the Libyan Arab Republic and adjacent areas; 1:2,000,000. U.S. Geol. Surv. Misc. GeoL Invest., Map I-350C.

Gourgaud, A. and Vincent, P.,2004, Petrology of two continental alkaline intraplate series at Emi koussi volcano, Tibesti, chad. Journal of volcanology and geothermal research, 129(4):261–290.

Gras, R., and B. Thusu, 1998, Trap architecture of the Early Cretaceous Sarir Sandstone in the eastern Sirt Basin, Libya, in S. D. Macgregor, J. T. R., Moody, and D. D.Clark-Lowes, eds., Petroleum geology of north Africa: Geological Society (London) Special Publication 132,p. 317–334.

Griffin, D., 2002, Aridity and humidity: two aspects of the late Miocene climate of North Africa and the Mediterranean. Palaeogeography, Palaeoclimatology, Palaeoecology, 182(1):65–91.

Griffin, D., 2006, The late Neogene Sahabi rivers of the Sahara and their climatic and environmental implications for the chad basin. Journal of the Geological Society, 163(6):905–921.

Gumati, Y.D., and Kanes, W.H., 1985, Early Tertiary subsidence and sedimentary facies—Northern Sirte Basin, Libya: American Association of Petroleum Geologists Bulletin, v. 69, p. 39–52.

Gumati,Y.D., and A. E. M. Nairn, 1991,Tectonic subsidence of the Sirte Basin, Libya: Journal of Petroleum Geology, v. 14, p. 93–102.

GWG (German Water Group), 1977, Hydrogeological study of groundwater resources in the Kufra Area, in German Water Engineering GmbH, Vol. 1-5, Tripoli, Libya, unpubl.

Hallett, D., 2002, Petroleum geology of Libya: New York, Elsevier, 503p.

Harding, T. P., 1984, Graben hydrocarbon occurrences and structural style.AAPG Bulletin, 68(3), 333-362.

Heaton, T.H.E., Vogel, J.C., 1981, “Excess air" in ground-water. J. Hydrol. 50, 201-216.

Heinl M, Brinkmann PJ., 1989, A ground water model for the Nubian Aquifer System. IAHS Hydrol Sci J 34(4)425–447

Hellström, B., 1940, The subterranean water in the Libyan desert. Geografiska Annaler, 22:206–239.

Hoelzmann P., Kruse H.-J., Rottinger F., 2000, Precipitation estimates for the eastern Sahara paleomonsoon based on a water balance model of the West Nubian Paleolake Basin: Global and Planetary Change, 26:105-120.

Ingerson,E ., and F. J. PearsonJ, r., 1964, Estimation of age and rate of motion of groundwater by the 14C-method, in Recent Researches in the Fields of Hydrosphere, Atmosphere and Nuclear Geochemistry, pp. 263-283, Maruzen, Tokyo.

International Atomic Energy Agency, Global Network for Isotopes in Precipitation

Jacob, H., & Sonntag, C., 1991, An 8 year record of the seasonal variation of 2H and 18O in atmospheric water vapour and precipitation at Heidelberg, Germany. Tellus B, 43(3), 291-300.

Kehinde, M. and Loehnert, E., 1989, Review of African groundwater resources. Journal of African Earth Sciences (and the Middle East), 9(1):179–185.

Klitzsch, E., 1971, The structural development of parts of north Africa since Cambrian time. In Symposium on Geology of Libya (Carlyle gray, ed.), Tripoli, Libya, pages 253–262.

Kroner, A., 1993, The Pan-African belt of northeastern and eastern Africa, Madagascar, southern India, Sri Lanka and east Antarctica; Terrane amalgamation during formation of the Gondwana Supercontinent, in Thorwiehe, U., and Schandelmeier, H., eds., Geoscientific research in Northeast Africa: Rotterdam, Netherlands, A.A. Balkema, p. 3–9.

Kuwairi, A., 2006, Water mining: the great man-made river, Libya. In Proceedings of the Institution of Civil Engineers. Civil engineering, volume 159, pages 39–43.

Lloyd, J. W., 1990, Groundwater resources development in the eastern Sahara. Journal of Hydrology, 119(1):71–87.

Lüning, S., Craig, J., Fitches, B., Mayouf, J., Busrewil, A., El Dieb, M., Gammudi, A., Loydell, D., McIlroy, D., 1999, Re-evaluation of the petroleum potential of the Kufra Basin (SE Libya, NE Chad): Does the source rock barrier fall?: Marine and Petroleum Geology, v. 16, p.693-718.

Mook, W. G., 1976, The dissolution-exchange model for dating groundwater with 14C, in Interpretation of Environmental Isotope and Hydrochemical Data in Groundwater Hydrology, pp. 213-225, International Atomic Energy Agency, Vienna.

Mamyrim, B.A., and I.N. Tolsikhin, 1984, Helium Isotopes in Nature. Elsevier.

Marine I. W., 1979, The use of naturally-occurring helium to estimate groundwater velocities for studies of geological storage of radioactive water. Water Resources Rex 15(5),1130-I 136.

Marty, B., Criaud, A., Fouillac, C., 1988, Low enthalpy geothermal fluids from the Paris sedimentary basin. Characteristics and origin of gases. Geothemics 17, 619-633.

Mccauley, J. F., Breed, C. S., Schaber, G. G., McHugh, W. P., Issawi, B., Haynes, C. V., ... & Kilani, A. E., 1986, Paleodrainages of the Eastern Sahara-The Radar Rivers Revisited (SIR-A/B Implications for a Mid-Tertiary Trans-Afnrcan Drainage System). Geoscience and Remote Sensing, IEEE Transactions on, (4), 624-648.

Mook, W. G., 1972, On the reconstruction of the initial 14C content of groundwater from the chemical and isotopic composition, in Proceedings of Eighth International Conference on Radiocarbon Dating, vol. l, pp. 342-352, Royal Society of New Zealand, Wellington.

Morgan, W. J.,1981, 13. Hotspot tracks and the opening of the Atlantic and Indian oceans. The Sea, ideas and observations on progress in the study of the seas, 7, 443.

Morgan, W. J., 1983, Hotspot tracks and the early rifting of the Atlantic,T ectonophysic9s4, , 123-139.

Murray, G., 1952, The artesian water of Egypt. Ministry of Finance and Economy, Survey of Egypt.

Occidental Petroleum Corporation, 1966, Analyses of Groundwater potentials and possible area for agricultural development in the Kingdom of Libya- Los Angeles, (unpubl. report).

Occidental Petroleum Corporation, 1970, Groundwater Geology and Hydrology of the Kufra Oasus (unpubl. report).

Ozima, M., and F.A. Podosek, 1983, Noble Gas Geochemistry. Cambridge University Press, Cambridge.

Pachur, H. and Hoelzmann, P., 2000, Late quaternary palaeoecology and palaeoclimates of the eastern Sahara. Journal of African Earth Sciences, 30(4):929–939.

Pachur, H., 1980, Climatic history in the late quaternary in southern libya and the western Libyan desert. The Geology of Libya, 3:781–8.

Pachur, H.-J., 1993, Palaeodrainage systeme im Sirte-Becken und seiner Umrahmung. Wurtzburger. Geographische Arbeiten 87, 17–34.

Pachur, H.J., 1996. The Geology of Syrte Basin – vol 1 – Reconstruction of paleodrainage systems in Syrte Basin and the area surrounding the Tibesti Mountains: Implications for the hydrological history of the region. First symposium on the sedimentary basins of Libya, Tripoli. Elsevier Eds.

Paillou, P., Tooth, S., & Lopez, S., 2012, The Kufrah paleodrainage system in Libya: A past connection to the Mediterranean Sea?. Comptes Rendus Geoscience.

Pallas, P., 1981, Water Resources of the Socialist People's Libyan Arab Jamahiriya. In: Salem, M. J. & Busrewil, M. T. (eds). Geology of Libya. Academic Press, London, 539-94.

Pearson, F. J., Jr., and B. B. Hanshaw, 1970, Sources of dissolved carbonate species in groundwater and their effects on carbon-14 dating, in Isotope Hydrology 1970, pp. 271-285, International Atomic Energy Agency, Vienna.

Pearson, F. J., Jr., and W. W. Swarzenki, 1974, 14C evidence for the origin of arid region groundwater, Northeastern Province, Kenya, in Isotope Techniques in Groundwater Hydrology 1974, pp. 95-108, International Atomic Energy Agency, Vienna.

Pearson, F. J., Jr., M. S. Bedinger, and B. F. Jones, 1972, Carbon-14 ages of water from the Arkansas Hot Springs, in Proceedings of Eighth International Conference on Radiocarbon Dating, vol. 1, pp. 330-341, Royal Society of New Zealand, Wellington.

Pim, R. and Binsariti, A., 1994, The Libyan great man-made river project. Paper 2. The water resource. Proceedings of the ICE-Water Maritime and Energy, 106(2):123–145.

Pinti, D.L., Marty, B., Andrews, J.N., 1997, Atmosphere-de- rived noble gas evidence for the preservation of ancient waters in sedimentary basins. Geology 25 (2), 111-114.

Ramos, E., Mariano, M., J. M. de Gibert, K. Tawengi, A. Khoja, and Ne´ stor D., 2006, Stratigraphy and sedimentology of the Middle Ordovician Haouaz Formation(Murzuq Basin, Libya). AAPG Bulletin, v. 90, no. 9, pp. 1309–1336.

Roberts M. L., Bench G. S., Brown T. A., Caffee M. W., Finkel R. C., Freeman S. P. H. T., Hainsworth L. J., Kashgarian M., Mc Aninch J. E., Proctor I. D., Southon J. R. and Vogel J. S.,1997, The LLNL AMS facility. Nucl. Instrum. Meth. B. 123, 57–61.

Robinson, C., El-Baz, F., Al-Saud, T. and Jeon, S., 2006, Use of radar data to delineate palaeodrainage leading to the Kufra Oasis in the Eastern Sahara. Journal of African Earth Sciences, 44, pp. 229–240.

Robinson, C.A., El-Baz, F., Ozdogan, M., Ledwith, M., Blanco, D., Oakley, S. and Inzana, J., 2000, Use of radar data to delineate palaeodrainage flow directions in the Selima sand sheet, Eastern Sahara. Photogrammetric Engineering and Remote Sensing, 66, pp. 745–753.

Roohi, M., 1996, A geological view of source-reservoir relationships in the western Sirt Basin, in M. J. Salem, A. S. El-Hawat, and A. M. Sbeta, eds., Geology of the Sirt Basin: Amsterdam, Elsevier, v. 1, p. 323-336.

Rusk, D. C., 2001, Libya: Petroleum potential of the underexplored basin centers—Atwenty-first-century challenge, in M.W. Downey, J. C. Threet, and W. A.Morgan, eds., Petroleum provinces of the twenty-first century: AAPG Memoir 74,p. 429–452

Sandford, K.,1935, Geological observations on the northwest frontiers of the anglo-Egyptian Sudan and the adjoining part of the southern Libyan desert. Quarterly Journal of the Geological Society, 91(1-4):323–381.

Schroter, T., 1996, Tectonic and sedimentary development of the central Zallah Trough (west Sirt Basin, Libya). First Symposium on the Sedimentary Basins of Libya, Geology of the Sirt Basin, vol. 3. (eds. M.J. Salem, M.T. Busrewil, A.A. Misallati and M.J. Sola), Elsevier, Amsterdam, p. 123-136.

Smith S. P. and Kennedy B. M.,1983, The solubility of noble gases in water and NaCl brine. Geochim. Cosmochim. Acta 47, 503–515.

Solomon, D.K. and P.G. Cook, 2000, 3He and 4He. In Cook, P.G., and A.L. Herczeg, Environmental Tracers in Subsurface Hydrogeology. Kluwer Academic Publishers, Boston, U.S.A.

Solomon, D.K., 2000, 4He in Groundwater. In Cook, P.G., and A.L. Herczeg, Environmental Tracers in Subsurface Hydrogeology. Kluwer Academic Publishers, Boston, U.S.A.

Solomon, D.K., Hunt, A., Poreda, J., 1996, Source of radiogenic helium 4 in shallow aquifers: implications for dating young groundwater. Water Resour. Res. 32, 1805–1813.

Sturchio, N., Du, X., Purtschert, R., Lehmann, B., Sultan, M., Patterson, L., Lu, Z., Müller, P., Bigler, T., Bailey, K., et al., 2004, One million year old groundwater in the Sahara revealed by krypton-81 and chlorine-36. Arxiv preprint physics/0402092.

Stute, M., Forster M., Frischkorn H., Serejo A., Clark J.F., Schlosser P., Broecker W.S. and Bonani G., 1995, Cooling of tropical Brazil (5°C) during the Last Glacial Maximum: Science 269:379-383.

Stute M. and Sonntag C., 1992, Paleotemperatures derived from noble gases dissolved in groundwater and in relation to soil temperature. In Isotopes of noble gases as tracers in environmental studies, pp. 111–122. IAEA, Vienna.

Stute M., Sonntag C., De´ak J. and Schlosser P., 1992b, Helium in deep circulating groundwater in the Great Hungarian Plain: Flow dynamics and crustal and mantle helium fluxes. Geochim. Cosmochim. Acta. 56, 2051–2067.

Stute, M., and Deak, J., 1989, Environmental isotope study (14C, 13C, 18O, D, noble gases) on deep groundwater circulation systems in Hungary with reference to paleoclimate. Radiocarbon 31, 902-918.

Stute, M., and Schlosser, P., 1993, Principles and applications of the noble gas paleothermometer, AGU monograph on``climate change in continental isotopic records". Geophysical Monograph 78, 89-100.

Stute M. and Schlosser P., 2000, Atmospheric noble gases. In Environmental tracers in subsurface hydrology (eds. Vol. P. Cook and A. L. Herczeg) pp. 349 –377. Kluwer Academic Publishers, Boston.

Swailem, F., Hamza, M., and Aly, A., 1983, Isotopic composition of groundwaters from Kufra (Libya) as indicator for groundwater formation.

Tamers, M. A., 1967, Surface-water infiltration and groundwater movement in arid zones of Venezuela, in Isotopes in Hydrology, pp. 339-351, International Atomic Energy Agency, Vienna.

Tamers, M. A., 1975, Validity of radiocarbon dates on groundwater, Geophys. Surv., 2, 217-239.

Tamers, M. A., and Scharpenseel. H. W.,1970, Sequential sampling of radiocarbon in groundwater, in Isotope Hydrology 1970, pp. 241- 256, International Atomic Energy Agency, Vienna.

Tipton and Kalambach, Inc., 1972, Feasibility of the Kufra aqriclutral project. Unpublished report. 109 PP.

Torgersen T. and Clarke W. B., 1985, Helium accumulation in groundwater, I: An evaluation of sources and the continental flux of crustal 4He in the Great Artesian Basin, Australia. Geochim. Cosmochim. Acta. 49, 1211–1218.

Torgersen T., 1980, Controls on pore-fluid concentration of 4He and 222Rn and calculation of 4He/222Rn ages. J Geochem. Explor. 13, 57-75.

Torgersen, T., Clarke, W.B., 1985, Helium accumulation in groundwater, I: an evaluation of sources and the continental flux of crustal 4He in the Great Artesian Basin, Australia. Geochim. Cosmochim Acta 49, 1211-1218.

Torgersen, T., Ivey, G.N., 1985, Helium accumulation in groundwater, II: a model for the accumulation of the crustal 4He deassing flux. Geochim. Cosmochim Acta 49, 2445-2452.

Torgerse T., M. A. Habermehl F. M. Phillips, D. Elmore, P. Kubik, B. G. Jones, T. Hemmick, and H. E. Gove, 1991, Chlorine 36 dating of very old groundwater, 3, Further studies in the Great Artesian Basin, Australia, Water R esour. Res., 27, 3201-3213.

Turner, B., 1980, Paleozoic sedimentology of the southeastern part of al Kufrah Basin, Libya: a model for oil exploration. The geology of Libya, 2:351–374.

Turner, B., 1991, Paleozoic deltaic sedimentation in the southeastern part of al kufrah basin, libya. The Geology of Libya, 5:1713–1726.

Van der Meer, F., and S. Cloetingh, 1993a, Late Cretaceous and Tertiary subsidence history of the Sirt Basin (Libya), an example of the use of backstripping analysis: ITC (International Institute for Geo-information Science and Earth Observation) Journal, v. 93, no. 1, p. 68–76.

Van der Meer, F., and S. Cloetingh, 1993b, Intraplate stresses and subsidence history of the Sirt Basin (Libya): Tectonophysics, v. 226, p. 37–58.

Van Houten, F. B., 1980, Latest Jurassic–Early Cretaceous regressive facies, northeast African craton: AAPG Bulletin, v. 64, p. 857–867.

Vittimberga, P. and Cardello, R. 1963, Sédimentologie et pétrographie du Bassin du Paléooique de Kufra. Premier Symposium Saharien, Tripoli, 1963. Rev. Inst. Fr. du Pétrole, 18, 10: 228-40.

Vogel, J. C., 1967, Investigation of groundwater flow with radiocarbon. pp 355-69 of Isotopes in Hydrology. Vienna, International Atomic Energy Agency.

Vogel, J. C., and D. Ehhalt, 1963, The use of carbon isotopes in groundwater studies, in Radioisotopes in Hydrology, pp. 383-395, International Atomic Energy Agency, Vienna.

Vogel, J. C., 1970,Carbon-14 dating of groundwater, in Isotope Hydrology pp. 235-237, International Atomic Energy Agency, Vienna.

Wallin, B., Gaye, C., Gourcy, L., and Aggarwal, P., 2005, Isotope methods for management of shared aquifers in northern africa. Ground water, 43(5):744–749.

Weiss R. F. and Kyser T. K., 1978, Solubility of krypton in water and seawater. J. Chem. Eng. Data. 23, 69–72.

Weiss R. F., 1970, The solubility of nitrogen, oxygen and argon in water and seawater. Deep-Sea Res. 17, 721–735.

Weiss R. F., 1971, Solubility of helium and neon in water and seawater. J. Chem. Eng. Data. 16, 235–241.

Wendorf, F., Schild, R., Said, R., Haynes, C. V., Gautier, A., & Kobusiewicz, M., 1976, The prehistory of the Egyptian Sahara. Science, 193(4248), 103-114.

Wennekers, J. H. N., K. F. Wallace, and I. Y. Abugares, 1996, The geology and ydrocarbons of the Sirt Basin: A synopsis, in M. J. Salem, A. J. Mouzoughi, and O. S. Hammuda, eds., The geology of the Sirt Basin: Amsterdam, Elsevier, v. 1, p. 3–56.

Wheida, E. and Verhoeven, R., 2006, Review and assessment of water resources in Libya. Water international, 31(3):295–309.

Wilson, M. and Guiraud, R., 1998, Late Permian to Recent magmatic activity on the African-Arabian margin of Tethys. In: Petroleum Geology of North Africa, (ed. D.S. Macgregor, R.T.J. Moody, D.D.Clark-Lowes), Geol. Soc. Special Publication No. 132, p. 231-264.

Wright, E. P. and Edmunds, W.M., 1971, Hydrogeological studies in Central Cyrenaica. In: Symposium on the Geology of Libya. University of Libya, Tripoli, pp. 459-481.

Wright, E., Benfield, A., Edmunds, W., and Kitching, R., 1982, Hydrogeology of the Kufra and Sirte Basins, eastern Libya. Quarterly Journal of Engineering Geology and Hydrogeology, 15(2):83–103.

Wüest, A., G. Piepke, and J. D. Halfmann,1996, Combined effects of dissolved solids and temperature on the density stratification of Lake Malawi (East Africa), in The Limnology, Climatology and Paleoclimatology of the East African Lakes, edited by T. C. Johnson and E. O. Odada, pp. 183– 202, Gordon and Breach Sci., New York.